

# **Parameters Retrieval of Heat Transfer systems using Inverse Optimization**

*A dissertation report submitted in partial fulfilment of the requirement for the award of*

*degree of*

**MASTER OF ENGINEERING**

**IN**

**THERMAL ENGINEERING**

**Submitted By**

**Sarvjeet Singh**

Roll No. 801783012

Under the Guidance of

Dr. Rohit Kumar Singla

Assistant Professor



**THAPAR INSTITUTE**  
OF ENGINEERING & TECHNOLOGY  
(Deemed to be University)

**DEPARTMENT OF MECHANICAL ENGINEERING**

**Thapar Institute of Engineering and Technology, Patiala**

**Punjab 147004, India**

**July, 2019**

*Dedicated to my  
Beloved Family*

## CERTIFICATE

---

I hereby certify that the thesis entitled **“Parameters retrieval of heat transfer systems using Inverse Optimization”** being submitted by **Mr. SARVJEET SINGH** to the Thapar Institute of Engineering and Technology Patiala for the award of the degree of Master of Engineering in Thermal Engineering is a record of bonafide research work carried out by him under my supervision and guidance. He has fulfilled the requirements for the submission of the thesis, which is best of my knowledge, has reached the requisite standard.

The material contained in this thesis has not been submitted, in part or in full to any other University or Institute for the award of any degree or diploma.

*Sarvjeet Singh*

Mr. Sarvjeet Singh

Roll-No-801783012



(Dr. Rohit Kumar Singla)

Assistant Professor

Department of Mechanical Engineering

TIET, Patiala, India

Date:- *15 July 2019*

Place *Patiala*

## ACKNOWLEDGEMENTS

---

First and foremost, I would like to extend my sincere thanks and gratitude towards my supervisor, Dr. Rohit Kumar Singla, Assistant Professor, Department of Mechanical Engineering, Thapar Institute of Engineering and Technology, Patiala for his continuous guidance, encouragement and strong support during the course of my M.E thesis. I am eternally grateful for his kindness, helpful guidance, discussions, and dazzling sense of humor. He truly exemplify the role of advisor. I am forever grateful for his kindness and contributions, not only towards my research but towards my professional growth as well.

I am grateful to Dr. Kavita Goyal, Assistant Professor, Department of Mathematics, Thapar Institute of Engineering and Technology, who provided useful suggestion and valuable advice regarding my research work. I would like to convey my deep gratitude to Ph.D. research Scholar Miss. Meenal Singhal, Department of Mathematics, without her, things would have been very difficult.

I express my special thanks to Mr. Charanjit Singh, Mr. Harcharn Singh and other technicians, who provided their technical support generously during the lab work. Without their support and practical tips as well as the good work environment in the Heat and Mass Transfer Lab, it would not have been possible to finish the experimental work so smoothly. I also express my gratitude towards my classmates and other supporting staff at the Thapar Institute of Engineering and Technology, Patiala, who directly or indirectly contributed towards my research.

A special thanks goes to my family for their encouragement and sacrifices. Their support and kind encouragements provided the essential foundation to thrive and success. I praise God, the Almighty, merciful and passionate, for providing me the strength and the motivation to proceed successfully.

**Patiala, July 2019**

  
**(Sarvjeet Singh)**

## ABSTRACT

---

---

This thesis is dealing with the numerical and experimental analysis of heat transfer systems to minimize the loss of heat transfer and maintaining the temperature as per our requirement. Fins are the one of the heat transfer system employed to dissipate the heat from the heating equipment. The race of maintaining the high efficiency from the least inputs tends to originate new technology in the field of heat transfer. Different types of configuration of fins are used for the purpose of heat transfer. Our body is also behave like a heat transfer system considered as bioheat system. Present work marked at applying the theory of parameter estimation by optimization techniques to a few engineering and bioheat problems involving heat transfer. For this, two heat transfer problems involving cylindrical pin fin and brain tissue have been considered. In addition, experimental data based parameter retrieval on a cylindrical pin fin is also undertaken. The work successfully reveals the application of one non-evolutionary optimization algorithms Golden Section Search Method (GSSM) for single parameter retrieval and one evolutionary optimization algorithms Differential Evolution (DE) for unknown multi-parameter retrievals. At first for the forward solution, MATLAB's inbuilt "pdepe" solver is applied for the cylindrical pin fin involving all temperature-dependent modes of heat transfer and discrete boundary conditions and finite element method is employed to solve the Pennes bioheat transfer equation as forward problem in cancerous brain. Furthermore, experiments are also done to get forward results on the pin fin of brass. Then, the GSSM and the DE are applied on these fin problems to inversely predict critical parameters such as heat flux, heat transfer coefficient, and perfusion rate. After estimating various parameters, the amount of satisfactory simulated measurement errors/noise are also evaluate.

Based on the literature survey, the research work initiates with the formulation and the solution of the recognized parabolic heat transfer problems on fins and bioheat transfer involving different levels of nonlinearities, for which either forward and/or inverse analyses were not found or less work done. Under this gaps are identified, two parabolic heat transfer problems are assumed. Initially, for the forward solution, the MATLAB's inbuilt "pdepe" solver is applied for the cylindrical pin fin of brass involving all temperature-dependent modes of heat transfer and discrete boundary conditions. Furthermore, a comparative experimental study is also conducted on a solid brass pin fin.

The experimental values are used for the theoretical analysis in MATLAB. Later, the GSSM and the DE, are applied on these bioheat and fin problems to inversely guess critical parameters such as the heat flux, heat transfer coefficient, perfusion rate. Due to the incompatibility of the GSSM for multi-parameter estimation, the DE is used as optimization technique for the multiple parameter retrievals. After estimating various parameters, the amount of satisfactory simulated measurement errors/noise are also evaluated. Different cases of heat input in the fin is studied like constant heat flux, variable heat flux, static heat flux in triangular manner and static heat flux in realistic form. For constant heat flux under static conditions, a tolerance level of 5% is acceptable for temperature with a maximum error of 3.72% in reconstruction. Linear triangular heat flux with on-off conditions under static conditions, a tolerance level of 3% is acceptable for temperature with a maximum error of 6% in reconstruction. Non-linear realistic heat flux under static conditions, a tolerance level of 4% is acceptable for temperature with a maximum error of 4% in reconstruction. The retrieved heat flux is well in agreement with the actual heat flux as confirmed by experiments. The maximum uncertainties in reconstructed heat flux are 5%, 6% and 2% for different voltage and current. It is also found that the present retrieval procedure is a real approach to estimate unknown regulatory parameters for practically filling a wanted output from a given system.

The concept of heat transfer analysis is also applied to retrieve parameters such as perfusion rate to estimate the presence, size, and location in parabolic bioheat transfer problems of brain tissue. The Pennes model is used for the heat transfer and solved by the Finite Element Method as forward problem. The gradient free Differential Evolution is used as the optimization method. The code is run for three times, and each time different combinations of the unknown parameters are found. It is observed that the maximum deviation of temperature field obtained from estimated value of ( $P_1, P_2, P_3, P_4, P_5, P_6$  and  $P_7$ ) from exact ones is found to be 0.008 %.

*Key words:* Non-linear pin fin, heat transfer, forward methods, inverse methods and perfusion rate.

# CONTENTS

---

---

<b>CERTIFICATE</b> .....	<b>i</b>
<b>ACKNOWLEDGEMENTS</b> .....	<b>ii</b>
<b>ABSTRACT</b> .....	<b>iii</b>
<b>CONTENTS</b> .....	<b>v</b>
<b>List of Figures</b> .....	<b>vii</b>
<b>List of Tables</b> .....	<b>x</b>
<b>Nomenclature</b> .....	<b>xi</b>
<b>CHAPTER 1</b> .....	<b>1</b>
<b>INRODUCTION</b> .....	<b>1</b>
1.1. Basics of heat transfer .....	1
1.2. Thermal systems .....	2
1.3. Concept of Inverse problems/methods .....	5
<b>CHAPTER 2</b> .....	<b>8</b>
<b>LITERATURE REVIEW</b> .....	<b>8</b>
2.1. Literature survey of Forward problems in thermal systems.....	8
2.2. Parameter retrieval in thermal systems using Inverse optimization.....	12
2.2.1. Parameter retrieval using gradient-based inverse optimization .....	12
2.2.2. Parameter retrieval using gradient-free inverse optimization methods .....	14
2.3. Summary and research gaps identified .....	20
2.4. Thesis objectives .....	21
<b>CHAPTER 3</b> .....	<b>22</b>
<b>FORMULATION AND SOLUTION METHODOLOGY</b> .....	<b>22</b>
3.1.1. Longitudinal circular pin fin with all temperature dependent thermal parameters .....	22
3.1.2. Estimation of multiple tumor parameter in brain tissue using inverse analysis techniques with Pennes bioheat model. ....	26

3.2. Solution techniques for forward (direct) problems .....	27
3.2.1 Experimental analysis for circular pin fin of brass.....	27
3.2.2. MATLAB’s inbuilt “pdepe” solver for 1-D Problem.....	29
3.2.3. FEM for 1-D bio heat Problem .....	31
3.3. Inverse optimization techniques for retrieving parameters.....	32
3.3.1. Optimization methods .....	32
<b>CHAPTER 4.....</b>	<b>36</b>
<b>RESULT AND DISCUSSION .....</b>	<b>36</b>
4. Forward Results and Inverse Results .....	36
4.1. Forward problem .....	36
4.1.1 Theoretical results.....	36
4.1.2. Experimental Results.....	46
4.2. Comparison of steady-state theoretical and experimental results of Pin fin.....	48
4.3. Retrieval of unknown parameters in thermal systems.....	49
4.3.1. Single parameter retrieval using GSSM (Pin Fin) .....	49
4.4.2. Multiple parameter retrieval using Differential Evolution .....	61
4.5. Estimation of multiple tumor parameter in brain tissue using inverse analysis techniques.....	67
4.5.1. Validation .....	68
4.5.2. Forward results .....	69
4.5.3. Inverse Results .....	70
<b>CHAPTER 5.....</b>	<b>74</b>
<b>CONCLUSION AND FUTURE DIRECTIONS.....</b>	<b>74</b>
5.1. Conclusion.....	74
5.2. Future Direction .....	76
<b>List of Publications .....</b>	<b>77</b>
<b>References.....</b>	<b>78</b>

## List of Figures

---

<b>Figure 1.1.</b> The schematic representation of forward problem.....	3
<b>Figure 1.2.</b> The schematic representation of inverse problem.....	5
<b>Figure 3.1.</b> Schematic of pin fin.....	23
<b>Figure 3.2.</b> Schematic of cancerous brain tissue.....	27
<b>Figure 3.3.</b> Experimental Setup.....	28
<b>Figure 3.4.</b> Schematic of pin fin with thermocouples.....	29
<b>Figure 3.5.</b> Flow chart of FEM.....	31
<b>Figure 3.6.</b> Flow chart for Golden Section Search Method (GSSM).....	33
<b>Figure 3.7.</b> Flow chart of Differential Evolution Algorithm.....	35
<b>Figure 4.1.</b> Validation of present solution methodology of pdepe tool by results with literature; $\beta=0.2, \theta_a=Q=0, N_c=1, N_r=0.2$ .....	37
<b>Figure 4.2.</b> Comparison of steady state temperature distribution for different boundary conditions at tip of the fin (a) different mode of heat transfer both at surface and tip (b) different mode of heat transfer at tip (c) different mode of heat transfer with $n=0 \gamma=0$ .....	40
<b>Figure 4.3.</b> Comparison of non-dimensional temperature ( $\theta$ ) for various values of $N_c$ with $N_r=0.1, n=1, N_{br}=0.002, Bi=0.07, \gamma=0.02, \beta=0.02, \theta_a=0.88, \tau=5$ .....	41
<b>Figure 4.4.</b> Comparison of non-dimensional temperature ( $\theta$ ) for various values of $N_r$ with $N_c$ $=2, n=1, N_{br}=0.002, Bi=0.07, \gamma=0.02, \beta=0.02, \theta_a=0.88, \tau=5$ .....	42
<b>Figure 4.5.</b> Comparison of non-dimensional temperature ( $\theta$ ) for various values of $n$ with $N_r=0.1, N_c=2, N_{br}=0.002, Bi=0.07, \gamma=0.02, \beta=0.02, \theta_a=0.88, \tau=5$ .....	43
<b>Figure 4.6.</b> Comparison of non-dimensional temperature ( $\theta$ ) for various values of $\beta$ with $N_r=0.1, N_c=2, n=1, N_{br}=0.002, \gamma=0.02, Bi=0.07, \theta_a=0.88, \tau=5$ .....	43
<b>Figure 4.7.</b> Comparison of non-dimensional temperature ( $\theta$ ) for various values of $\gamma$ with $N_r=0.1, N_c=2, n=1, N_{br}=0.002, \beta=0.02, Bi=0.07, \theta_a=0.88, \tau=5$ .....	44
<b>Figure 4.8.</b> Comparison of non-dimensional temperature ( $\theta$ ) for various values of $N_{br}$ with $N_r=0.1, N_c=2, n=1, Bi=0.07, \gamma=0.02, \beta=0.02, \theta_a=0.88, \tau=5$ .....	45
<b>Figure 4.9.</b> Comparison of non-dimensional temperature ( $\theta$ ) for various values of $Bi$ with $N_r=0.1, N_c=2, n=1, N_{br}=0.002, \gamma=0.02, \beta=0.02, \theta_a=0.88, \tau=5$ .....	45
<b>Figure 4.10.</b> Transient temperature distribution from experimental setup (a) dimensional temperature and (b) non-dimensional temperature for $V=80$ V and $I=0.027$ A.....	46

<b>Figure 4.11.</b> Transient temperature distribution from experimental setup (a) dimensional temperature and (b) non-dimensional temperature for $V=70$ V and $I=0.022$ A.....	47
<b>Figure 4.12.</b> Transient temperature distribution from experimental setup (a) dimensional temperature and (b) non-dimensional temperature for $V=60$ V and $I=0.018$ A.....	47
<b>Figure 4.13.</b> Transient non-dimensional temperature distribution (a) Experimental setup ( $\tau=2.226$ ). (b) From MATLAB ( $\tau=5$ ) .....	48
<b>Figure 4.14. (a)</b> Temperature distribution with respect to distance, with different time steps. (b) Noisy temperature data with distance, when measurement error of 0%, 1%, 2%, 4%, 5% are added. ....	50
<b>Figure 4.15. (a)</b> Retrieved flux using GSSM, with initial guesses converging towards the retrieved value without measurement error (b) Variation of objective function with number of iterations in GSSM without measurement error. (c) Retrieved flux using GSSM, with initial guesses converging towards the retrieved value, with measurement error of 1%, 2%, 4%, 5% in temperatures. (d) Variation of objective function with number of iterations in GSSM, with measurement error of 1%, 2%, 4%, 5% in temperatures. ....	51
<b>Figure 4.16.</b> Retrieved triangular heat flux (0% error), when exact $\Phi$ in case (b) of Table 4.4 is used in forward analysis.....	54
<b>Figure 4.17.</b> Retrieved triangular heat flux (with 1%, 2%, 4%, 5% error), when exact $\Phi$ in case (b) of Table 4.4 is used in forward analysis.....	54
<b>Figure 4.18.</b> Retrieved realistic heat flux (0% error), when exact $\Phi$ in case (c) of Table 4.4 is used in forward analysis.....	56
<b>Figure 4.19.</b> Retrieved realistic heat flux (with 1%, 2%, 4%, 5% error), when exact $\Phi$ in case (c) of Table 4.4 is used in forward analysis. ....	57
<b>Figure 4.20.</b> Retrieved heat flux when experimental temperature profile is used in the inverse analysis (heat flux is input for longer duration), with error bars indicating uncertainties for different voltage and current. ....	59
<b>Figure 4.21.</b> Variation of estimated unknown parameters; (a) objective function ( $F$ ) (b) heat flux ( $\phi$ ), (c) heat transfer coefficient ( $h$ ), with iterations of DE without measurement error, $e_r=0$ . ....	63
<b>Figure 4.22.</b> Comparison of actual and reconstructed non-dimensional temperature field for cylindrical pin fin, $e_r=0$ .....	64

<b>Figure 4.23.</b> Variation of estimated unknown parameters; (a) objective function ( $F$ ) (b) heat flux ( $\phi$ ), (c) heat transfer coefficient ( $h$ ), with iterations of DE without measurement error, $e_r \neq 0$ .....	66
<b>Figure 4.24.</b> Comparison of actual and reconstructed temperature field of the fin considering the different error, $e_r \neq 0$ . ....	67
<b>Figure 4.25.</b> Comparison of the present result for temperature distribution for single layer normal brain tissue with Das (2013).....	68
<b>Figure 4.26.</b> Comparison of the present result for temperature distribution for multi-layer brain tissue with Das (2013) .....	69
<b>Figure 4.27.</b> Comparison of Temperature distribution in the brain tissue with (a) different boundary with multiple tumor of same size (b) multiple tumor of different size and (c) multiple tumor with different size-location.....	70
<b>Figure 4.28.</b> Comparison of temperature distribution in the brain tissue with and without tumor.....	71
<b>Figure 4.29.</b> (a)Variation of objective function ( $F$ ) with iterations of DE (b) Comparison of estimated and exact values of perfusion rate, $\eta_b$ in 1-D brain tissue.....	73
<b>Figure 4.30.</b> Comparison of actual and reconstructed non-dimensional temperature field for brain tissue. ....	73

## List of Tables

---

---

<b>Table 4.1.</b> Input parameters taken from experimental test rig for forward analysis. ....	38
<b>Table 4.2.</b> Non-dimensional parameters with range based on feasible experimental input and final parameters values used during forward analysis. ....	39
<b>Table 4.3.</b> Relative error in recovered heat flux, with measurement error in temperature, for a case when heat flux is assumed to be constant. ....	52
<b>Table 4.4.</b> Heat flux corresponding to different cases: .....	53
<b>Table 4.5.</b> Relative error in recovered heat flux, with measurement error in temperature, for a case when heat flux is assumed to be triangular. ....	55
<b>Table 4.6.</b> Relative error in recovered heat flux, with measurement error in temperature, for a case when heat flux is assumed to be realistic. ....	58
<b>Table 4.7.</b> Estimated heat flux using the temperatures obtained by experiments during morning ( $M1, M2$ ), afternoon ( $AF1, AF2$ ) and evening ( $E1, E2$ ). ....	60
<b>Table 4.8.</b> Comparison of values for different runs of DE with temperature field of pin fin containing no measurement error, $e_r=0$ .Range: $[\phi, h_b] = [0-10; 2-25]$ ;.....	62
<b>Table 4.9.</b> Comparison of values for different runs of DE with temperature field of pin fin containing measurement error, $e_r \neq 0$ .Range: $[\phi, h_b] = [0-10; 2-25]$ .....	65
<b>Table 4.10.</b> Properties of brain tissue and tumor [57],[41] .....	71
<b>Table 4.11.</b> Comparison of values for different runs of DE with temperature field of pin fin containing no measurement error, $e_r=0$ .Range: $[P_1, P_2, P_3, P_4, P_5, P_6, P_7] = [0.0001-0.01]$ ;..	72

## Nomenclature

---

<b>Symbols</b>	<b>Description</b>
$A$	surface area of the fin, [m <sup>2</sup> ]
$A_{cs}$	cross-sectional area of the fin, [m <sup>2</sup> ]
$Bi$	Biot number
$C_p$	specific heat capacity at constant pressure, [J/kg-K]
$CR$	crossover probability
$d$	diameter of the fin, [m]
$e_r$	error
$F$	objective function.
$h$	convective heat transfer coefficient, [W/(m <sup>2</sup> K)]
$k$	thermal conductivity, [W/(m-K)]
$L$	length of the fin, [m]
$n$	exponent for variable heat transfer coefficient
$N_{br}$	radiation parameter at boundary
$N_c, N_r$	convection, radiation parameter
$P$	perimeter of the fin, [m]
$P_1, P_3, P_5$	perfusion rate of normal tissue, [s <sup>-1</sup> ]
$P_2, P_4$	perfusion rate of tumor, [s <sup>-1</sup> ]
$P_6, P_7$	perfusion rate of bone and scalp, [s <sup>-1</sup> ]
$q$	heat flux [W/m <sup>2</sup> ]
$Q$	heat generation, [W/m <sup>3</sup> ]
$r$	radius of the fin, [m]
$S$	scaling factor
$T$	temperature, [K]
$t$	time, [s]
<b>Greek Symbols</b>	
$\beta$	constant, describing the variation of thermal conductivity
$\gamma$	constant, describing the variation of heat transfer coefficient
$\delta$	the slope of thermal emissivity-temperature curve [K <sup>-1</sup> ]

$\varepsilon$	emissivity
$\eta$	perfusion rate, [s <sup>-1</sup> ]
$\theta$	dimensionless temperature [T/T <sub>b</sub> ]
$\tilde{\theta}$	dimensionless reconstructed temperature,
$\theta_a$	dimensionless ambient temperature [T <sub>a</sub> /T <sub>b</sub> ]
$\xi$	dimensionless length of fin
$\rho$	density, [kg/m]
$\sigma$	Stefan-Boltzmann constant [5.67×10 <sup>-8</sup> W/(m <sup>2</sup> K <sup>4</sup> )]
$\Phi$	dimensionless heat flux
$\lambda$	the slope of thermal conductivity-temperature curve [K <sup>-1</sup> ]
$\tau$	dimensionless time

*Subscript*

$a$	ambient
$b$	base
$bd$	blood
$c$	convection
$m$	metabolism
$r$	radiation
$s$	spatial

# CHAPTER 1

## INRODUCTION

---

---

Heat has always been thought to be something that produces in us a sensation of warmness and one would think that nature of heat is one of the first things understood by manhood. In the nineteenth century, we had a factual physical understanding of the nature of heat. Many practices that occur in nature arbitrarily and without any order are in fact ruled by some noticeable or not so noticeable physical laws. Therefore with the progress in the science and technology the differential equations are used to investigate the wide variety of problems in science and engineering. In the following section heat transfer is explained in complete manner.

### 1.1. Basics of heat transfer

Heat transfer is a process of exchange of thermal energy from higher temperature to lower temperature between two systems or within the systems. There are various ways by which heat is transferred between the systems that are thermal conduction, thermal convection, and radiation. All the techniques have their own phenomena for exchange thermal energy and have their own significance on the system. The extended surfaces are most preferred technique for exchanging or enhancing the thermal energy from one system to another, which are also known as fins [1]. By Newton's law of cooling the heat transfer by convection can be varies by changes the three factors that are temperature gradient between the objects, convection heat transfer coefficient and increasing the surface area of the object. Increasing the temperature gradient is not easy in practical way. In similar way to increase the convection heat transfer coefficient, we should have some external way like fan and etc. but it made the system more complex, bulky and costly, so we have last choice to increase the surface area of the objects that can be easily achieved by using the fins. As the fins are attached to the object which increases the surface area so that more area comes in the contact of the external fluid and more convection take place, it directly increases the heat transfer rate. In most of the applications, such type of heat transfer ways are used in our practical life, as it is economical and simple to use. Fins can be broadly divided as longitudinal fin, radial

fin and Pin fin. There are various applications of the fins in our practical life. Fins are used in the air-cooled I.C. engines [1], [2], refrigeration condenser tubes, automobile radiator, electric transformers, Semiconductor, reciprocating air compressors, heat sinks of laptops/servers and many more. Bioheat transfer in tissue contains heat absorption, heat generation, heat transmission, evaporation, heat radiation, and conduction, etc. It is a very complex procedure which couples with temperature circulation, tissue strain, stress on the tissue and warm harm of tissue. The event of thermal exchange is one of the normally watched marvels running from a straight forward natural action (hypothermia, hyperthermia, digestion and some more) to complex mechanical procedures. Furthermore, regularly these phenomenon are related (change in temperature prompts a change in thickness/focus) and henceforth happen all the while. In addition, the joint investigation of these two phenomenon produces an effective and reasonable examination of frameworks. Scarcely any models where thermal exchange are considered together incorporate drying, evaporative cooling, cooling tower, perspiring, burning of fuel bead and removal cooling of re-emergence vehicles from space.

## **1.2. Thermal systems**

A thermal framework is an unpredictable gathering of coupled parts (some of them thermal), appearing regular organized conduct. For instance, a cooler is a thermal framework which is a blend of channels, blower, electric engine, heat exchangers, valves, protection, packaging, entryways, light, and so on and these segments connect together to accomplish a shared objective of cold generation inside the fridge. The investigation of thermal frameworks is exceptionally testing a direct result of the unpredictable idea of thermal exchange phenomenon along with the nearness of nonlinear terms in the administering conditions because of temperature-subordinate properties of the framework. Like other building subjects, the effect(s) of the thermal exchange phenomenon on a framework can either be contemplated tentatively or scientifically/computationally in the wake of accomplishment administering conditions with the assistance of numerical displaying. The exploratory investigation is the best alternative, yet frequently it isn't possible to lead analyzes under the essential conditions. This might be because of the infeasible trial setup, theoretical framework, related cost, labor and time. In such circumstances, a scientific/computational investigation can be utilized to break down the framework's conduct. The scientific/computational investigation can foresee the framework/item's

conduct before it is really created and exposed to the viable application. Along these lines, from one perspective, scientific/computational examination saves us from really running costly and tedious tests, and, then again, it empowers us to take remedial measures before conclusive advancement of the item. These direct/forward problems have a place with the class of well-presented problems. On the off chance that an issue is well-presented, at that point it is commonly simple to numerically explain it. The odds that the numerical arrangement of a well-presented issue is steady utilizing a stable numerical calculation are very high. Along these lines, direct/forward problems are anything but easy to deal with numerically. The schematic representation of forward problem is presented by a block diagram in Fig. 1.1.

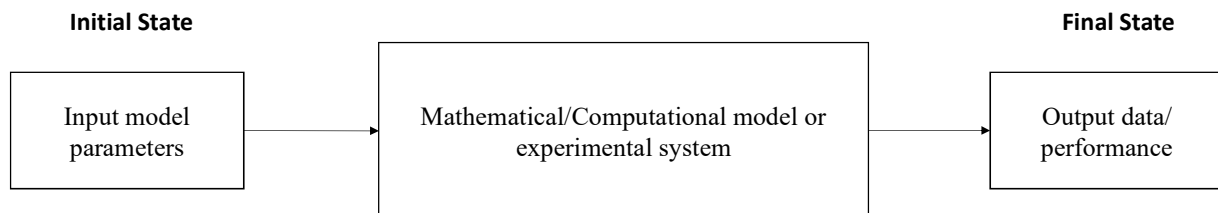


**Figure 1.1.** The schematic representation of forward problem.

The extended surfaces are most preferred technique for exchanging or enhancing the thermal energy from one system to another, which are also known as fins [1]. By Newton's law of cooling the heat transfer by convection can be varies by changes the three factors that are temperature gradient between the objects, convection heat transfer coefficient and increasing the surface area of the object. Increasing the temperature gradient is not easy in practical way. In similar way to increase the convection heat transfer coefficient, we should have some external way like fan and etc. but it made the system more complex, bulky and costly, so we have last choice to increase the surface area of the objects that can be easily achieved by using the fins. As the fins are attached to the object which increases the surface area so that more area comes in the contact of the external fluid and more convection take place, it directly increases the heat transfer rate. In most of the applications, such type of heat transfer ways are used in our practical life, as it is economical and simple to use. Fins can be broadly divided as longitudinal fin, radial fin and Pin fin. There are various applications of the fins in our practical life. Fins are used in the air-cooled I.C.engines [1], [2], refrigeration condenser tubes, automobile radiator, electric transformers, Semiconductor, reciprocating air compressors, heat sinks of laptops/servers and many more. Human body is also act as a thermal system. It produces heat by several biochemical reactions at cellular level, and

preserves its temperature inside a short-range by various thermoregulatory contrivances [3]. Bioheat transfer in tissue contains heat absorption, heat generation, heat transmission, evaporation, heat radiation, and conduction, etc. The heat transfer in alive tissues, known as bioheat transfer, is an intricate phenomenon that depends on the thermodynamics of the organic system, its thermal constitutive constraints and the thermal response to external incitement, e.g., electromagnetic or ultrasonic waves used in cancer treatments. The overall thermal manner of the human body is the united result of heat generation and heat transfer at several scales, the learning of bioheat transfer is especially applicable to the field of thermal medicine, since experimental temperature data is not widely available. Temperature measurement methods are mostly offensive as well as costly and provide a restricted number of measurement points. Every human organ has diverse thermophysical properties, and in nearly all organs and soft tissue (except bones and epidermis) the metabolic heat is formed. The human body in spite of the complex heat transfer processes that happen within it, is kept at a closely constant core temperature, usually between  $36.5^{\circ}\text{C}$  and  $37.1^{\circ}\text{C}$ , by lively thermoregulation. The temperature of the skin depends on the ambient temperature as well as heat transfer by convection and radiation with the environments. Non-invasive temperature measurement methods, such as magnetic resonance thermal imaging, let volumetric temperature measurements. Though, they are limited due to its high cost and low thermal resolution. Some therapeutic applications based on the knowledge of bioheat transfer contain either raising or dropping temperature from normal body temperature, viz., hyperthermia and hypothermia respectively. Hyperthermia may be defined as increasing the temperature of a certain area of the body above normal for a definite period of time, typically between 30 and 90 min. The most common methods to induce hyperthermia are established on heat deposition from electromagnetic or ultrasound sources, where the organic tissues change the immersed energy into heat causing a temperature increase. In 1948, Pennes [4] was the leading to propose and validate experimentally an analytical bioheat transfer model with a heat loss term due to blood perfusion besides perfusion, Pennes' model also accounted for thermal storage, internal and/or external sources caused heat conduction and heat generation. Other accurate bioheat transfer models have been recommended. Though, Pennes' model is the most widely adopted because of simplicity and acceptable accuracy if no large thermally significant blood vessels are close to the analyzed heated region.

### 1.3. Concept of Inverse problems/methods

There are many latest models available for various frameworks for which the reconstructed arrangements exceptionally take after comparing with the experimental measures. In this way, latest models are broadly used to get forward (direct) answers for different sort of physical frameworks/issues as talked about in the above section. Actually, the inverse problems in the physical framework's concern about the recovery of incomprehensible physical parameters, thermal properties, limit conditions, introductory conditions and geometry of that framework for the given yield/execution parameters of the framework. In another manner, we should have suitable data about the forward model of the problem so as to take care of an inverse problem. The inverse problems regularly are not well-presented in the Hadamard's sense [5] of well-posedness. It must to be noticed that among the three states of well-presented problems proposed by

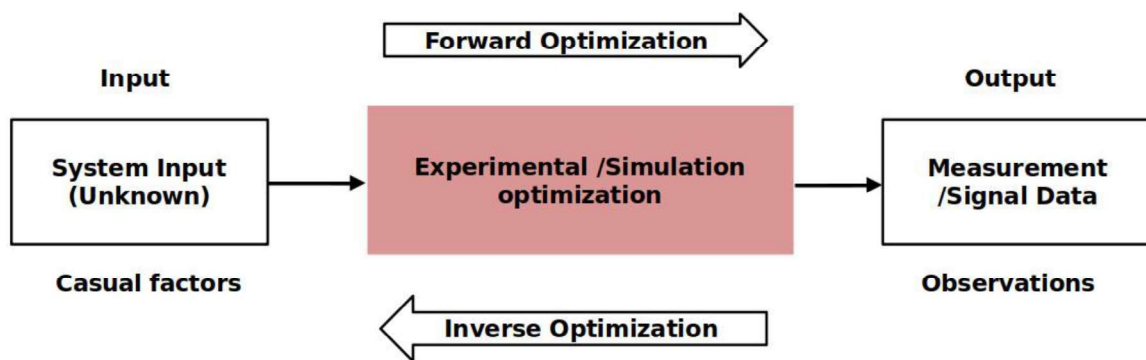


**Figure 1.2.** The schematic representation of inverse problem.

Hadamard's (for example presence, uniqueness, and security), the state of toughness is regularly damaged by opposite problems. In this manner inverse problems are not well-presented problems and thus taking care of the inverse problems numerically is a repetitive task. They are testing in light of the fact that their answers can be hard to accomplish, and when one is discovered it might be infeasible dependent on limitations. Or in other word, inverse problems can't be settled straight away utilizing customary logical or numerical methods. The schematic representation of inverse problem is presented by a block diagram in Fig.1.2.

Scientifically, when we apply a regularization/adjustment system to an inverse problem, a objective is built with the assistance of which, we can acquire the real arrangement of our inverse issue. This target capacity includes the squared distinction among careful and evaluated execution

of the framework. For the minimization of the objective work, improvement strategies are required. By and large, deterministic just as stochastic advancement procedures are utilized to limit the objective work. In this manner, the problem of taking care of an inverse problem is changed over into problem of improving objective work. Inverse also helpful in the bio heat transfer problems also to estimate the perfusion rate, heat generation or any other parameter. It can detect the cancerous affection in any part of the body. The enhancement procedure will keep running over various emphases until the stopping criteria is met. More is the quantity of emphases, increasingly exact is the procedure yet higher is the computational expense. So there is a compromise among exactness and computational expense.

Specific instances of thermal frameworks where the inverse enhancement methods are connected incorporate heaters, chambers for fast thermal handling of semiconductor wafers, utility and compound broilers, metal and glass cooling, infrared heaters, and numerous others. Besides, the converse improvement systems are likewise valuable to recover thermal parameters in broadened surfaces, heat exchangers, and permeable media and so on with conductive, convective and additionally radiative thermal move phenomenon. The traditional optimization techniques are useful in finding the best solution or unrestrained maxima or minima of continuous and differentiable functions. There are two types of optimization methods i.e. deterministic methods and evolutionary methods. A deterministic methods, for which given the same input information will always give the same output information. Deterministic methods includes steepest descent method, conjugate gradient method, Newton Raphson method, quasi-newton method, and Levenberg Marquardt method. Evolutionary algorithms (EAs) are one type of met heuristics that are identified as population, which are basically algorithms where the knowledge comes from interactions between several candidate solutions. Some of the evolutionary algorithms are genetic algorithm, differential algorithm, particle swarm and etc.

Inverse optimization systems are utilized to take care of inverse problems in numerous parts of science and innovation, for example, building applications, arithmetic, therapeutic science, natural science, water contamination, stargazing and some more. There is a wide scope of uses, for example, forecast of land area for groundwater, oil and gas assets, tomography for the reproduction of inner organs, electromagnetic remote detecting, estimation of material properties, and so forth, for which inverse optimization methods are utilized. Some increasingly handy applications where inverse optimization strategies are utilized in thermal frameworks are referenced beneath, these

procedures are utilized to estimate the thermal conductivity of a cooled ingot during steel treating. These systems are utilized for the estimation of thermal contact resistance between two metals during the thermal trade of vitality. In the next chapter of this thesis, the detailed literature survey has been presented.

## CHAPTER 2

### LITERATURE REVIEW

---

---

In almost all the branch of engineering, heat transfer problems are met which cannot be resolved by thermodynamic reasoning alone but need an analysis founded on heat transfer analysis. Many thermal systems like engineering and household appliances are considered on the principles of heat transfer like heating and air conditioning system, refrigerator, computer and etc. The human body is continually rejecting heat to its surroundings and behave as thermal system. As per the literature, wide area of the heat transfer are used by the researcher for the analysis. Many different forward and inverse methods are used to estimate the unknown parameters like thermal conductivity, heat transfer coefficient and etc. The researcher had done analytical, semi-analytical, numerical and experimental study on the fins to understand the thermal analysis of the fins. All the methods have their own significance. As for the study of inverse analysis, there should be a forward method which adopted by the researcher to meet the requirement. Some of the work found in the literature are as discussed to understand the work and advancements made in the inverse work for the estimation.

#### 2.1. Literature survey of Forward problems in thermal systems

The solution of forward problem is obtained by solving the mathematical model in the form of partial differential equation by using suitable numerical or non-numerical technique. By solving the computational modal the solution comes in the form of temperature or some exact solutions or equations. Some of the literature found on the forward problem.

**Donea.**, [6], presented the finite element analysis to solve the non-linear steady state heat transfer problems. The nonlinearity arises due the temperature dependent properties like thermal conductivity and radiation heat transfer take place between parts of the 2-D structure and environment. The researcher had showed the various examples considering various boundary conditions. Kirchhoff's transformation method adopted with the iterations are made to find out the

temperature distribution in two-dimensional structure with temperature-dependent thermal conductivity and radiation.

**Baughan *et al.***, [7], compared the results of the transient method and heated-coating methods for measurement of heat transfer coefficient in a duct. Both the methods impose the isotherm on the surface by employ the liquid crystal. In experimental setup, there is a duct in which diffuser and heater section are divided. Heat transfer results of both the method are found be comparable near the stagnation region but away from the stagnation region, there is some variation fin out due to the boundary conditions. It is found that transient method is very useful for handling of complex problems but heated-coating method is not gives accurate results for complex problem.

**Kiwan and Al-Nimr**, [8], concluded that porous fin has more heat transfer as compared to the conventional fin. The porosity of fin increase the more performance of the fin and also save the material. Finite Element Method is used to solve the governing and boundary equations. The effect of different design and operating parameter are also studied like Darcy number, Ra number and etc. As the value of Ra increases the heat transfer rate is also increasing.

**Coskun and Atay**, [9], implemented the Variational iteration method (VIM) to study the fin efficiency of convective straight fin with temperature-dependent thermal conductivity. As VIM gives the analytical solution of the non-linear problem. Researcher concluded that with the increasing thermal conductivity non-linearity also going to increase. The result of the VIM are compared with the results from the ADM and fund in good agreement. The thermo-geometric parameters also affects the solution of the problem. As it shows more accurate than the Adomian Decomposition Method (ADM), also shows the acceptable results with the non-linearity.

**Singh, Kumar and Kumar**, [10], studied the numerical results obtained for the solution of model related to the diffusion-dispersion during flow through multiparticle system. The MATLAB “pdepe” solver is used to solve the governing partial differential equation. The results obtained from this is comparable with the earlier analytical and numerical work. It shows the better accuracy than other work. This it is conclude that the present method is simple, convenient and elegant to solve the two boundary value problems.

**Wang and Yang**, [11], adopted the Finite element method (FEM) to study the T-shaped fin in 2-D. The study reveals the analysis of heat transfer in the fin. There are some parameters are maintained

to be unknown. The temperature at the root of the fin is also analyzed and error study also done to understand the variation with the incorrect data.

**Moitsheki and Harley**, [12], studied the steady heat transfer through pin fin in 2-D. A constant base temperature is maintained at the base of the fin. The method of separation of variable is adopted for the study of governing equations in linear form. When the equation in the non-linear form symmetry reduction result in construct the number of ordinary equations. Researcher also analyzed the heat flux, fin efficiency, and entropy. The Kirchhoff transformation is applied to linearize the non-linear differential equation and the dynamics of the heat transfer also studied.

**Lin et al.**, [13], Studied the 2-D irregular shape configuration of fin to different boundary value problem. Finite element method and finite difference method is used for the study. The adopted method is also applied on the various fins also to know the effectiveness of the method.

**Singh et al.**, [14], examined the unsteady heat conduction through the short fin by implement the quasi-steady theory and exact solution. Different tip conditions are considered for the analysis. The solution obtained by the quasi-steady solution for shortfin are compared with the exact unsteady solution. There is non-dimensionalized parameter variation with temperature distribution is also made. The results obtained from both the methods are quiet comparable with each other.

**Shah et al.**, [15], investigated the thermal behavior of the cylindrical fin using the Ansys APDL Software. Different materials are taken to study the transient and steady-state analysis. A constant temperature is maintained at the base of the fin and convective boundary is maintained at the top the fin. It is conclude that copper has high heat transfer rate due to the high value of thermal conductivity. The result obtained from the transient analysis are in good agreement with steady-state analysis.

**L.A.**, [16], examined the performance of pin fin by using the pin fin apparatus. He used fin material of different type i.e. brass, copper and aluminium so that it should be comparable. The efficiency of fin for various material is investigated and heat transfer enhancement also take into consideration. A forced convection is utilized for the purpose. Experimental setup consist of a heater input heat flux at one end and other end is kept open, thermocouples are attached on the surface of the pin to collect the temperature. After study the temperature distribution in different type of fin material. Researcher calculate the value of various non- dimensional parameter like

Reynolds number, Nusselts number to find out the heat transfer coefficient and efficiency of the material. As a result, it is found that copper has high thermal conductivity than other two i.e. brass and aluminum.

**Reddy *et al.***, [17], had made the temperature distribution analysis on a composite pin fin by conducting experiments and using FEM on Ansys. The author carried out the experiments to find the temperature distribution in the pin fin made of composite material. There is also numerical study is done by using the ANSYS (FEM) to analysis the steady-state distribution of the pin fin. The experimental results are compared with the results of the simulation in Ansys. Both the results are in good agreement with each other for temperature distribution on the fin tip

**Cui *et al.***, [18], A node-based smoothed finite element method is presented for the smoothed temperature domain and the accuracy of the NS-FEM are examined by the various several numerical examples considering different boundary conditions. The accuracy of the present method is found very high as compared to the traditional FEM and node-based smoothed finite element method NS-FEM.

**Sevilgen**, [19], analyzed the convective straight fin with temperature-dependent thermal conductivity by using CFD and MATLAB. The heat transfer characteristics of straight fin are analyzed by numerical methods. Two different cases are studied having linear and constant thermal conductivity. The CFD results are in good agreement with the result of MATLAB solver. The 1-D and 3-D numerical solution can be easily implement to get combine solutions.

**Jooma and Harley**, [20], analyzed the conductive, convective and radiative porous radial fin with transient condition. Researcher used the Crank-Nicolson finite difference method to solve the model describing the problem of the porous fin with or with incorporating Newton-Raphson method. The results obtained from the CN method are validated with the Differential Transformation Method (DTM). The dynamical system analysis is also done to check the stability of the proposed method.

**Gupta and Singh**, [21], made the analytical thermal analysis on straight triangular fins of steel and aluminium. The linear governing equations and boundary conditions of heat transfer are solved by MATLAB. There are different boundary conditions are made, constant temperature is applied at the base of the fin and fin tip have insulated and convective boundary are applied. The study concludes

that the MATLAB is quite efficient in solve the thermal behavior of the fin. As the value of heat flux and surface area is increases the efficiency and effectiveness of the fin also increases. The heat flow rate in case of aluminium is more than the steel.

**Das and Kundu**, [22], deal with the rectangular fin involving temperature dependent properties considering all modes of heat transfer. The problem is solved by the numerical based Runge-Kutta method of fourth order. The results of the forward method is validated with results available in the literature used methods such as ADM, Galerkin and BVP methods.

Many established methods had used by the researcher to solve the forward problems. The forward problem involving the heat transfer by the fin is solved by the well-known methods like DTM, FEM, FDM, R-K method and experimentally. In the next subsection literature survey on the different type of inverse optimization is discussed.

## **2.2. Parameter retrieval in thermal systems using Inverse optimization**

Many work had done on the estimation of the unknown parameters by using suitable inverse techniques. Some of the techniques found in the literature are as discussed. From forward method, we get the temperature field, which is further used as the input for the inverse technique. The unknown parameters such as thermal conductivity, heat transfer coefficient, internal heat generation and etc. should be retrieved using inverse optimization. The accuracy of inverse methods likely to depend on both forward method and optimization technique selected for the inverse retrieval method.

### **2.2.1. Parameter retrieval using gradient-based inverse optimization**

The gradient-based optimization techniques always gives result of same input as same output. It takes much time to solve the objective function to give as desired maxima or minima. Some of the gradient-based optimization methods used by the researcher for their work found in the literature described as below.

**Chen and Lin**, [23], adopted the hybrid numerical Laplace transform and control volume to estimate the temperature-dependent thermal conductivity and heat capacity simultaneously in the material in 1-D. Thermocouples are used to measure the temperature inside the material. The temperature distribution is obtained from the Laplace transform used as the forward method and these

temperature values are further used as input in the control volume method (inverse method). The result obtained from the present numerical method is found in good agreement with the literature.

**Chen, Chang and Hsu**, [24], estimated the transient heat flux of a pin fin base of 2-D using inverse method. The Direct problem is solved by the finite volume method for obtaining the temperature distribution and for inverse problem conjugate gradient method is used. This method don't need any prior information of the functional form of the unknown parameters. The temperature distribution obtained by the stimulated value of the heat flux is comparable with the temperature distribution obtained by the exact heat flux value.

**Chen, Yang, and Lee**, [25], applied conjugate gradient method on annular fin to estimate the space and time-dependent heat transfer coefficient. The temperature distribution at measuring positions of the fin is obtained by using finite volume method. Conjugate gradient method (CGM) is used for solving the inverse problem. The thermal/mechanical coupling effect also taken in consideration which increases the complexity of the governing equation. The stimulated results are in good agreement with exact value of the temperature distribution on that positions.

**Wang and Yang**, [11], estimated the internal heat generation and root temperature simultaneously of the T-shaped fin. Finite element method is adopted to study the fin in 2-D numerically. The sequential algorithm using finite element method and least square method is used to estimate the internal heat generation. Different type of configuration square configuration, optimal configuration and rectangular. The effect of error is also analyzed. One step estimate is able to find the unknown heat flux of the different configurations.

**Mota *et al.***, [26], applied Bayesian approach to simultaneously estimate the heat capacity, thermal conductivity and heat flux of a non-linear heat conduction problem in 1-D. The Markov chain Monte Carlo method is adopted to solve the inverse problem. Experimental work also did in which a specimen is heated with an oxyacetylene torch. The inverse solution is also applied on the experimental work. Simulated data is used for check the accuracy of the present inverse method.

**Lin *et al.***, [13], proposed the method to estimate the heat flux boundary conditions for the irregular shape of fins. The sensors are used to calculate the temperature at selected locations. The sequential method with the combination of finite element method is used to study the heat flux estimation for the different type of the fins, sensor locations, number of sensors and function of heat flux boundary

also. The error study is also made to estimate the accuracy of the method. The results are also validated.

**Lee *et al.***, [27], applied the inverse heat transfer study on the functionally graded fin to estimate the time-dependent base heat flux. The direct problem is solved by the numerical method of Laplace transformation and finite difference to know the temperature distribution along the locations of the fin. For the inverse method, conjugate gradient method (CGM) is used. The sensitivity and error study is also proposed in the work. It is concluded that no prior information is needed to perform functional form of the unknown quantity to apply inverse algorithm.

**Bamdad *et al.***, [28], applied the gradient-based conjugate gradient method on the rectangular fin considering convective-conductive heat transfer problem. The forward problem is solved by the Lattice Boltzmann Method and the results are validated with the analytical and finite difference method. Further, the inverse algorithm (CGM) is applied to retrieve the unknown boundary heat flux. It is concluded that the conjunction of CGM with LBM gives very much accurate values of the unknown heat flux.

**Chen *et al.***, [29], applied the conjugate gradient method on the irregular fin made up of functionally graded material. The unknown parameter is taken as the base heat flux at three different locations. The accuracy of the inverse method is also analyzed by adding error in the measure temperature. Sensitivity study is also taken, it shows that no prior information is need to retrieve the unknown quantity.

**Huang *et al.***, [30], A fin array is studied in the work using Levenberg-Marquardt method and CFD commercial software to obtain the optimal shape and diameter to satisfy the prescribed temperature profile. The numerical results shows that the height of the fin becomes shorter and diameter increases. The numerical result of the pin fin array are compare with the experimental results of pin fin array and found to be in good agreement with the numerical results.

Basically the many work had done with the Conjugate gradient method to solve the different types of heat transfer problem in fin. More over Levenberg-Marquardt method is also employed for the optimization.

### **2.2.2. Parameter retrieval using gradient-free inverse optimization methods**

Gradient free or evolutionary optimization methods, these methods are gives the global as well as local maxima and minima. Due to gradient free, it optimized the solution in less time as compared to gradient-based methods. Some of the optimization used by the researcher for their work like GA, DE, and etc. found in the literature are described as

**Raudensky et al.**, [31], presented the capability of genetic algorithm used as the inverse algorithm to retrieve the unknown parameters in the one-dimensional heat conduction problem. The forward data used by the inverse method is may be numerically obtained or experimentally. Genetic algorithm is capable of solving the both error-free and noisy data. It is capable of optimized the single parameter retrieval and multi-objective function.

**Babu and Sastry** [32], used the new proposed technique to estimate the effective heat transfer parameter in trickle bed reactor using the combination of orthogonal collocation method and Differential Evolution (DE). The forward results are compared with the radial temperature profile method. The present method take less time to convergence as compared with other techniques without compromising the accuracy of the solutions.

**Chiwiacowsky et al.**, [33], applied the different inverse methods on the 1-D heat conduction problem of slab to estimate the initial condition. The Conjugate gradient method, quasi-newton method and genetic algorithm is applied to minimize the objective function. The problems are considered in the domain of space and time.

**Taler** [34], presented the two method to estimate the heat transfer coefficient in the smooth tube placed in the staggered tube arrangement. The two methods are Levenberg Marquardt method and single decomposition method are used for heat transfer coefficient. The results obtained from the method are in good agreement. The uncertainty is also studied by adding the Gaussian error. The present study demonstrates that no prior data is need about the temperature field in the fluid.

**Copiello and Fabbri** [35], optimized the heat transfer in wavy fin cooled by the laminar flow condition as virtue of forced convection. The forward problem is solved by the finite element method to compute the temperature distribution and velocity. The genetic algorithm is adopted to solve the multi-objective function to maximize the heat transfer and minimize the heat resistance.

**Alghamdi**, [36], developed mathematical model of direct and inverse problem for the flat probe which is subjected to the time-dependent heat flux at one end. Other end is made insulated, the temperature distribution in the probe is obtained by method of variation of parameters. The analytical Levenberg-Marquardt method is used as the inverse approach for the work. Experiments were conducted on the flat probe of stainless steel. Different heat flux profile function is also studied. Thus it is concluded that the estimated heat flux profile is in satisfactory agreement with the exact heat flux profile.

**Mota *et al.***, [26], Markov Chain Monte Carlo Method is used as the forward method to estimation of unknown parameters of skin tumor. Bayesian Framework is used for the estimation of the surface temperature of cancerous portion. The unknowns are thermal conductivity, blood perfusion rate and density and etc.

**Mitra and Balaji**, [37], employed the inverse method to estimate the location and size of the tumor inside the hemispherical breast. Forward problem solved by the finite element based commercial software COMSOL. After that Artificial neural network used to minimize the objective function to get the prescribed temperature field. Two cases are done with internal heat generation and with heat generation. The numerical result and the result obtained from the infrared camera are also compared. The ANN in conjunction with FEM gives very precise accuracy results.

**Das**, [38], applied the inverse problem on the conduction-convection fin with temperature-dependent thermal conductivity to estimate the thermal conductivity and conductive-convective parameters. There are 100 points are taken for the obtaining the temperature distribution. The analytical decomposition method is used as the forward method to find the temperature distribution in the fin. The obtained temperature distribution is further used as the input for the inverse method. The Nelder-Mead simplex search method is used as the inverse method. The results obtained from the inverse method is in quite good agreement with the exact results. The unknown parameters conduction-convection ( $N$ ) and thermal conductivity ( $K$ ) are estimated simultaneously. Multiple combinations of the unknowns' parameters have been found to satisfy the given temperature field. The study of the effect of error, number of measurement points and sensitivity is also done.

**Huang and Chang**, [39], applied the inverse problem on the heat sink modules with encapsulated chip for optimizing design parameters in 3-D. The direct problem is solved by the finite volume method and Levenberg-Marquardt method is adopted for solving inverse problem. Aluminum and

copper heat sinks are compared to find the suitable design of heat sink. It is concluded that larger heat transfer area does not assure better thermal performance. Copper heat sink has better thermal performance due to its high thermal conductivity than the Aluminum heat sink.

**Das**, [40], applied the genetic algorithm (GA) for retrieving the unknown parameters such as thermal conductivity and thermal conductivity in cylindrical fin geometry. Finite difference method is used as forward method to obtain the temperature field from some of the known values. The estimation is done for single and multi-parameters simultaneously. The temperature obtained from the forward method is served as the input for the inverse method (GA), the results of the optimization method observed as the combination of unknown parameters to satisfy the given temperature field. The effect of error on parameters estimation is also studied. It is concluded that the work is useful for selecting the any combination to satisfy the prescribed temperature field.

**Das, Singh and Mishra**, [41], considered 1-D bioheat equation to find out the size and location of the tumor inside the brain and breast. For this Pennes bioheat equation is solved by the Finite Volume Method (FVM), maintain one side adiabatic and other at constant temperature. The results are also validated with the literature and are found in good agreement. The estimation is done for varying the size and location of the tumor and inverse method direct search method gives accurate result. Error study also done to check the accuracy of the applied algorithm conjunction with FVM.

**Das and Ooi**, [42], applied the inverse method to estimate the unknown parameter of rectangular fin having temperature dependent heat transfer coefficient. The unknown parameters are thermal conductivity, heat transfer coefficient and exponent of the heat transfer coefficient. Analytical Adomian decomposition method is used as the forward method to obtain the temperature distribution. Only at three locations on the fin temperature distribution is obtained which is further used in the simulated annealing (SM) as inverse algorithm. Due to the correlated nature of the parameters, many feasible combinations of the unknowns are obtained. It offers the flexibility in selecting the fin material according to the need. This method is suitable where only at discrete points temperature is available, it helps to find the properties of the fin which satisfy the prescribed temperature field.

**Bhowmik et al.**, [43], proposed the use of Adomian decomposition method (ADM) in combination with the differential evolution (DE) to simultaneously estimate the dimensions of hyperbolic and rectangular profile fin. The non-linear governing equation is modeled and the insulated and

convective boundaries are maintained. Heat transfer coefficient and thermal conductivity is maintained temperature dependent. The ADM is used as the direct method to obtain the temperature field along the different profile of fin. The inverse scheme based on the differential evolution, provide the different combinations of the unknowns. Differential evolution is evolutionary method, it takes less computational time and are easily implemented for estimating the multiple unknown parameters. In present study 100 iterations, population size of 30 and cross over ratio,  $CR= 0.9$  and scaling factor,  $S=0.7$  considered. Error study is also done to judge the accuracy of the inverse method. The temperature field obtained from the any of the combination value is satisfy the prescribed temperature filed. Thus researcher concluded that as there is many combinations are obtained so there is more choices to select the parameter of the fin.

**Das**, [44], applied the inverse problem on conductive-convective and radiative cylindrical porous fin. Five unknown parameters are estimated simultaneously by the approach i.e. porosity, emissivity, thermal conductivity, thickness, and permeability. For the solution of direct problem numerical based Rung-Kutta method is adopted for obtaining temperature distribution in the fin. Inverse problem is solved by the hybrid evolutionary-nonlinear programming optimization algorithm (DE-NLP). The results are obtained in the combinations of the parameters which satisfy the prescribed temperature field. Then the effect of error and sensitivity is also done to check the accuracy of this hybrid optimization technique. The result obtained from the inverse method is satisfactory with the exact results. Thus the combination of values of unknown parameters obtained from the method provide an opportunity for selecting the any combination of available material to satisfy the temperature distribution. Thus it is found that the hybrid combination gives more accurate and fast results than individual method.

**Panda et al.**, [45], presents the analytical solution of the rectangular fin to estimate the thermal conductivity and heat transfer coefficient across the fin surface and fin tip. The temperature distribution along the fin is obtained by the homotopy analysis method for insulated and convective fin tip boundary. Genetic algorithm (GA) is used as the inverse method to estimate the unknowns. The solution leads to many feasible combination of the unknown parameters which satisfy the temperature field. It provide the flexibility to select any of the combination of fin materials, fin dimensions, and thermal conditions to achieve the desired heat transfer. It is also investigated that the allowable error is limited to 10%-12% to achieve satisfactory reconstruction of temperature field.

**Das and Mishra**, [46], applied the curve fitting as the inverse method to identify the properties of melanoma of 2-D hemispherical breast. Lower portion of the hemisphere made at constant temperature and upper portion to the convection, sides are insulated. The surface skin temperature are obtained by the Finite Volume Method (FVM) and these temperature is then used for inverse analysis to find out the unknown parameters like blood perfusion rate, size, and location.

**Panda and Das**, [47], estimated the fin dimensions, convective and radiative parameters of radial porous fin. All modes of the heat transfer take place i.e. conduction, convection, and radiation. The temperature distribution along the fin is obtained by finite difference method as forward method. For the solution of inverse problem genetic algorithm (GA) is used which gives results in form of combination of unknown parameters which satisfy the given temperature field. It provides the flexibility to select any of the combination to achieve the heat transfer duty.

Human body is also act as a thermal system. It produces heat by several biochemical reactions at cellular level, and preserves its temperature inside a short-range by various thermoregulatory contrivance. Bioheat transfer in tissue contains heat absorption, heat generation, heat transmission, evaporation, heat radiation, and conduction, etc. Some the work found in the literature done in past years discussed as below

**Bhowmik and Reepaka**, [48], estimated the thermal characteristics of the cancerous tissue inside the skin in 3-D. Three ways of heat transfer take place i.e. convection, radiation, and evaporation. The skin has different type of layers and all have their different properties like perfusion rate, density, and thermal conductivity. The heat transfer in the skin is modeled by Pennes model and solved by the commercial software COMSOL. Two different inverse methods are used i.e. genetic algorithm and simulated annealing. The results of both the methods are within the range as prescribed by us. As in the comparison, the simulated annealing give more accurate results as compared to the genetic algorithm. The unknown parameters, heat transfer coefficient “ $h$ ”, depth of penetration, “ $d$ ”, blood perfusion rate “ $\eta_b$ ” and metabolic heat generation, “ $q$ ” are equivalent to the exact values.

**Agrawal**, [49], estimated the heat flux on a plate having electron beam is act as heating source. The infrared camera is used for obtaining the temperature distribution in the plate due to the heating. The governing equations are solved by the Fourier transformation, Duhamel theorem for direct problem and Newton Leibnitz equation is used for inverse problem. The formulation is done on the MATLAB and the results are validated with the results obtained by the ANSYS. It is concluded that the

experimental temperature obtained from the heating can also use formulation in the MATLAB to perform inverse problem.

**Creence *et al.***, [50], Finite Element Method in combination with Genetic algorithm is used to estimate the blood perfusion rate of the cancerous breast. Three different type of analysis had done i.e. crossover analysis, population size analysis, and heat generation analysis.

**Kumar and Nagarajan**, [51], proposed the method of estimation of unknown boundary heat flux of a fin using Bayesian approach. Experimental setup consist of rectangular mild steel fin and having aluminium base plate. A constant heat flux is provided at the base of the fin. The forward model is studied with the ANSYS and artificial neural network (ANN) to reduce the cost and time. The Markov Chain Monte Carlo algorithm along with Bayesian approach is used for the estimation of heat flux from surrogated data. The sensitivity study of the estimated temperature with the unknown parameters is also done. It is concluded that forward method ANN can reduce the cost and time whereas Bayesian approach provides results in better estimation process and quantifies the uncertainty accurately.

**Bahador, Keshtkar and Zariee**, [52], Studied the numerical and experimental investigation on breast tumor to estimate the parameters by using inverse algorithms. For the solution of forward problem to solve the bioheat equation Finite volume method is used and for the sake of experiment image processing is also done, the temperature calculated from the melanoma body. The numerical results are compared with to validate the formulation and found to be in well agreement. The gradient free genetic algorithm is used for the optimization task. The error between the both the approaches found to be 8-10 % for depth and 0.01-1% for heat generation in the tumor.

In past year, the gradient free methods are used in fast manner, due to the fast computational results. Some of the methods that are used by the researcher to solve the heat transfer problem of fins and bio heat are genetic algorithm, Differential evolution, Golden section search method, ANN and etc.

### **2.3. Summary and research gaps identified**

The literature review depicts the mastery amount of work had done in the field of inverse analysis linked with the heat transfer in fins and bio heat. Many of the traditional as well as latest methods

had used by the researchers to solve the forward as well as inverse problem. By studying all the work following research gaps are identified-

- i. Limited literature is found for the inverse analysis in the solid pin fin using experimental data as forward approach.
- ii. Non-linear analysis of Solid pin fin is limited in the literature with numerical techniques such as FEM, FVM, Runge- kutta method and ADM
- iii. The prediction of the parameters like convection heat transfer coefficient, constant or functional heat flux, thermal conductivity of solid pin fin by using inverse analysis have to be carried out.
- iv. Comparison of result from the Inverse analysis for theoretical and experimental is limited in the literature.
- v. The prediction of multiple tumor using inverse is limited in literature for the brain considering all the layers.

## **2.4. Thesis objectives**

After reading the work done in the field of inverse analysis on heat transfer system like fins and bio heat from literature, books and journals, thesis were decided the following objectives-

- i. Implementation of solution techniques to the heat transfer problems with realistic situation based temperature dependent thermal parameters.
- ii. To estimate the heat flux and convective heat transfer coefficient of fin/extended surface using an inverse method from simulation/experimental noisy data.
- iii. Estimation of multiple tumour parameter in brain tissue using inverse analysis techniques with Pennes bioheat model.

## CHAPTER 3

### FORMULATION AND SOLUTION METHODOLOGY

---

In this section, we consider two problems on heat transfer. The first problem involved circular pin fin of brass having temperature dependent thermal properties. All modes of heat transfer are considered. The second problem is related to bioheat transfer, in which brain tissue has been considered for analyses. As from First law of thermodynamics or law of conservation of energy principle, the energy can neither be created nor be destroyed throughout a process it can only changes from one form to another [1], [2]. Thus the energy balance for any system go through any process may be expressed as the net rise and fall in the total energy of the system throughout a process is equal to the difference among the total energy entering and total energy exit the system throughout that process. Energy can be moved to or from a system by work, heat, and mass flow.

$$E_{in} - E_{out} = E_{system}$$

#### **3.1.1. Longitudinal circular pin fin with all temperature dependent thermal parameters**

In the present work, a cylindrical pin fin with temperature-dependent thermal properties is considered as shown in Figure 3.1. This fin is used to dissipate the heat generated from an electronic device by the mode of conduction, convection, and radiation. One end of the fin is provide with heat flux and another end is subjected to a variety of boundary conditions varying from simplest such as an insulated tip, isothermal boundary, convective tip, radiative tip, to realistic ones such as the combined convective and radiative tip.

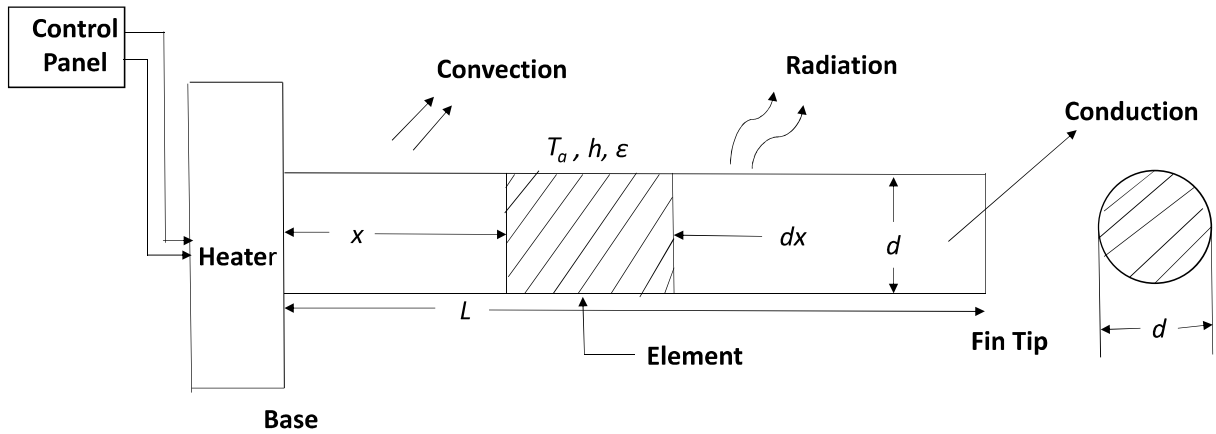


**Figure 3.1.** Schematic of pin fin.

Assumptions made during the analysis are:

1. No heat is generated within the fin.
2. The cross-sectional area of the fin is considered uniform.
3. Heat conduction occurs in one-dimension only.
4. Contact thermal resistance is considered negligible.

The governing equation for the above problem has been derived below by considering a small element in the direction of heat transfer,  $x$  as shown in Figure 3.

According to the Fourier law, the heat conducted into the element at the position  $x$  ( $Q_x$ ) and conducted out at the position  $x+dx$  ( $Q_{x+dx}$ ) are given by the following equations,

$$Q_x = -k(T)A_{cs} \left[ \frac{\partial T}{\partial x} \right]_x \quad (1)$$

$$Q_{x+dx} = -k(T)A_{cs} \left[ \frac{\partial T}{\partial x} \right]_{x+dx} \quad (2)$$

Heat emitting out of the element due to the process of convection and radiation is given by,

$$Q_{conv.} = h(T)P dx(T - T_a) \quad (3)$$

$$Q_{rad} = \epsilon(T)\sigma P dx(T^4 - T_a^4) \quad (4)$$

Energy stored in the element is given by  $\rho c_p A \frac{dT}{dt}$ . An energy balance on the element leads to the following equation

$$Q_x = Q_{(x+dx)} + Q_{conv.} + Q_{rad.} + \rho c_p A \frac{dT}{dt} \quad (5)$$

$$Q_x - Q_{(x+dx)} - Q_{conv.} - Q_{rad.} = \rho c_p A \frac{dT}{dt} \quad (6)$$

$$\frac{\partial}{\partial x} \left( k(T) A_{cs} \left[ \frac{\partial T}{\partial x} \right] \right) - h(T) P(T - T_a) - \varepsilon(T) \sigma P(T^4 - T_a^4) = \rho c_p A \frac{\partial T}{\partial t} \quad (7)$$

Where ' $h(T)$ ' is the non-linear heat transfer coefficient and ' $k(T)$ ' is the temperature-dependent thermal conductivity and ' $\varepsilon(T)$ ' are temperature dependent emissivity which are expressed as

$$k(T) = k_a [1 + \lambda(T - T_a)] \quad (8)$$

$$h(T) = h_b \left( \frac{T - T_a}{T_b - T_a} \right)^n \quad (9)$$

$$\varepsilon(T) = \varepsilon_a [1 + \delta(T - T_a)] \quad (10)$$

Here  $k_a$  is the thermal conductivity at the ambient air temperature of the fin, ' $h_b$ ' is the heat transfer coefficient at the base temperature, and ' $\varepsilon_a$ ' is the emissivity at ambient temperature. ' $\lambda$ ', ' $n$ ' and ' $\delta$ ' are respectively the parameters defining the variation of thermal conductivity, heat transfer coefficient and emissivity with respect to the temperature. The governing equation is associated with left and right tip boundary conditions, where the left one is fixed

$\left( -k(T) A_{cs} \left[ \frac{\partial T}{\partial x} \right]_x = q \text{ at } x = 0 \right)$  and different boundary conditions are imposed at right tip.

Following cases are considered for the right end tip.

**Case-1: Insulated Tip.**

$$-k(T) A_{cs} \left[ \frac{\partial T}{\partial x} \right]_x = 0 \quad x=L \quad (11)$$

**Case-2: Isothermal Tip.**

$$T = T_{tip} \quad x=L \quad (12)$$

**Case-3: Convection Tip.**

$$-k(T)A_{cs} \left[ \frac{\partial T}{\partial x} \right]_x = h(T)A(T - T_a) \quad x=L \quad (13)$$

**Case-4: Radiative Tip**

$$-k(T)A_{cs} \left[ \frac{\partial T}{\partial x} \right]_x = \varepsilon(T)\sigma A(T^4 - T_a^4) \quad x=L \quad (14)$$

**Case-5: Convective and radiative Tip**

$$-k(T)A_{cs} \left[ \frac{\partial T}{\partial x} \right]_x = h(T)A(T - T_a) + \varepsilon(T)\sigma A(T^4 - T_a^4) \quad x=L \quad (15)$$

The above governing equation and: associated the boundary conditions are non-dimensionalized using the following quantities.

$$\theta = \frac{T}{T_b}; \theta_a = \frac{T_a}{T_b}; \quad N_c = \frac{h_b PL^2}{k_a A_{cs}}; \quad \beta = \lambda T_b; \quad \gamma = \delta T_b; \quad N_r = \frac{\varepsilon_o \sigma PL^2 T_b^3}{K_a A_{cs}}; \quad \tau = \frac{k_o t}{L^2 \rho c_p}; \quad \xi = \frac{x}{L};$$

$$Bi = \frac{h_b L}{k_a}; \quad \Phi = \frac{qL}{k_a T_b}; \quad N_{br} = \frac{\varepsilon_o \sigma L T_b^3}{k_a};$$

**Governing equation:-**

$$\frac{\partial}{\partial \xi} \left[ \frac{\partial \theta}{\partial \xi} + \beta \theta \frac{\partial \theta}{\partial \xi} - \beta \theta_a \frac{\partial \theta}{\partial \xi} \right] - N_c \left( \frac{\theta - \theta_a}{1 - \theta_a} \right)^n (\theta - \theta_a) - N_r [1 - \gamma(\theta - \theta_a)] (\theta^4 - \theta_a^4) = \frac{\partial \theta}{\partial \tau} \quad (16)$$

**Dimensionless boundary conditions:**  $-[1 + \beta(\theta - \theta_a)] \frac{\partial \theta}{\partial \xi} = \Phi$  at  $\xi = 0$ , together with

**Case-1: Insulated Tip.**

$$-[1 + \beta(\theta - \theta_a)] \frac{\partial \theta}{\partial \xi} = 0 \quad \xi=1 \quad (17)$$

**Case-2: Isothermal Tip.**

$$\theta = \theta_{ip} \quad \xi=1 \quad (18)$$

**Case-3: Convective Tip.**

$$-[1 + \beta(\theta - \theta_a)] \frac{\partial \theta}{\partial \xi} = Bi.(\theta - \theta_a) \left[ \frac{\theta - \theta_a}{1 - \theta_a} \right]^n \quad \xi=1 \quad (19)$$

**Case-4: Radiative Tip**

$$-[1 + \beta(\theta - \theta_a)] \frac{\partial \theta}{\partial \xi} = N_{br} [(1 - \gamma(\theta - \theta_a))(\theta^4 - \theta_a^4)] \quad \zeta=1 \quad (20)$$

### Case-5: Convective and radiative Tip

$$-[1 + \beta(\theta - \theta_a)] \frac{\partial \theta}{\partial \xi} = Bi.(\theta - \theta_a) \left[ \frac{\theta - \theta_a}{1 - \theta_a} \right]^n + N_{br} [(1 - \gamma(\theta - \theta_a))(\theta^4 - \theta_a^4)] \quad \zeta=1 \quad (21)$$

### 3.1.2. Estimation of multiple tumor parameter in brain tissue using inverse analysis techniques with Pennes bioheat model.

The Pennes bioheat transfer model has been used for guessing temperature distributions in living tissues for more than a half century. The equation was recognized by performing an order of experiments calculating temperatures of arterial blood and tissue in the relaxing human fore arm of helpers and derived a thermal energy conservation equation: the well-known bioheat transfer equation (BHTE). The equation comprises a special term that expresses the heat interchange between blood flow and solid tissues. The blood temperature is supposed to be constant arterial blood temperature. Pennes bio heat equation is considered as the most general equation to describe the thermal equation of tissue matrix. Attention is given to 1-D brain tissue as shown in the Fig. 3.2. The brain is divided into three parts i.e. scalp, bone and brain tissue in which multiple tumor is present. The heat transfer in the living tissue is governed by the Pennes bioheat equation [53],

$$\rho c_p \frac{\partial T}{\partial t} = k \frac{\partial^2 T}{\partial x^2} + \underbrace{\eta_{bd} \rho_{bd} c_{pbd} (T_a - T)}_{\text{Source term}} + Q_m + Q_s \quad (22)$$

Where in the above equation,  $\rho_b$  is the density,  $c_{pb}$  is the specific heat of the blood,  $T_a$  is the arterial blood temperature,  $Q_m$  metabolic heat generation,  $k$  thermal conductivity and  $Q_s$  is the distributed volumetric heat source due to spatial heating. The arterial temperature is maintained as 37°C. The initial condition and boundary conditions are-

$$T_{(x,0)} = 36 \text{ } ^\circ\text{C} \quad (23)$$

$$\left. \frac{\partial T}{\partial t} \right|_{x=0} = 0 \quad (24)$$

$$T|_{x=L} = T_L = 39 \text{ } ^\circ\text{C} \quad (25)$$

$$T|_{x=L} = h(T_a - T) \quad (26)$$

Eqn. (22) represents a transient heat conduction problem. Towards the numerical solution, we follow the procedure of the FEM, which is discussed in next section.

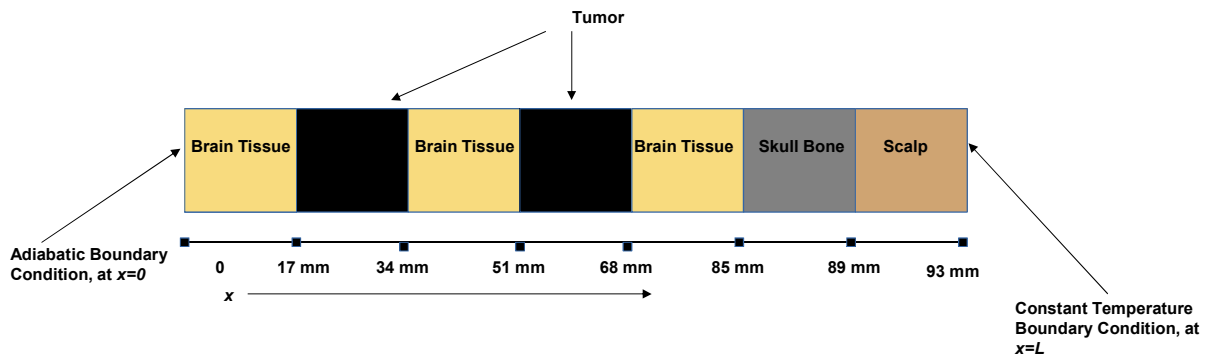


**Figure 3.2.** Schematic of cancerous brain tissue.

### 3.2. Solution techniques for forward (direct) problems

The solution of forward problem or the direct problem is feed to the inverse system so that the new estimated parameters are evaluated and the reconstructed temperature field generated by the new parameters is compared with the direct problem temperature that we get in the form of solution of forward problem. In present study there are two methods are adopted to get the temperature field i.e. experimental, and computational (numerical).

#### 3.2.1 Experimental analysis for circular pin fin of brass.

Experiments were conducted with a cylindrical brass fin, as shown in Fig. 3.3. The apparatus comprised a horizontal 10 mm diameter rod of brass, having 350 mm length. At the interval of 50 mm, eight K-type thermocouples were used to record the surface temperature whereas an additional thermocouple was used for measuring ambient temperature. An electric heater of 240V was connected to one end of a brass rod, which was responsible for generating heat flux with a power of 30 Watts at 240V AC. The other end of the rod was kept open to the environment. This allowed cooling via convection and radiation. Further heat resistant matt black paint was done on the outside of the rod so that emissivity is close to 1. The heat transfer setup consist of the data acquisition system, data logger, and control panel and heat transfer unit. There is voltage regulator on the heat transfer service unit, to control the voltage according to the requirement of the

experiment and three digital display showing value of current, voltage and the temperature of the thermocouples. As the voltage is increases the temperature of the first thermocouple T1 also increases. For different values of heat flux, the temperature profile of the rod had been noted through data logger. Temperature measurements were recorded until the system attained its steady state. The temperatures is noted for different environment condition i.e. morning, afternoon and evening. For the sake of accuracy experiments are done for three times for each case. After completion of experiment, take the readings and switch off the voltage supply. Allow the system to reach ambient condition, before continue with next experiment. The obtained thermal data involved uncertainty due to measurements. The relative uncertainty in the input temperature is 0.0156, with relative uncertainties in voltage ( $V$ ) and current ( $I$ ) being 0.03144 and 0.06542 respectively. To minimize the uncertainty involved, three measurements under the same conditions were recorded, whose average was utilized in the study.

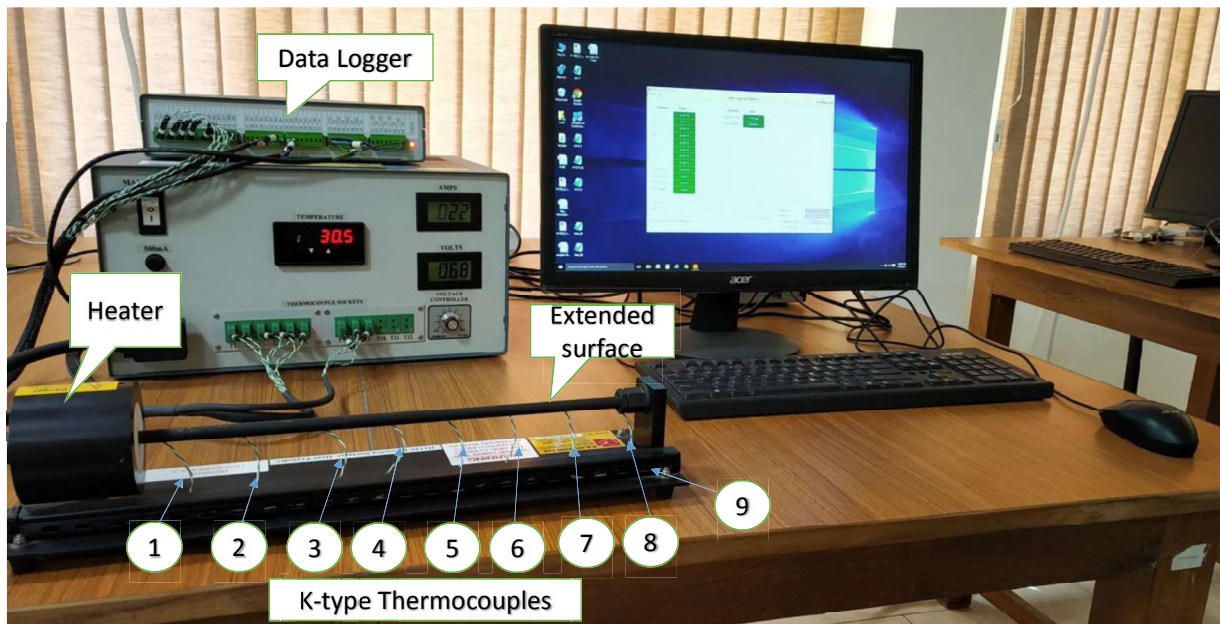


**Figure 3.3.** Experimental Setup.

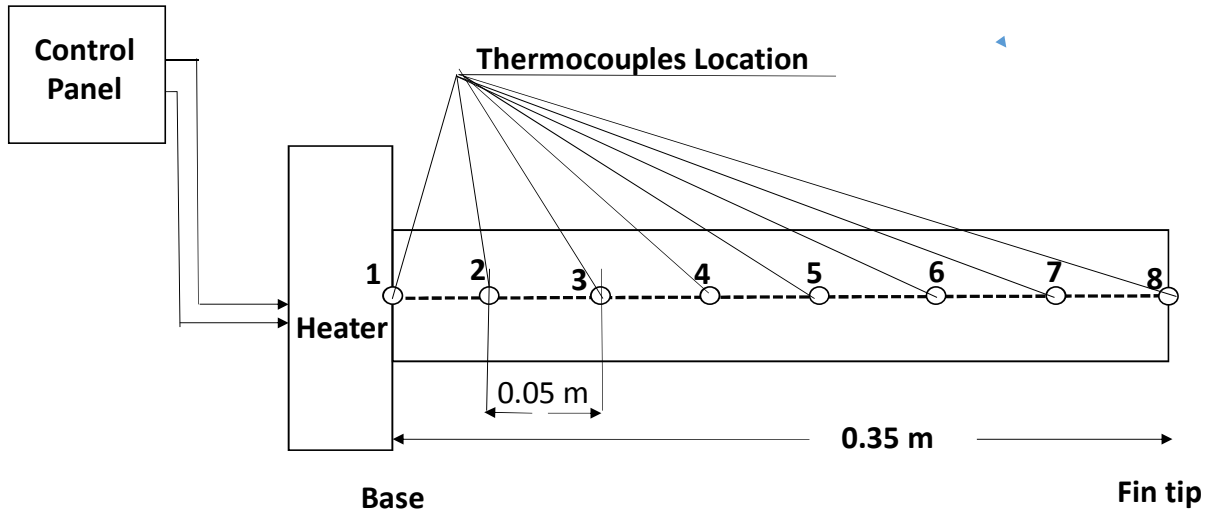


Figure 3.4. Schematic of pin fin with thermocouples.

### 3.2.2. MATLAB's inbuilt "pdepe" solver for 1-D Problem.

MATLAB's inbuilt tool 'pdepe' is used to solve time-dependent partial differential equations (PDEs) of parabolic and elliptic type, which are encountered in many scientific problems. Such a tool converts a PDE into a number of ODEs after space and time discretization. These ODEs are further solved using a time integrating technique.

The detailed implementation steps include:

1. The PDE at hand should be rewritten the following form

$$c\left(x, t, u, \frac{\partial u}{\partial x}\right) \frac{\partial u}{\partial t} = x^{-m} \frac{\partial}{\partial x} \left( x^m f\left(x, t, u, \frac{\partial u}{\partial x}\right) \right) + s\left(x, t, u, \frac{\partial u}{\partial x}\right), \quad t_0 \leq t \leq t_f \text{ \& } a \leq x \leq b \quad (27)$$

where  $m$  can be 0, 1, or 2, corresponding to slab, cylindrical, or spherical symmetry, respectively.

$f\left(x, t, u, \frac{\partial u}{\partial x}\right)$  is the flux term and  $s\left(x, t, u, \frac{\partial u}{\partial x}\right)$  is the source term.

2. An initial condition has to specified which is satisfied at  $t = t_0$  and all  $x$ , given by

$$u(x, t_0) = u_0(x) \quad (28)$$

3. The boundary condition is written in the following form,

$$p(x, t, u) + q(x, t) f\left(x, t, u, \frac{\partial u}{\partial x}\right) = 0, \text{ for all } t \text{ and for } x=a \text{ or } x=b \quad (29)$$

4. Next, three function files containing  $c, f, s$  and  $u_0$  and  $p, q$  are created ( `pdex1pde`, `pdex1ic`, `pdex1pbc` can be referred in the Matlab code given in the appendix).

5. Mesh for  $x$  and  $t$  (using `linspace` Matlab function) is created and `pdepe` is called in the command window as `sol = pdepe(m,@pdex1pde,@pdex1ic,@pdex1bc,xi,tau);`

6. The solutions are then plotted for post-processing.

For our research work, we have to use `Pdepe` to solve equation (16) for  $0 \leq \xi \leq 1$  for times  $\tau \geq 0$ .

0. Comparing equation (16) and (27), we get the following

$$\begin{aligned}
 m &= 0 \\
 f &= \left[ \frac{\partial \theta}{\partial \xi} + \beta \theta \frac{\partial \theta}{\partial \xi} - \beta \theta_a \frac{\partial \theta}{\partial \xi} \right] \\
 s &= -N_c \left( \frac{\theta - \theta_a}{1 - \theta_a} \right)^n (\theta - \theta_a) - N_r \left[ 1 - \gamma(\theta - \theta_a) \right] (\theta^4 - \theta_a^4) \\
 c &= 1
 \end{aligned}$$

The PDE satisfies the initial condition  $\theta(x, 0) = 0.88$  for all  $x$ . By comparing the value of left side

boundary condition  $-[1 + \beta(\theta - \theta_a)] \frac{\partial \theta}{\partial \xi} = \Phi$  at  $\xi = 0$  with the equation (29), we get  $pl = \Phi$  and

$ql = 1$ . Further, comparing equations (17-21), with equation (29), we get the following functions  $p$  and  $q$  for the right tip:

**Case-1: Insulated Tip**

$$pr=0 \qquad qr=1 \qquad (30)$$

**Case-2: Isothermal Tip**

$$pr = \theta - \theta_{tip} \Big|_{\xi=1} \qquad qr=0 \qquad (31)$$

**Case-3: Convection Tip.**

$$pr = Bi.(\theta - \theta_a) \left[ \frac{\theta - \theta_a}{1 - \theta_a} \right]^n \Big|_{\xi=1} \qquad qr=1 \qquad (32)$$

**Case-4: Radiative Tip.**

$$pr = N_{br} \left[ (1 - \gamma(\theta - \theta_a)) (\theta^4 - \theta_a^4) \right] \Big|_{\xi=1} \qquad qr=1 \qquad (33)$$

**Case-5: Convective and radiative Tip.**

$$pr = Bi.(\theta - \theta_a) \left[ \frac{\theta - \theta_a}{1 - \theta_a} \right]^n + N_{br} \left[ (1 - \gamma(\theta - \theta_a)) (\theta^4 - \theta_a^4) \right] \Big|_{\xi=1} \qquad qr=1 \qquad (34)$$

### 3.2.3. FEM for 1-D bio heat Problem

The Finite Element Method (FEM) is a numerical tool used for solving problems of mathematical problems and engineering in the fields of heat transfer, fluid flow, structural analysis, mass transport. The analytical solution of these difficulties generally need the solution to boundary value difficulties for partial differential equations. A system of algebraic equations is made by the formulation of FEM problems. In FEM, the complex shape of the module is split into minor units called elements. The simple equations that model these finite elements are then gathered into a bigger system of equations that models the entire problem. We used the FEM simulation tool to resolve the mathematical model with the initial and boundary conditions, and offer results. The forward part of the problem involved the numerical simulation of heat transfer phenomena in a cancerous brain by using the Pennes bioheat transfer equation using FEM. The Equation (22) was spatially discretized by the FEM. Once Equation (22) is discretized by the FEM, a system of the form rises

$$[K][T]=[F]$$

$K$ =Property, (Stiffness, conductivity and viscosity and etc.)

$T$ =Behavior, (Displacement, temperature, velocity, electric potential and etc.)

$F$ =Action, (Force, heat source, charge and etc.)

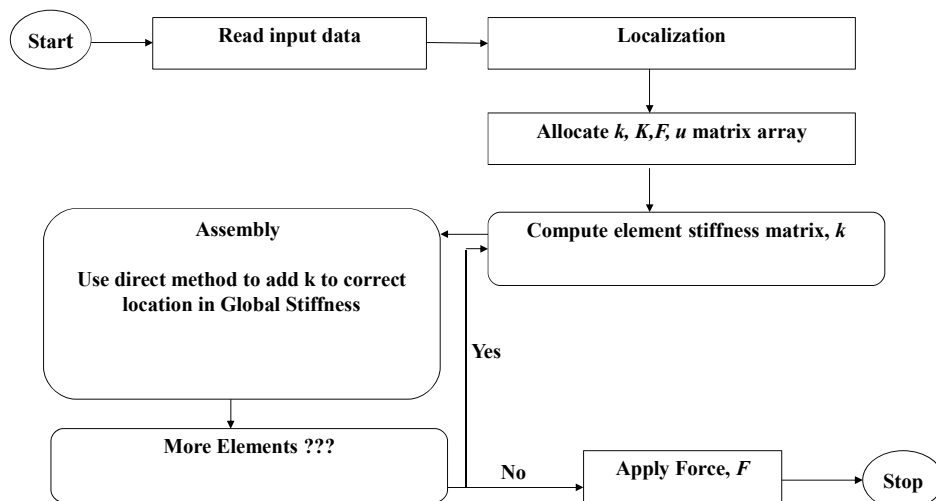


Figure 3.5. Flow chart of FEM.

### **3.3. Inverse optimization techniques for retrieving parameters**

An inverse analysis in science is the process of calculating the causal factors from set of observations that produced them. The obtainable literatures show that most of the studies on solid pin fins are aimed at manipulative the steady-state temperature distributions from the information of thermo-physical properties using suitable boundary conditions of the fin. One of the methods of attaining the temperature profile is to perform an experiment by keeping proper boundary conditions. But the experimental procedure takes long time for the analysis/results, so for the sake of saving the time, money and manpower, a computational study is desirable. In order to computationally attain the wanted task, the governing heat transfer equation desires to be solved by using a suitable method employing known thermo-physical properties and boundary conditions.

#### **3.3.1. Optimization methods**

The traditional optimization methods are useful in detecting the best solution or unrestrained maxima or minima of continuous and differentiable functions. There are two types of optimization methods i.e. deterministic methods and evolutionary methods. A deterministic methods, for which given the same input information will always give the same output information. Deterministic methods includes Newton Raphson method, steepest descent method, conjugate gradient method, Levenberg Marquardt method and quasi-newton method, and. Evolutionary algorithms (EAs) are one type of met heuristics that are identified as population, which are basically algorithms where the knowledge comes from interactions between several candidate solutions. In the instance of EAs, besides applying agitations to solutions (mutation), they also generate novel solutions from recombination of present ones (crossover). Some of the evolutionary algorithms are genetic algorithm, differential algorithm, particle swarm and etc.

##### **3.3.1.1. Golden section search method**

In the current work, GSSM is used as one variable search technique to optimize the given objective function by iteratively shrinking the guessed range. GSSM was proposed by Kiefer [54] and is a variant of Fibonacci search method. The simplest method of its kind, GSSM does not require gradient calculations, hence reduces the computational cost significantly. The method converges fast as it optimizes using direct search approach.

The method starts by describing an initial guessed range ( $\phi_{max} - \phi_{min}$ ). The algorithm then refines the guesses as

$$a = \phi_{min} + (1-r)(\phi_{max} - \phi_{min})$$

$$b = \phi_{max} - (1-r)(\phi_{max} - \phi_{min})$$

Where  $r = \frac{\sqrt{5}-1}{2} = 0.618$  satisfying the property,  $r = \frac{1}{1+r}$  here 'r' is called inverse golden

number, which is responsible for deriving the name of the method. These new points  $a, b$ , are at a distance of 'r' from the original  $\phi_{max}, \phi_{min}$ . The objective function is then calculated for  $a, b$  using objective function equation, as  $f(a), f(b)$ . If  $f(a) < f(b)$ , then discard interval to right of b, i.e., keep  $\phi_{max} = \phi_{min}$  and  $\phi_{max} = b$ , otherwise  $\phi_{max} = \phi_{min}$  and  $\phi_{min} = a$ , in the next iteration. The interval then reduces to  $[\phi_{max}, b]$  or  $[a, \phi_{max}]$  respectively. The whole point of doing this lies in the fact that while reducing the interval to achieve a minimum objective, the ratio, often called reduction ratio,  $\frac{\phi_{max} - \phi_{min}}{b - \phi_{min}}$  and  $\frac{\phi_{max} - \phi_{min}}{\phi_{max} - a}$  remains 1.618, which is the golden number. The iterations above are continued until a fixed number of iterations are crossed or the objective function achieves a sufficiently small value.

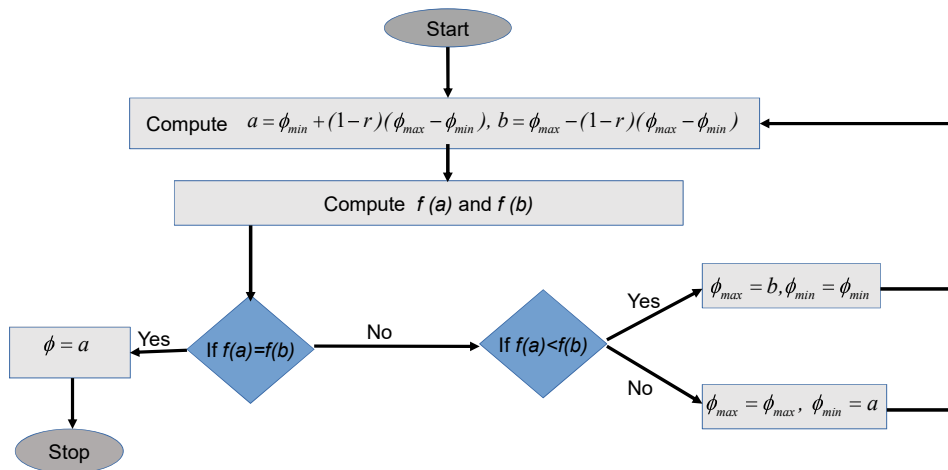


**Figure 3.6.** Flow chart for Golden Section Search Method (GSSM).

### **3.3.1.2. Differential evolution algorithm**

Differential evolution is gradient free algorithm, thus they even applied for objective function which are difficult to differentiate. The differential evolution method is a vigorous and simple search optimization method for estimation of multi-objective function [55]. DE is the mutation scheme that makes DE self-adaptive and the selection process. In DE, all results have the same chance of being nominated as parents without requirement of their fitness value. DE works on a greedy choice process. DE algorithm is a stochastic optimization method reducing an objective function that can model the problem's objectives while including constraints. The process mainly has three benefits; fast convergence, finding the true global least irrespective of the initial parameter values, and using a few regulator parameters. Being easy to use, fast and simple, very easily adjustable for integer and discrete optimization, quite operative in nonlinear constraint. Optimization together with penalty functions and beneficial for optimizing multi-modal exploration spaces are the extra important features of DE. The DE algorithm is a population based algorithm like genetic algorithms by means of the like operators; mutation, crossover and selection. The main alteration in creating better solutions is that genetic algorithms depend on crossover while DE depend on mutation operation. The algorithm uses mutation operation as exploration mechanism and choice operation to direct the exploration toward the particular regions in the search space. The DE algorithm also uses a non-uniform crossover that can take child vector constraints from one parent more often than it does from others. By means of the components of the present population members to build trial vectors, the recombination (crossover) operator professionally shuffles data about effective combinations, permitting the search for a better solution space.

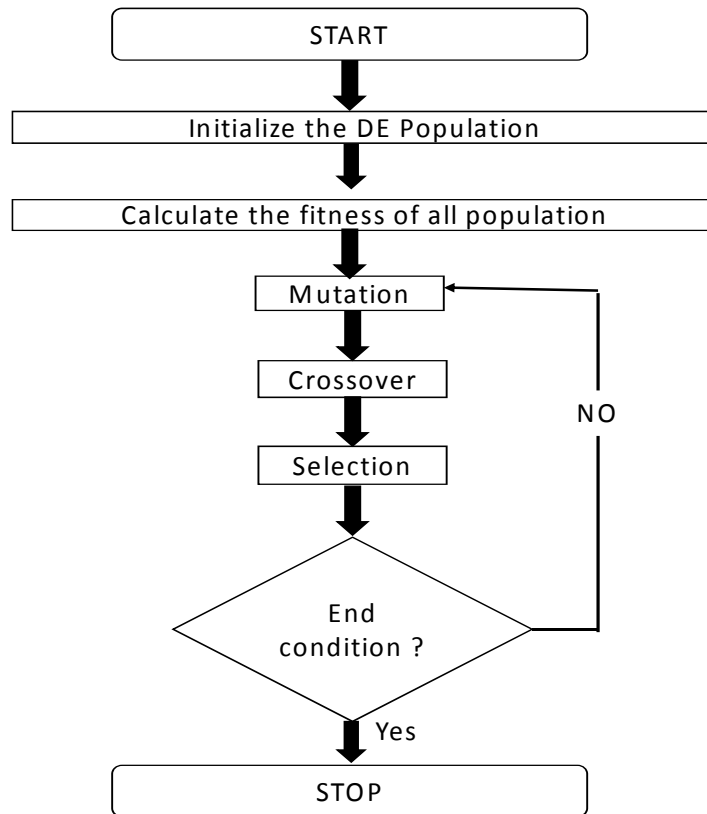


**Figure 3.7.** Flow chart of Differential Evolution Algorithm

#### 4. Forward Results and Inverse Results

Two heat transfer problems are taken for the analyses. The first problem involved circular pin fin of brass having temperature dependent thermal properties. The second problem is related to bioheat transfer, in which brain tissue has been considered for analyses. The MATLAB's pdepe solver is used to solve the forward heat transfer problem in the fin case. The bio heat transfer related problem is firstly solved by the pdepe for the single layer, but on addition of multiple layer the pdepe tool is unable to solve the interface boundary condition problem. In order to resolve the problem Finite element method is adopted to solve multi-layer problem in bio heat transfer. After getting the forward results for above discussed problem, inverse method is adopted for each case. The results of the forward and inverse methods are discussed in the next sub section for both the problems.

#### 4.1. Forward problem

This section describes the forward results obtained by employing the forward method on the pin fin problem.

##### 4.1.1 Theoretical results

The solution of governing equation (16) of circular pin fin with various boundary conditions (17-21) were obtained using MATLAB based pdepe tool. The obtained results i.e. temperature distribution are compared with literature for a simplest case without internal heat generation, insulated and constant temperature tip conditions. Further, the comparison was presented in Fig. 4.1. and found to well in agreement with the results obtained in [22] literature by RK-4 for conductive–convective and radiative fin at  $\beta=0.2$ ,  $\theta_a=Q=0$ ,  $N_c=1$ ,  $N_r=0.2$ .

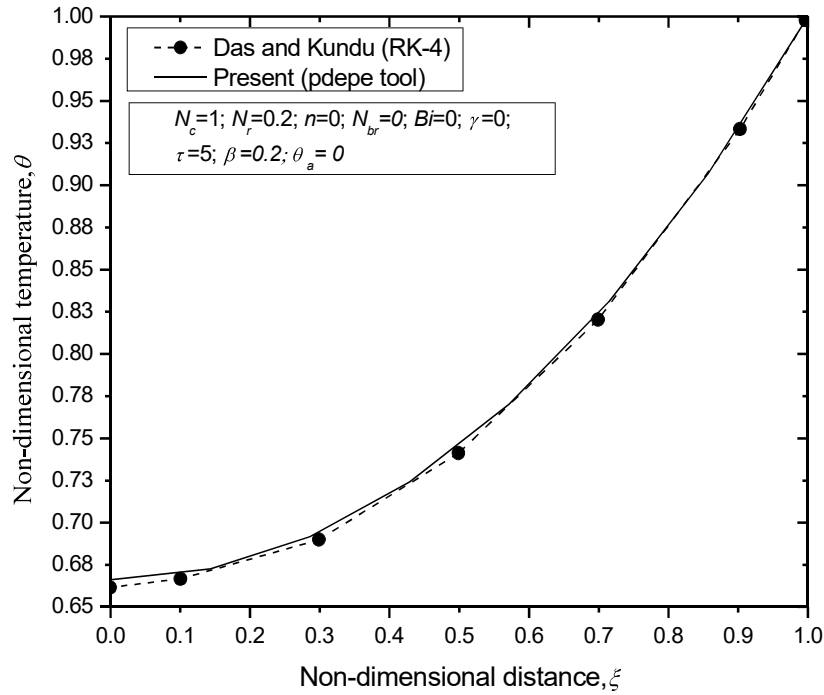


**Figure 4.1.** Validation of present solution methodology of pdepe tool by results with literature;  $\beta=0.2$ ,  $\theta_a=Q=0$ ,  $N_c=1$ ,  $N_r=0.2$ .

The different values of non-dimensional entities ( $N_c$ ,  $N_r$ ,  $n$ ,  $\theta_a$ ,  $\beta$ ,  $\gamma$ ,  $Bi$  and  $N_{br}$ ) considered in the forward method based on the experimental measurements for test rig as shown in Figure 3.1. The measured experimental parameters are presented in Table 4.1. These values are further used to consider feasible non-dimensional parameters for forward analysis along with the range of few assumed parameters as mentioned in Table 4.2. Based on the above-selected parameters, the solution i.e., temperature distribution was obtained using numerical technique as discussed in solution methodology. The forward analysis was conducted for the nonlinear heat transfer problem with all temperature dependent thermos-physical parameters. In the present research work, the boundary conditions have been considered from simplest (Insulated tip) to most critical one (Simultaneous convective and radiative tip). This Work discusses two major points, one the variation of different modes of heat transfer on the temperature distribution either on surface or tip of the extended surface and secondly above the variation of parameters on the temperature distribution.

**Table 4.1.** Input parameters taken from experimental test rig for forward analysis.

Property	Value
Brass fin density, $\rho$	8520 kg/m <sup>3</sup>
Specific heat at constant pressure of the fin, $c_p$	375 J/kg-K
The thermal conductivity of the fin, $k$	121 W/m-K
Base temperature, $T_b$	298 K
Ambient Temperature, $T_a$	295 K
Length of the fin, $L$	0.35 m
Diameter of fin, $d$	0.01 m
Material of the fin	Brass
Active cross-sectional area, $A$	$7.854 \times 10^{-5}$ m <sup>2</sup>
Perimeter of fin, $P$	0.0314 m

In the first part, the mode of heat transfer varies to analyze the performance via temperature. As in Figure 4.2 (a), the case with radiation mode having maximum temperature as compare to other cases such as convective, convective and radiative. It is found because of the less value of the non-dimensional parameter  $Nr$ , which was determined from experimental setup and unavailability of convection term in governing equation, (16). It means that the more heat transfer occurs from only convective case and then convective-radiative case both at surface and tip of the fin as compare to the radiative case. The inconsistency comes in the insulated case, as in this case both the convection and radiation term take place from surface (in governing equation) so that due the availability of ‘n’ more heat transfer take place at surface and the no heat transfer at tip. The constant temperature at tip condition is an independent case and found less temperature profile as  $\theta_{\xi=1} = 1$  was considered.

**Table 4.2.** Non-dimensional parameters with range based on feasible experimental input and final parameters values used during forward analysis.

Range	values
$3 \leq h_b \leq 25$	$h_b = 5$
$0 \leq \varepsilon_o \leq 1$	$\varepsilon_o = 0.95$
$1.3 \leq N_c \leq 10$	$N_c = 2$
$0.1 \leq N_r \leq 0.5$	$N_r = 0.1$
$0.001 \leq N_{br} \leq 0.004$	$N_{br} = 0.002$
$0.0086 \leq Bi \leq 0.07$ -	$Bi = 0.07$
$\beta$	0.02
$\tau$	0.02
Time step, $d\tau$	0.4167
Grid size, $d\zeta$	0.1429
Final time, $\tau$	5

In Figure 4.2(b), it is considered that the heat transfer occurs by all mode on the surface and tips conditions various and the possible comparisons has been presented. It is found from Figure 4.2(b) that the convective tip condition has higher temperature followed by the others but it is not acceptable in real phenomena of heat transfer. The temperature profile of insulated tip condition should have the maximum temperature profile but it is found that the convective heat transfer decreases at the tip with the temperature dependent heat transfer coefficient i.e. due of 'n' value. As 'n' temperature dependent heat transfer constant take place in both governing and boundary so that it made opposite effects on tip surface. On surface, it increases the heat transfer but at tip or boundary, it decreases the heat transfer so that our trend might be in different order but these trends are very much correct. In

order to validate these trends, a case has been considered with constant heat transfer coefficient and constant emissivity i.e.  $n = 0$  and  $\gamma = 0$ .

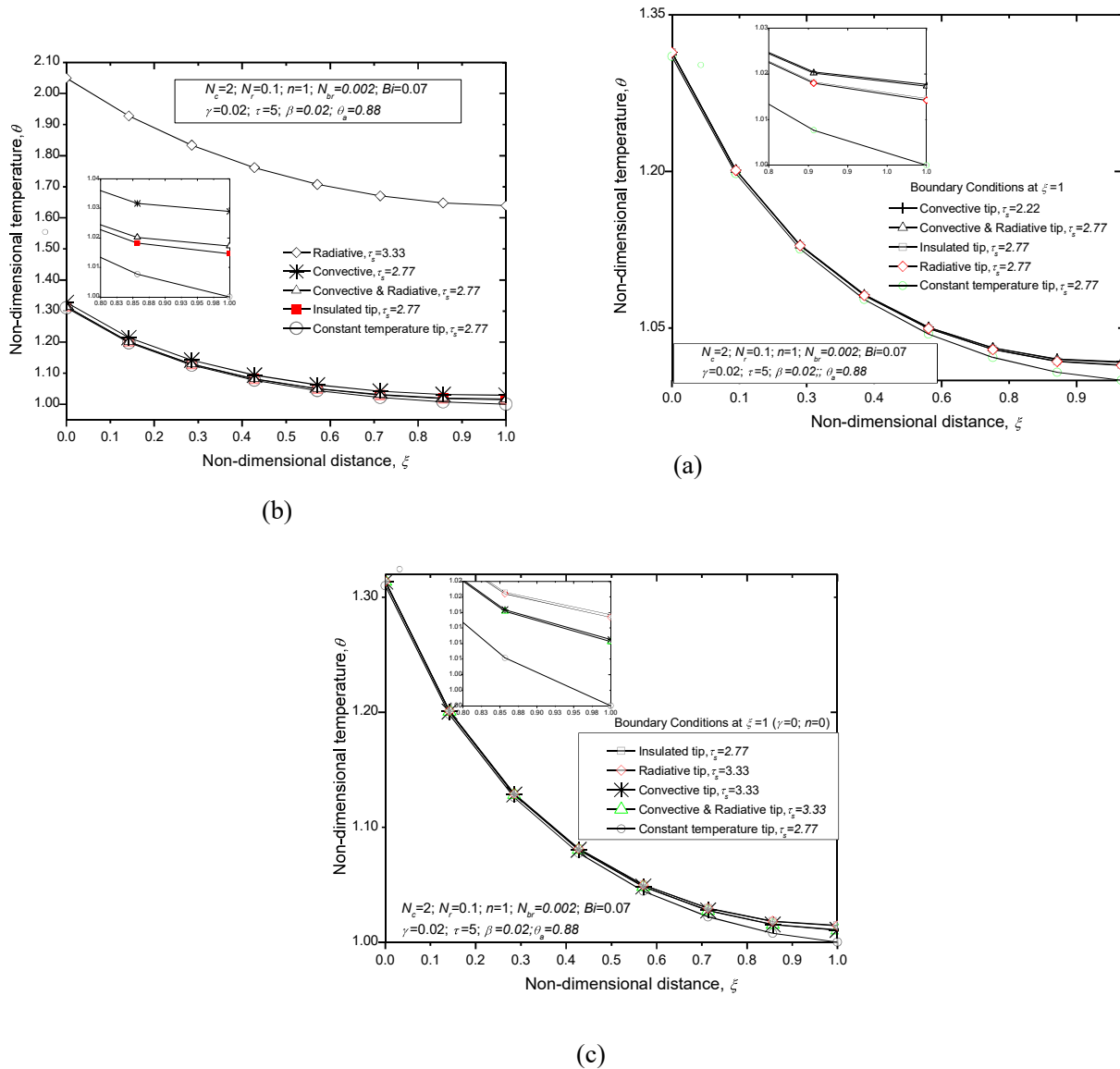


**Figure 4.2.** Comparison of steady state temperature distribution for different boundary conditions at tip of the fin (a) different mode of heat transfer both at surface and tip ( b) at tip (c) with  $n=0$  and  $\gamma=0$

As shown in Figure 4.2(c), the trends of temperature distribution found to be in right sequence by the actual theoretical phenomena. Insulated tip having maximum temperature followed by radiative tip than convective tip and last combined effect of radiation and convection on the tip. This leads us to say that our approach and code is very much correct to move to the next part of

this research work i.e. parametric study of individual parameter on performance in terms of temperature distribution.

A consideration of Figure 4.3. represents the effect of conduction-convection parameter,  $N_c$  on the temperature distribution in the fin. As the value of  $N_c$  increases, the local temperature in the fin decreases.

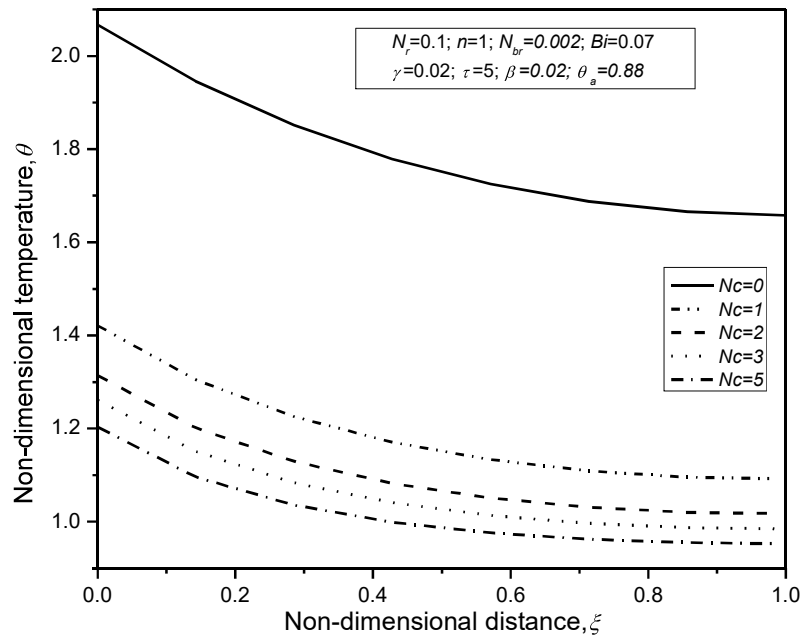


**Figure 4.3.** Comparison of non-dimensional temperature ( $\theta$ ) for various values of  $N_c$  with  $N_r=0.1$ ,  $n=1$ ,  $N_{br}=0.002$ ,  $Bi=0.07$ ,  $\gamma=0.02$ ,  $\beta=0.02$ ,  $\theta_a=0.88$ ,  $\tau=5$

As the convection takes place by the buoyancy forces which are encouraged by the density difference between both the fluids. It shows that the higher value of  $N_c$  have more heat transfer rate which leads to decrease of temperature distribution. Next, the effect of conduction-radiation parameter,  $N_r$  has been discussed in Figure 4.4. on temperature distribution. The influence of conduction-radiation parameter,  $N_r$  leads to decrease the temperature profile with the increase of parameter, which is the very much intuitive to understand as discussed in Figure 4.4.

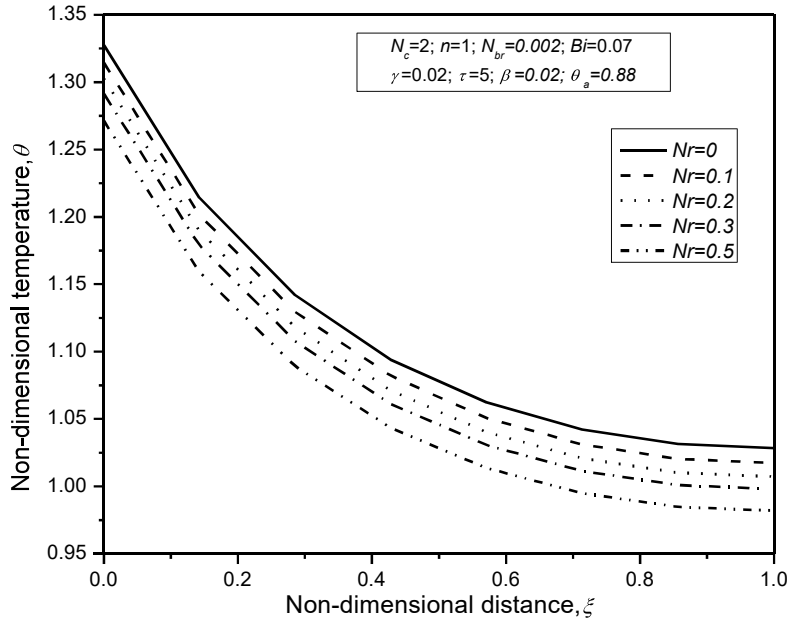


**Figure 4.4.** Comparison of non-dimensional temperature ( $\theta$ ) for various values of  $N_r$  with  $N_c = 2$ ,  $n = 1$ ,  $N_{br} = 0.002$ ,  $Bi = 0.07$ ,  $\gamma = 0.02$ ,  $\beta = 0.02$ ,  $\theta_a = 0.88$ ,  $\tau = 5$ .

It is clear from Figure 4.3 and 4.4 that the conductive-convection parameter and conduction-radiation parameter leads to increase heat transfer rate as it increases.

Next, the results and discussion are presented for the all the temperature-dependent parameters such as exponent of variable heat transfer coefficient,  $n$  (Figure 4.5), temperature-dependent thermal conductivity parameters,  $\beta$  (Figure 4.6), and temperature dependent radiative parameter,  $\gamma$  (Figure 4.7). The overall impact of exponent of variable heat transfer coefficient,  $n$  has been investigated and found that the rate of heat transfer increases as  $n$  value increases as shown in Figure 4.5. It is because of increasing heat transfer coefficient,  $h$ , with increase of temperature. Moreover, it is found that the effect of temperature dependent parameter of thermal conductivity and emissivity are insignificant in the present work as shown in Figure 4.6 and 4.7. It concludes that the effect of temperature-dependent heat transfer coefficient is very important both at surface and tip of fin in the present work.

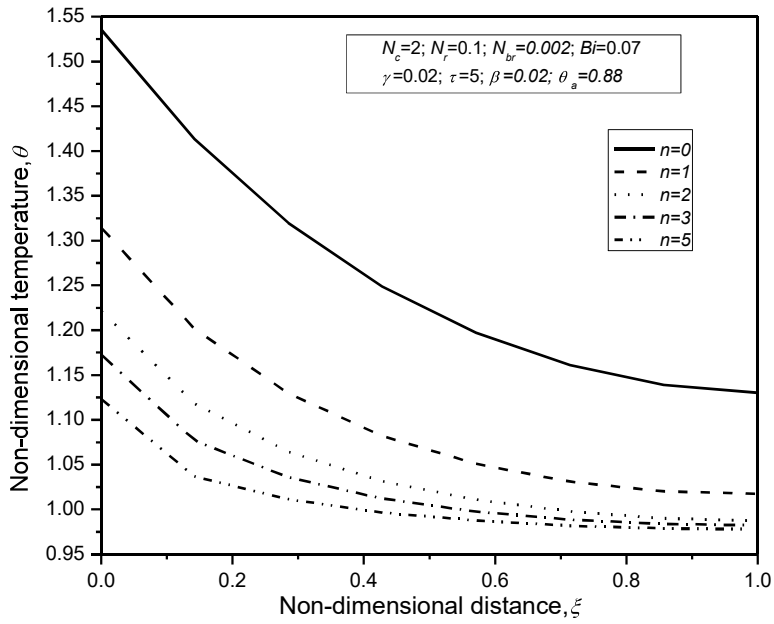


**Figure 4.5.** Comparison of non-dimensional temperature ( $\theta$ ) for various values of  $n$  with  $N_r=0.1$ ,  $N_c=2$ ,  $N_{br}=0.002$ ,  $Bi=0.07$ ,  $\gamma=0.02$ ,  $\beta=0.02$ ,  $\theta_a=0.88$ ,  $\tau=5$ .

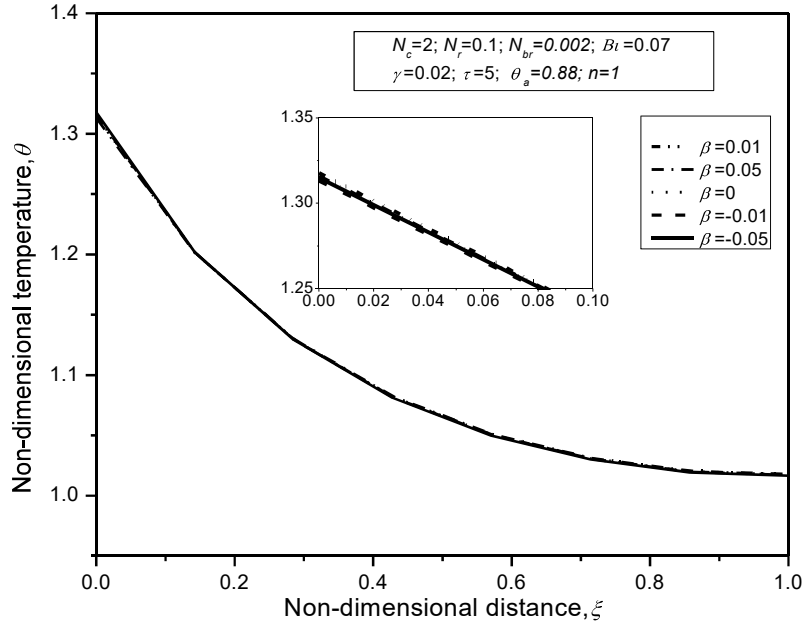


**Figure 4.6.** Comparison of non-dimensional temperature ( $\theta$ ) for various values of  $\beta$  with  $N_r=0.1$ ,  $N_c=2$ ,  $n=1$ ,  $N_{br}=0.002$ ,  $\gamma=0.02$ ,  $Bi=0.07$ ,  $\theta_a=0.88$ ,  $\tau=5$ .

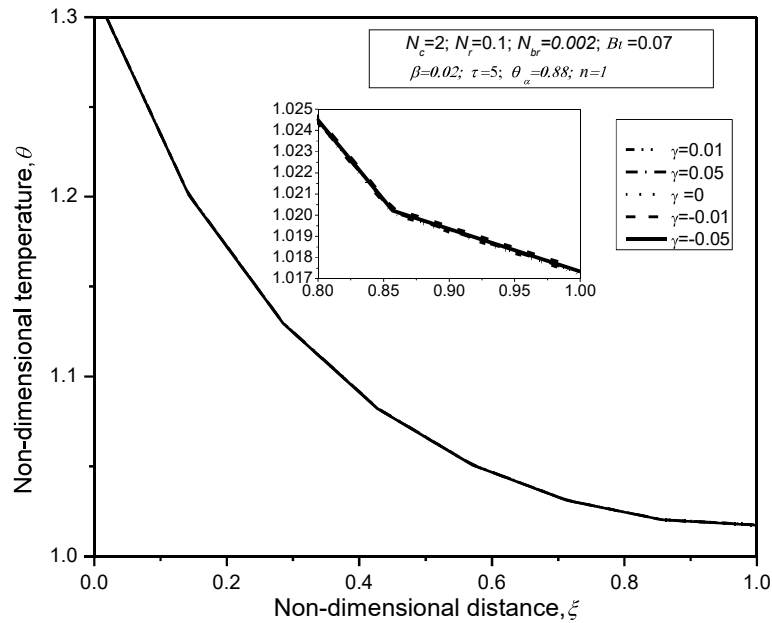


**Figure 4.7.** Comparison of non-dimensional temperature ( $\theta$ ) for various values of  $\gamma$  with  $N_r=0.1$ ,  $N_c=2$ ,  $n=1$ ,  $N_{br}=0.002$ ,  $\beta=0.02$ ,  $Bi=0.07$ ,  $\theta_a=0.88$ ,  $\tau=5$ .

The impact of tip parameters i.e., radiative parameter of boundary,  $N_{br}$  and Biot number,  $Bi$  have been presented in Figure 4.8 and Figure 4.9, respectively. The rate of heat transfer increases with the increase of radiative parameter of boundary,  $N_{br}$ . It is because of increasing radiative heat exchange from tip surface to environment with increase of  $N_{br}$ . Figure 4.9 shows the effect of Biot ( $Bi$ ) number on heat transfer rate in the fin, increasing the value of ‘ $Bi$ ’ number leads to a lower heat transfer rate at fixed value of other non-dimensional parameters. This is due to the negative effect of constant heat transfer coefficient,  $n$  at tip of the fin as discussed earlier. Finally, it is found that the temperature distribution increases with increase in Biot number,  $Bi$ .

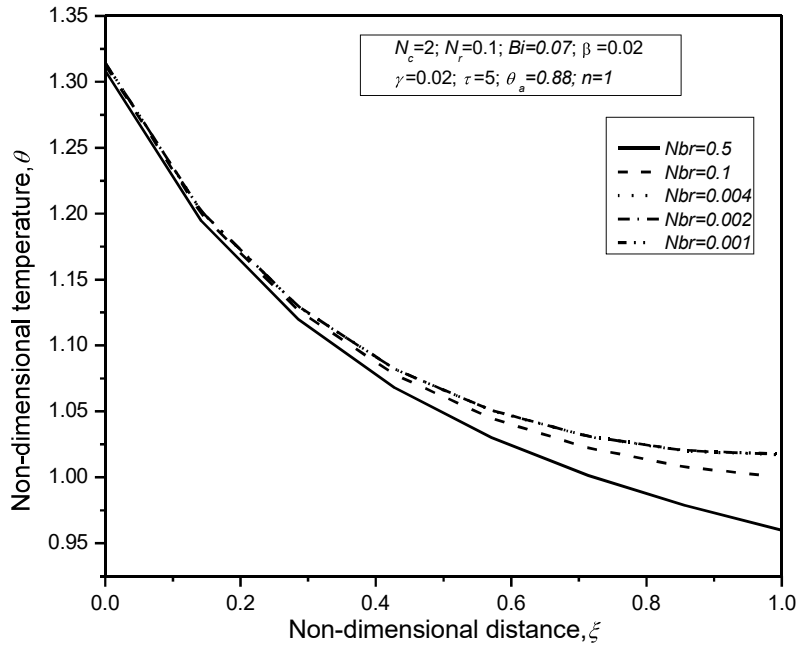


**Figure 4.8.** Comparison of non-dimensional temperature ( $\theta$ ) for various values of  $N_{br}$  with  $N_r=0.1$ ,  $N_c=2$ ,  $n=1$ ,  $Bi=0.07$ ,  $\gamma=0.02$ ,  $\beta=0.02$ ,  $\theta_a=0.88$ ,  $\tau=5$ .

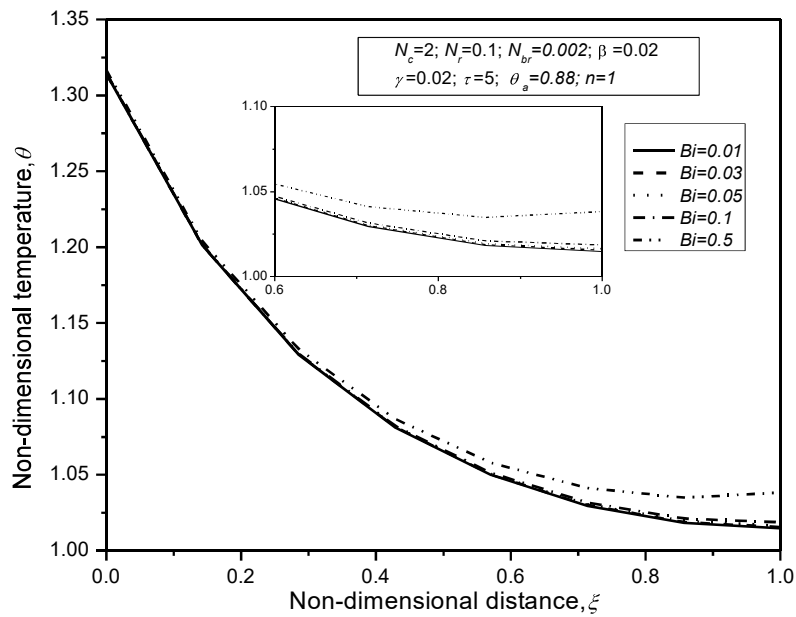


**Figure 4.9.** Comparison of non-dimensional temperature ( $\theta$ ) for various values of  $Bi$  with  $N_r=0.1$ ,  $N_c=2$ ,  $n=1$ ,  $N_{br}=0.002$ ,  $\gamma=0.02$ ,  $\beta=0.02$ ,  $\theta_a=0.88$ ,  $\tau=5$

### 4.1.2. Experimental Results

Experiments are done on the extended surface heat transfer setup as shown in the Figure 3.3. One side of the cylindrical pin fin is attached with the heater and other is open to convection and radiation. The experiments are performed for different values of voltage (80V, 70V, and 60V) to analyze the difference in temperature profiles.

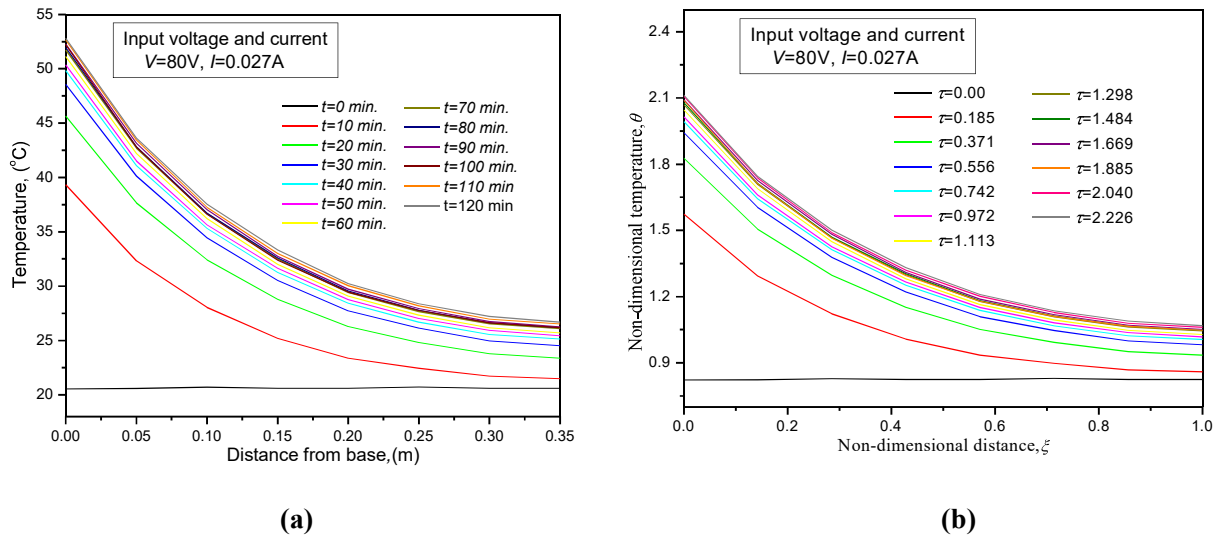
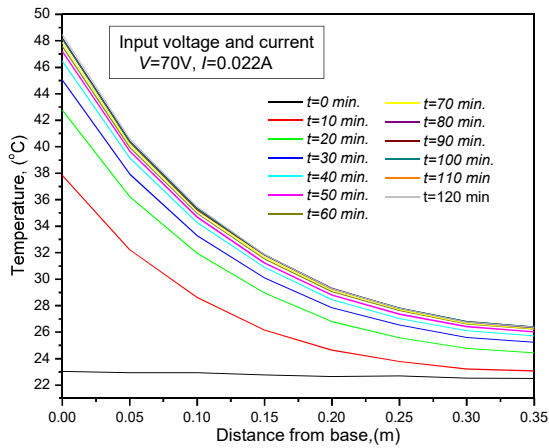
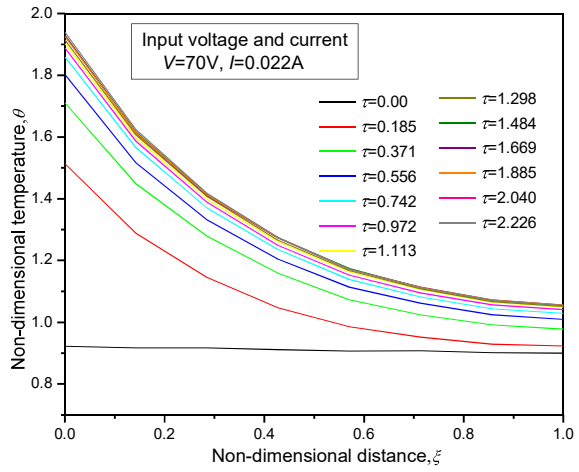


**Figure 4.10.** Transient temperature distribution from experimental setup (a) dimensional temperature and (b) non-dimensional temperature for  $V=80\text{ V}$  and  $I=0.027\text{ A}$

The experimental results of temperature data versus space and time is presented in Figure 4.10, 4.11 and 4.12 for the thermocouple which are attached to the surface of the pin fin. The heater is remain on until the steady state is not reached. When the steady state is observed, the heater is turned off and all the temperature data that is saved in data logger obtained with the help of computer. It is examined from the above-mentioned figures that as the voltage is increases corresponding current is also varies and the temperature profile is also affected. In case of 80V, the temperature profile have higher value compared to other voltage values (70V, 60V). The obtained temperature profile is also represented in non-dimensional form of temperature ' $\theta$ ' so that it can be comparable with the analytical results obtained with the help of MATLABs inbuilt Pdepe function.

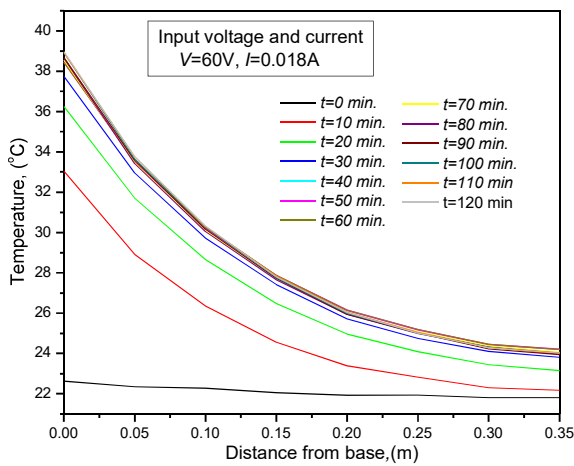


(a)

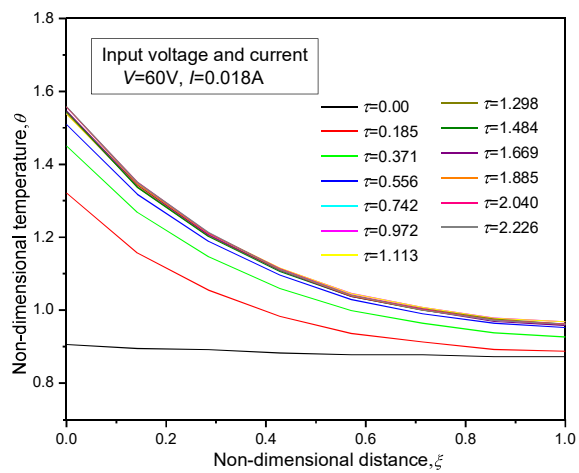


(b)

**Figure 4.11.** Transient temperature distribution from experimental setup (a) dimensional temperature and (b) non-dimensional temperature for  $V=70$  V and  $I=0.022$  A



(a)

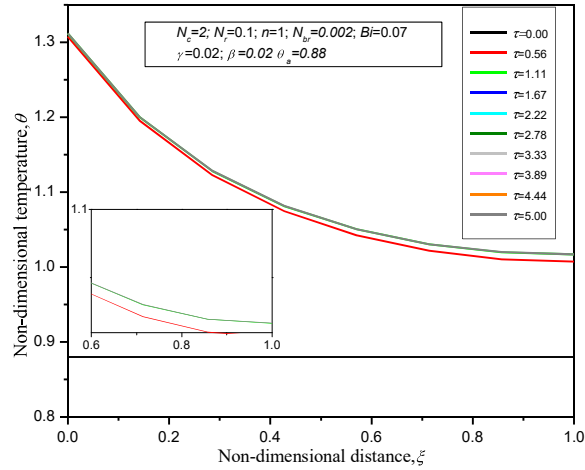


(b)

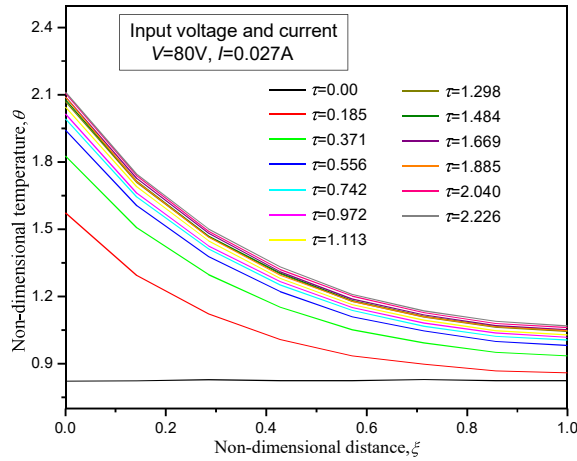
**Figure 4.12.** Transient temperature distribution from experimental setup (a) dimensional temperature and (b) non-dimensional temperature for  $V=60$  V and  $I=0.018$  A

## 4.2. Comparison of steady-state theoretical and experimental results of Pin fin

From analysis of the Figure 4.13, it shows that there is variation in the temperature profile for both the approaches, due to the unavailability of exact value of heat transfer coefficient ( $h_b$ ) and heat flux ( $\phi$ ) in the forward method. The inverse methods is employed to retrieve this unknown parameters.



(a)



(b)

**Figure 4.13.** Transient non-dimensional temperature distribution (a) From MATLAB ( $\tau = 5$ ) (b) Experimental setup ( $\tau = 2.226$ ).

### 4.3. Retrieval of unknown parameters in thermal systems

To retrieve the value of the unknown parameters, we can use inverse methods. For this, a direct problem is solved from that the temperature profile is obtained. These temperature profile is then used as the input for the inverse method. In present study, Golden Section Search Method and Differential Evolution method is used as inverse methods for the retrieval of single and multiple parameters.

#### Least Square Method

The objective function is chosen in the least square sense, as it results in optimal value of parameters by minimizing the sum of squared residuals as

$$f(\Phi) = \|\theta(\Phi) - \tilde{\theta}\|^2 \text{ or } \|\theta(\Phi)_i - \tilde{\theta}_i\|^2 \quad (35)$$

Here “ $\theta$ ” is the exact temperature obtained from the forward method, “ $\tilde{\theta}$ ” is the reconstructed temperature field obtained by using the parameter retrieved from the inverse analysis and “ $i$ ” is the time steps. By tuning the objective critically, parameters values are selected, which best fits the data points (temperature in this case). The model is developed in such a sense that it provides the difference between the actual and predicted values of temperature, called residual. The aim of this objective function is to minimize the associated error, appeared as a part of inverse calculations. The smaller is the objective function, the better are the unknowns determined via inverse.

#### 4.3.1. Single parameter retrieval using GSSM (Pin Fin)

Golden Section Search Method is gives very accurate results for the single parameters estimation, in the present work it is used to obtain the value of heat flux for different type cases

##### Case 1. To retrieve constant heat flux (static)

GSSM has proved to be an excellent method for the inverse when a single parameter is to be retrieved. Inverse algorithm runs until the objective function,  $f(\Phi) = \|\theta(\Phi) - \tilde{\theta}\|^2$  or  $\|\theta(\Phi)_i - \tilde{\theta}_i\|^2$  for the  $i^{\text{th}}$  step achieve a sufficiently small value.

Given thermal data in the form of temperature profile with respect to distance for different time steps, is shown in figure 4.14 (a). Temperatures are perturbed for errors as 1%, 2%, 4%, 5% and their plots with distance are shown in figure 4.14 (b), which are then utilized in the inverse analysis to retrieve heat flux, independent of time in this case. In figure 4.15(a), the initial guesses are taken to be  $[\phi_{max}, \phi_{min}] = \{ 0, 10 \}$ , and  $\phi$  decrease gradually to an optimal value 0.98, with the corresponding objective function's value  $O(10^{-10})$  as shown in figure 4.15(b), right after the 17<sup>th</sup> iteration. Similar results are obtained when measurement error of 1%, 2%, 4%, and 5% is added to the temperature measurements as shown in figure 4.15(c), 4.15(d) for convergence of vertices and objective function respectively with a number of iterations. The retrieved heat flux is compared with the exact 0.98 in Table 4.3. As the associated errors are statistical in nature, thus retrieval of  $\Phi$  is repeated thrice for three realizations of the temperature and the maximum error in each case has been highlighted. It can clearly be seen from Table 4.3 that with an increase in measurement error for temperature, there is an increase in the relative error of retrieved heat flux. But a sudden jump is seen from 3.7% to 9.8% in error (output) when the corresponding error (input) is changed from 5% to 10% respectively.

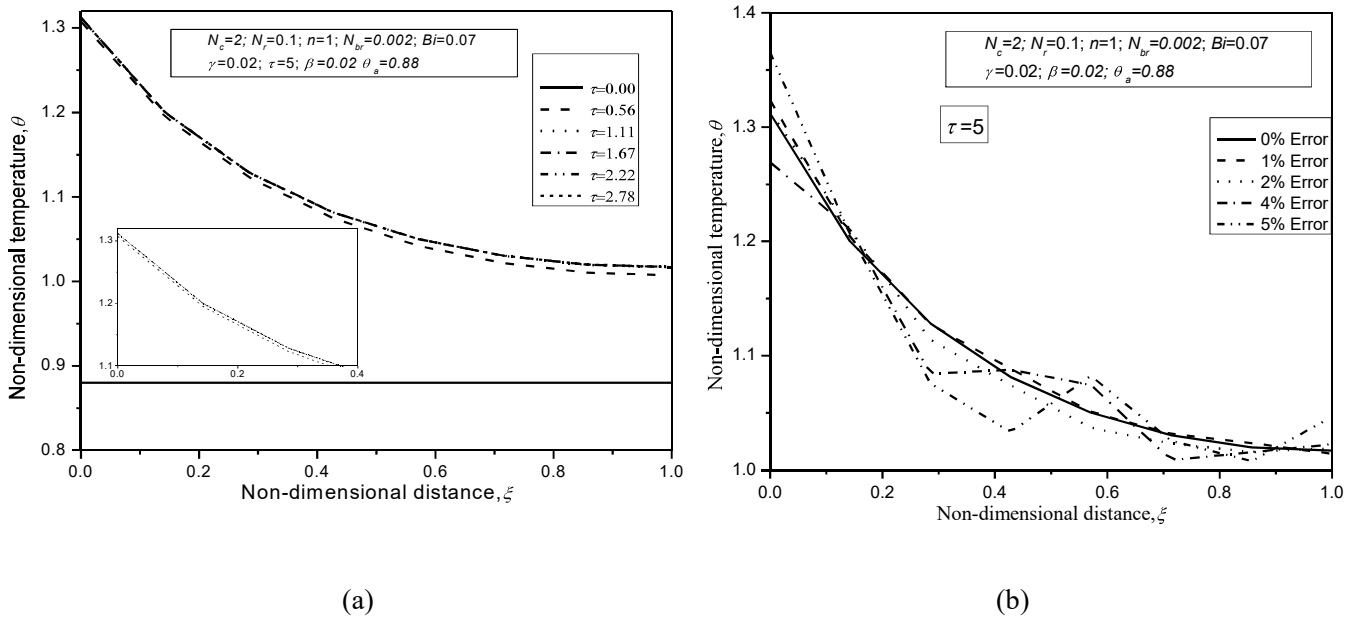
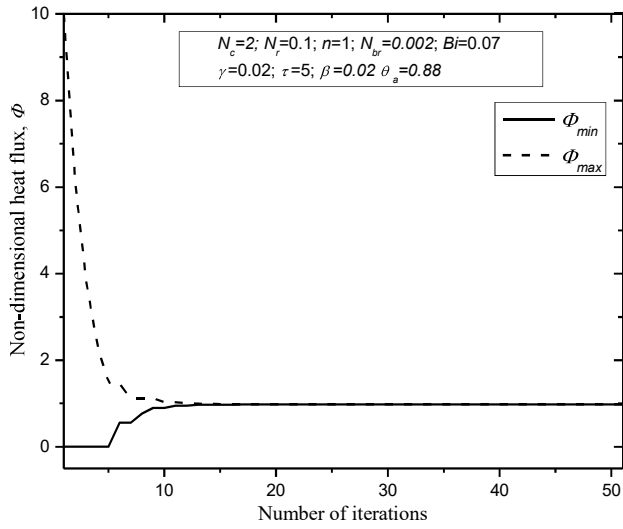
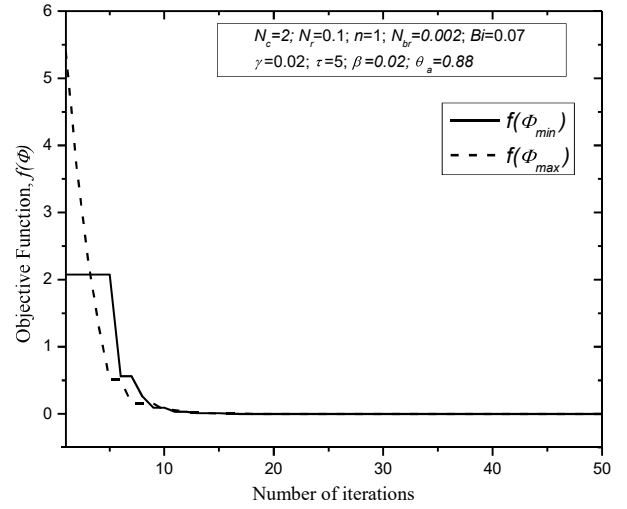


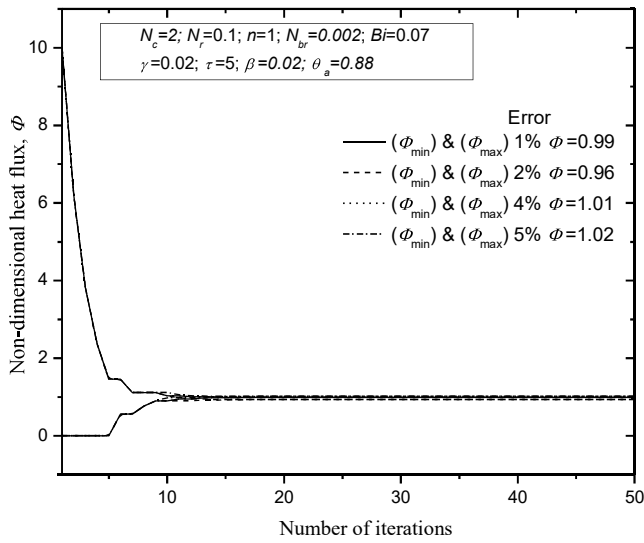
**Figure 4.14 (a)** Temperature distribution with respect to distance, with different time steps. **(b)** Noisy temperature data with distance, when measurement error of 0%, 1%, 2%, 4%, 5% are added.



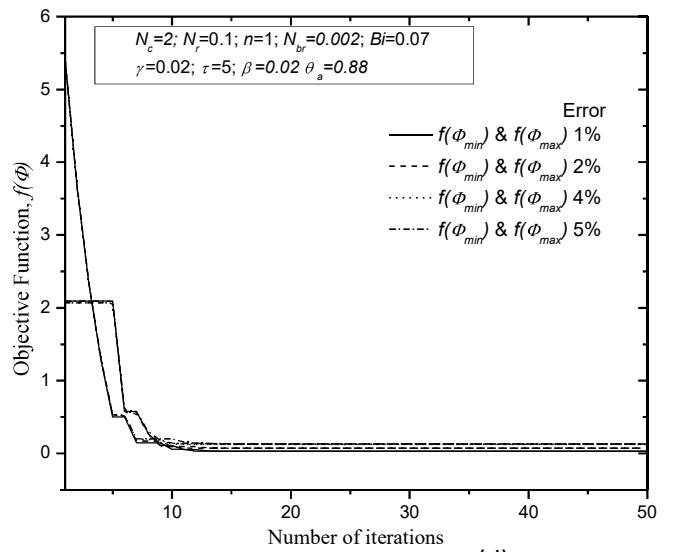
(a)



(b)



(c)



(d)

**Figure 4.15.** (a) and (b) Retrieved flux and variation of objective function using GSSM, with iterations without measurement error (c) and (d) Retrieved flux and objective function using GSSM, with iterations and measurement error of 1%, 2%, 4%, 5% in temperatures.

**Table 4.3.** Relative error in recovered heat flux, with measurement error in temperature, for a case when heat flux is assumed to be constant.

Error (%) Temperature	Heat flux (Exact value)	Heat flux (Retrieved)	Relative error in heat flux (%)
0	0.98	0.98	0
1		0.992035934	1.228156476
		0.986552201	0.668591943
		0.991598289	1.183498837
2		0.957271244	2.319260785
		0.962609396	1.774551416
		0.977082838	0.297669569
3		1.008599033	2.918268688
		1.001779005	2.222347451
		0.993679258	1.395842684
4		1.013800252	3.449005317
		1.010480843	3.11029006
		0.956496615	2.398304578
5		1.016517989	3.726325347
		0.974429615	0.568406629
		0.948040078	3.261216532
10		0.883704466	9.826074881
		0.945141426	3.55699734
		0.900020905	8.161132122

**Table 4.4** Heat flux corresponding to different cases:

a.	$\Phi = 0.98$ , (constant )
b.	$\Phi = \begin{cases} \Phi \tau, & 0 \leq \tau \leq \tau_1, \\ \Phi \tau_1 \left( \frac{\tau - \tau_2}{\tau_1 - \tau_2} \right), & \tau_1 < \tau \leq \tau_2, \\ 0, & \text{otherwise.} \end{cases} \quad [56]$
c.	$\Phi = \begin{cases} \Phi \sqrt{1.5\tau} & 0 \leq \tau \leq \tau_1 \\ \Phi \sqrt{1.5\tau_1} & \tau_1 < \tau \end{cases} \quad [49]$

**Case II: To retrieve linearly varying triangular heat flux with on-off conditions (when the functional form of heat flux is known)**

Assuming that the exact heat flux varies linearly, power in the form of flux is provided initially, which acts as a linear function of time until a maximum required heat is generated within the system. This heat then starts decreasing again linearly with respect to time. Such an assumption is valid [56] and corresponds to the on-off situation which is required in many practical applications. The application of such a system is found when the time of auto cut of any heating system is required. The temperature profile obtained using this flux is then utilized to retrieve flux. During the inverse process, it has been assumed that the functional form of heat flux is known apriori. Such retrieval is compared with that of exact flux and is shown in figure 4.16 and the trend comes out to be in a triangular fashion. It clearly justifies the exact assumed heat flux, described in the literature [56] for particular on-off situations of heating systems. Figure 4.17 represents the retrieval of heat flux when measured temperatures involved contains 1%, 2%, 4%, 5% random errors. The maximum relative error for each case has been highlighted in Table 4.5. The objective function, evaluated through equation,  $f(\Phi) = \|\theta(\Phi) - \tilde{\theta}\|$  is observed to be of the order of  $10^{-3}$ . As the error in temperature is increased from 3% to 4%, an exponential increase is observed for error in estimated heat flux. Thus, by an inverse analysis, it can be depicted that the maximum 6% error bound is acceptable, to maintain temperature profile within a range of 3%.

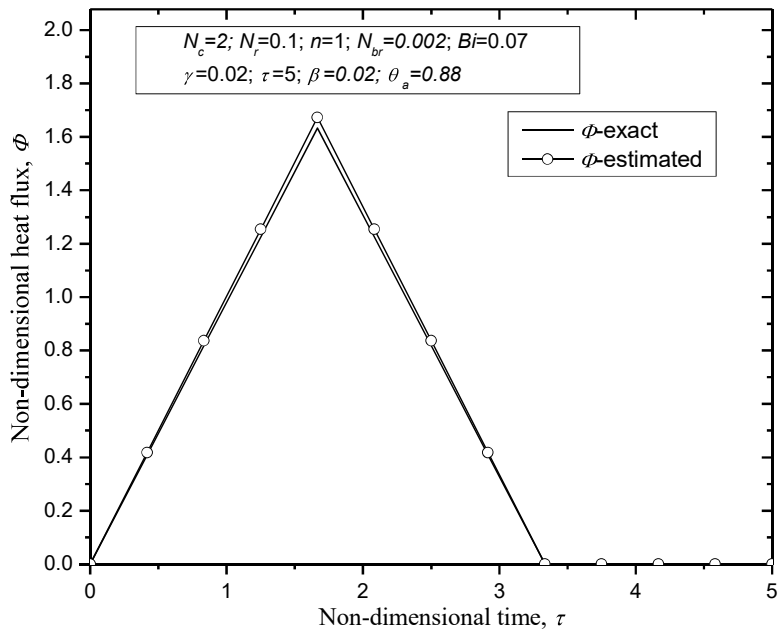


**Figure 4.16.** Retrieved triangular heat flux (0% error), when exact  $\Phi$  in case (b) of Table 4.4 is used in forward analysis.

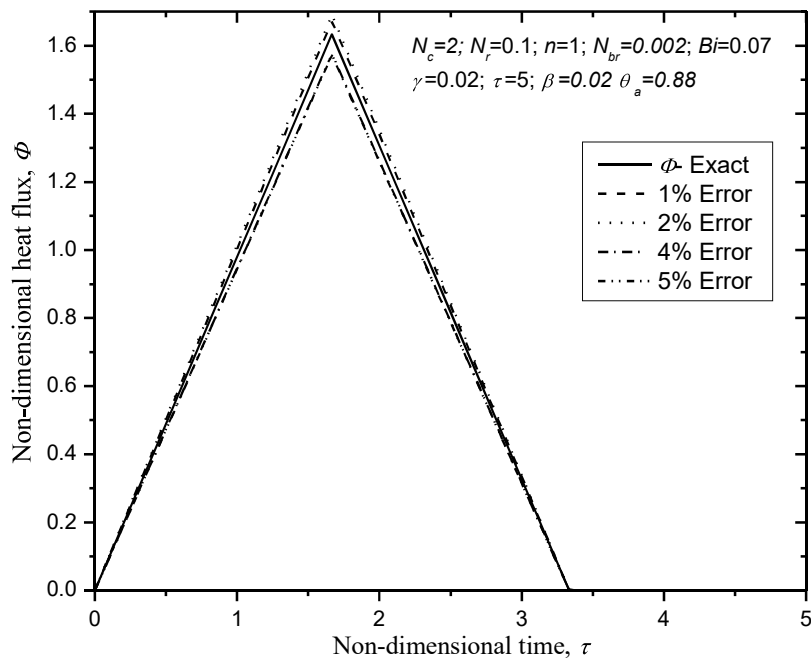


**Figure 4.17.** Retrieved triangular heat flux (with 1%, 2%, 4%, 5% error), when exact  $\Phi$  in case (b) of Table 4.4 is used in forward analysis.

**Table 4.5.** Relative error in recovered heat flux, with measurement error in temperature, for a case when heat flux is assumed to be triangular.

Error (in %) Temperature	Heat flux (Exact value)	Heat flux (Retrieved)	Relative error (%)	Objective Function
0	0.98	1.003698524	2.418216685	$6.95 \times 10^{-4}$
1		1.004108646	2.460065933	0.001240457
		0.955303403	2.520060928	0.001021717
		1.003849064	2.433577997	0.001331056
2		1.014991977	3.57060991	0.005234984
		0.935292177	4.562022742	0.004576284
		0.955106731	2.540129444	0.003735003
3		0.963758833	1.657261939	0.007504802
		1.035021695	5.614458669	0.01066376
		1.015020963	3.573567627	0.010863074
4		0.946527648	3.415546077	0.015742544
		1.006619232	2.71624814	0.020599025
		1.074709996	9.664285339	0.01760026
5		0.944263597	3.646571742	0.017581203
		1.014145922	3.484277761	0.027756475
		1.058483234	8.008493273	0.020935925

**Case III: To retrieve realistic heat flux (when the functional form of heat flux is known)**

Power in the form of heat flux is provided to the system. In this case, it was assumed that the heat flux being supplied, increases non-linearly with time. Due to such variation, temperature first increases and then after a certain duration becomes stagnant. After such a time, the system as a whole is said to achieve its steady state. Yet, the nature of heat flux described corresponds to the real heating up situation. Authors here thus considered it as an important study to observe the retrieval, when input temperatures were calculated through forward method, using  $\Phi$  as described in Table 4.2, case (c). Such a trend of heat flux is very close to real situation, making the whole process of retrieval extremely close to reality, as discussed in the literature [49]. In the first case when a static study of reconstruction is made, the functional form of heat flux is assumed to be known. The reconstructed heat flux matches almost exactly with that of exact flux when no error was present in the input temperatures as shown in figure 4.18. Further, the effect of perturbation in heat flux with the deviation of input temperature is compared in figure 4.19. The maximum deviation is seen in heat flux when 5% error in temperature was incorporated, as depicted clearly by figure 4.19. This estimation is further confirmed by Table 4.6, where a maximum relative error has been highlighted in each case, for the errors being random in nature. A 4% cut-off is observed for this case in temperature, with a maximum of 4% error.

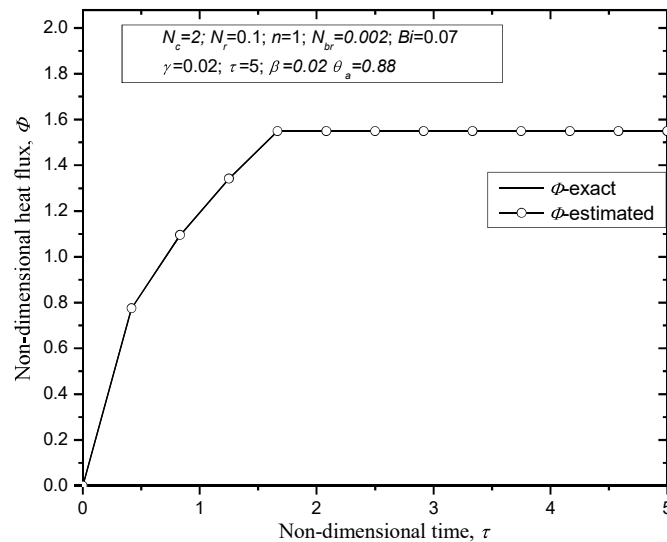


**Figure 4.18.** Retrieved realistic heat flux (0% error), when exact  $\Phi$  in case (c) of Table 4.4 is used in forward analysis.

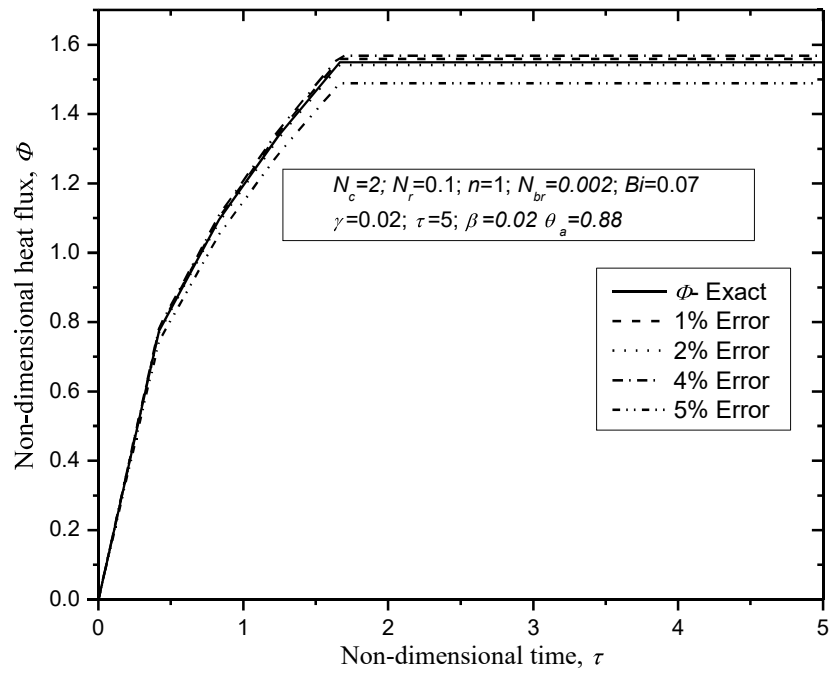


**Figure 4.19.** Retrieved realistic heat flux (with 1%, 2%, 4%, 5% error), when exact  $\phi$  in case (c) of Table 4.4 is used in forward analysis.

**Table 4.6.** Relative error in recovered heat flux, with measurement error in temperature, for a case when heat flux is assumed to be realistic.

Error (in %) Temperature	Heat flux (Exact value)	Heat flux (Retrieved)	Relative Error (%)	Objective Function
0	0.98	0.980000001	$O(10^{-8})$	$2.43 \times 10^{-18}$
1		0.985874944	0.5994841	0.001266
		0.990277259	1.0486999	0.000902
		0.999212793	1.960489	0.001406
2		0.9744729	0.5639898	0.006064
		0.9744729	0.5639898	0.00728
		1.001323309	2.1758479	0.00473
3		0.984944755	0.5045668	0.012164
		0.992773101	1.3033777	0.013374
		1.023755357	4.4648324	0.017592
4		0.991545154	1.1780769	0.019463
		0.963708509	1.662397	0.018463
		0.9744729	0.5639898	0.025282
5		0.942049749	3.8724746	0.044949
		0.9744729	0.5639898	0.03176
		1.02571509	4.6648051	0.031215

**Case IV: Retrieval of heat flux using experimental temperature data, when heat flux is input for a longer duration:**

Taking non-dimensional experimental parameters as given in Table 4.2, Figure 4.20, shows the retrieved heat flux for a case when experimental temperatures have been utilized for  $V=80\text{V}$  and  $I=0.027\text{A}$ ,  $V=60\text{V}$  and  $I=0.018\text{A}$  and  $V=70\text{V}$  and  $I=0.022\text{A}$ , till  $\tau = 2.226$ , a time when system attained its steady state. A similar trend is observed in both cases. This confirms the computed results. These plots cannot be compared one on one, as there is always an uncertainty in the experiments. Few parameters like  $h, \beta, \gamma$  are not exactly available for experiments. These parameters can only be guessed, which may then include huge errors, for comparison purposes. The relative uncertainty in the input temperature obtained from the experiments has been calculated using the formula,  $\frac{\Delta\theta}{\bar{\theta}}$ ,  $\bar{\theta} = \frac{\max(\theta) + \min(\theta)}{2}$ ,  $\Delta\theta = \frac{\max(\theta) - \min(\theta)}{2}$ . The obtained uncertainty in temperature is 0.0156. This uncertainty further depends on uncertainty in input voltage ( $V$ ) and ( $I$ ).

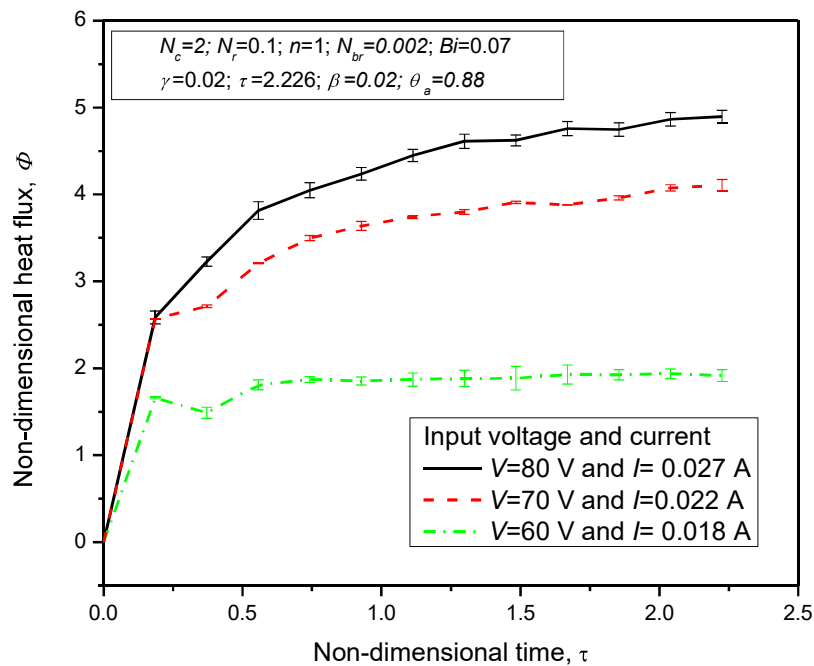


**Figure 4.20.** Retrieved heat flux when experimental temperature profile is used (heat flux is input for longer duration), with error bars indicating uncertainties for different voltage and current.

Relative uncertainties calculated using the same expressions for voltage ( $V$ ) and current ( $I$ ) is 0.03144 and 0.06542 respectively. These relative uncertainties affect the reconstruction as seen in figure 4.20. The maximum uncertainties in reconstructed heat flux are 5%, 6% and 2% for  $V=80V$  and  $I=0.027A$ ,  $V=60V$  and  $I=0.018A$  and  $V=70V$  and  $I=0.022A$  respectively. A closer look at the retrieved heat flux is seen in Table 4.7, for temperatures measured at different times, voltages and currents.

**Table 4.7.** Estimated heat flux using the temperatures obtained by experiments during morning ( $M1$ ,  $M2$ ), afternoon ( $AF1$ ,  $AF2$ ) and evening ( $E1$ ,  $E2$ ).

$\tau$	V=80V I=0.027A		V=60V I=0.018A		V=70V I=0.022A	
	M1	M2	AF1	AF2	E1	E2
0	0	0	0	0	0	0
0.1855	2.682409	2.490045	1.650933	1.667621	2.574025	2.570889
0.371	3.312981	3.14194	1.44195	1.536577	2.732311	2.691396
0.5565	4.006169	3.621319	1.760866	1.861246	3.212357	3.200486
0.742	4.223896	3.874449	1.839468	1.90039	3.549234	3.448579
0.9275	4.391775	4.082661	1.811503	1.897519	3.73217	3.541935
1.113	4.603978	4.291775	1.798906	1.942187	3.768807	3.712823
1.2985	4.800137	4.421964	1.793923	1.970653	3.852519	3.745339
1.484	4.767204	4.474801	1.757125	2.014028	3.935678	3.883219
1.6695	4.951445	4.563022	1.822464	2.03579	3.884922	3.873523
1.855	4.933076	4.559007	1.868569	1.981518	3.915837	4.004959
2.0405	5.053506	4.674008	1.884718	1.992023	4.006492	4.146135
2.226	5.070239	4.722193	1.851074	1.983638	3.973856	4.239564

#### 4.4.2. Multiple parameter retrieval using Differential Evolution

Differential evolution is gradient free algorithm, thus they even applied for objective function which are difficult to differentiate. As per the problem we have only temperature field,  $\theta$  and the two unknown parameters ( $\phi, h_b$ ) of cylindrical pin fin. The temperature field,  $\theta$  can be obtained by using the forward methods (numerically/analytically/semi analytically) or experiments. In the present work, we obtain the temperature field,  $\theta$  using the numerical method by adopting MATLAB's inbuilt pdepe tool, as described in the above section. We have two unknowns ( $\phi, h_b$ ). The objective function needed to be minimized as mentioned below

$$\text{Minimize: } F = \{\theta - \tilde{\theta}(h_b, \phi)\}^2 \quad (36)$$

Where  $\theta$  is the exact temperature obtained by MATLAB's Pdepe tool as forward approach. The temperature field,  $\tilde{\theta}$  corresponds the guessed value of unknowns ( $\phi, h_b$ ) to be optimized by DE in iterative manner. By considering the measurement error,  $e_r$  in the exact field, the objective function is reformed as below

$$\text{Minimize: } F = \{[\theta + e_r] - \tilde{\theta}(h_b, \phi)\}^2 \quad (37)$$

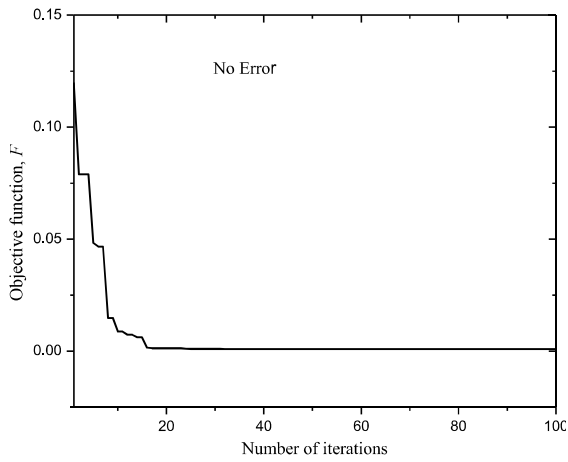
The optimization process has been terminated when the objective function ( $F$ ) acquired the minimum value after multiple iterations. In present work, 100 iterations are taken. The idea of differential evolution (DE) is suggested by Storn and Price [55]. In the present work, the population size of 30, scaling factor,  $S=0.7$  and crossover probability,  $CR=0.9$  has been considered for DE algorithm. In present work, MATLAB based Pdepe tool is used for solving the non-linear governing equation for conductive, convective and radiative pin fin having temperature dependent properties. MATLAB is used as forward method for obtaining the temperature field,  $\theta$  of pin fin. Differential evolution is used as inverse method for estimating the unknown parameter ( $\phi, h_b$ ) which satisfy the prescribed temperature field,  $\theta$  of the fin. The accuracy of the forward method (Pdepe) is validated with the results available in the literature obtained by (RK-4) [22] and found in satisfactory agreement as shown in Figure 4.1. The experimental study is also done on the brass pin fin setup. The input values are taken from the experimental outcomes in the MATLAB's pdepe coding like  $k, L, d, A_{cs}$  and etc. as shown in Table 4.1. The non-dimensional temperature distribution for both experimental and numerical method with non-dimensional time, ( $\tau$ ) is shown in Figure 4.13. The

study is done on the convective and radiative tip. The non-dimensional time, ( $\tau$ ) for both the approaches is different to achieve the steady state. DE used to find the values of these unknowns, we consider a cylindrical brass pin fin having flux at one end and other end is free to the environment. There are two unknown parameter ( $\phi$ ,  $h_b$ ) are estimated by numerical method as forward method and for inverse differential evolution (DE) is adopted. The four different run have been considered by DE to get confidence in the retrieved parameters which comes in the range provided by us, shown in Table 4.8. It shows the comparison of estimated and exact values of different unknowns, ( $\phi$ ,  $h_b$ ) obtained by using DE.

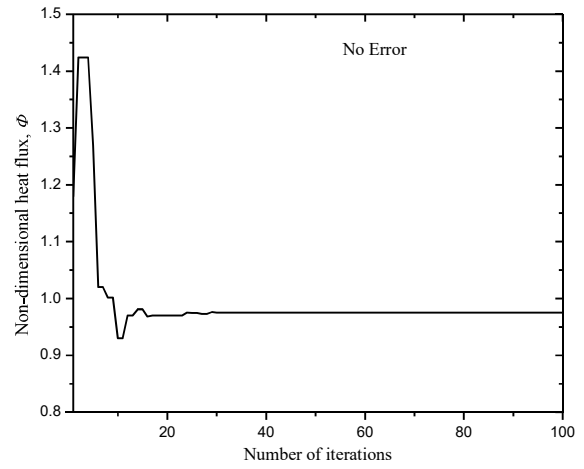
First case is without error,  $e_r=0$ , it is observed that for all runs are showing same results with same objective function value. The iterative variation of unknown parameters ( $\phi$ ,  $h_b$ ) and objective function ( $F$ ) using DE and without measurement error,  $e_r=0$  are shown in Fig. 4.21 (a-c). The obtainable iterative variation equals to the first run of the DE in Table 4.8. The unknown parameters get updated well beyond 30 iterations and function ( $F$ ) continuous decreases and remain same after 25 iterations. The objective function have value  $F \approx 0$  ( $10^{-4}$ ) for all the runs for estimation of unknowns, ( $\phi$ ,  $h_b$ ).

**Table 4.8.** Comparison of values for different runs of DE with temperature field of pin fin containing no measurement error,  $e_r=0$ . Range: [ $\phi$ ,  $h_b$ ] = [0-10; 2-25];

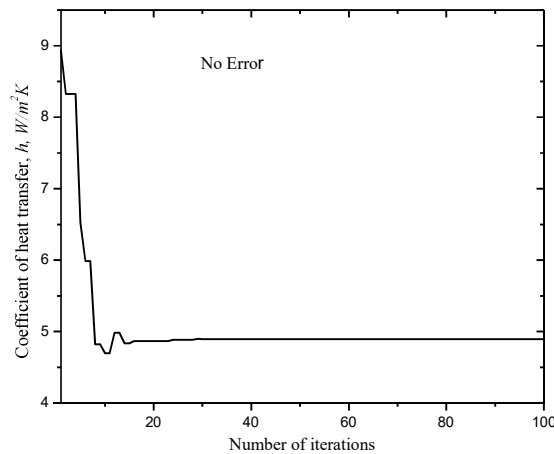
Run	Heat flux, $\phi$	Coefficient of heat transfer, $h_b$ (W/m <sup>2</sup> K)	( $N_c$ , $Bi$ )	Fitness function, $F$
Exact values considered in the forward problem				
	0.98	-	(2,0.07)	
<i>Estimated parameters</i>				
1	0.97	4.89	(1.97,0.01)	$9.35 \times 10^{-4}$
2	0.97	4.89	(1.97,0.01)	$9.35 \times 10^{-4}$
3	0.97	4.89	(1.97,0.01)	$9.35 \times 10^{-4}$
4	0.97	4.89	(1.97,0.01)	$9.35 \times 10^{-4}$



(a)



(b)



(c)

**Figure 4.21.** Variation of estimated unknown parameters; (a) objective function ( $F$ ) (b) heat flux ( $\phi$ ), (c) heat transfer coefficient ( $h$ ), with iterations of DE without measurement error,  $e_r=0$ .

Based on the estimated values of the unknown parameters, a new temperature field is reconstructed and compared with the actual temperature field as shown in Fig, 4.22. The actual and reconstructed temperature field are excellent match with each other. In the next case, the measurement error has been considered in the objective function as in Eq. 37. There are four different measurement errors considered such as  $e_r=1\%$ ,  $e_r=3\%$ ,  $e_r=5\%$  and  $e_r=10\%$  for further study. The estimated values for

unknown parameters using DE from a temperature field with measurement error has been presented in Table 4.9. The four runs using DE have been taken for accurate retrieval. In the present study, the retrieved values are very much similar in each run of DE along with objective function value. This is representing the unique solution of inverse problem. In figure 4.23, the iterative variation of unknown parameters ( $\phi$ ,  $h_b$ ) and objective function ( $F$ ) using DE have been depicted for measurement errors,  $e_r \neq 0$  in Figure 35 (a-c), respectively. The unknown parameters get updated well beyond 22 iterations and function ( $F$ ) continuous decreases and remain same after 20 to 100 iterations and made very less change also on adding error also.

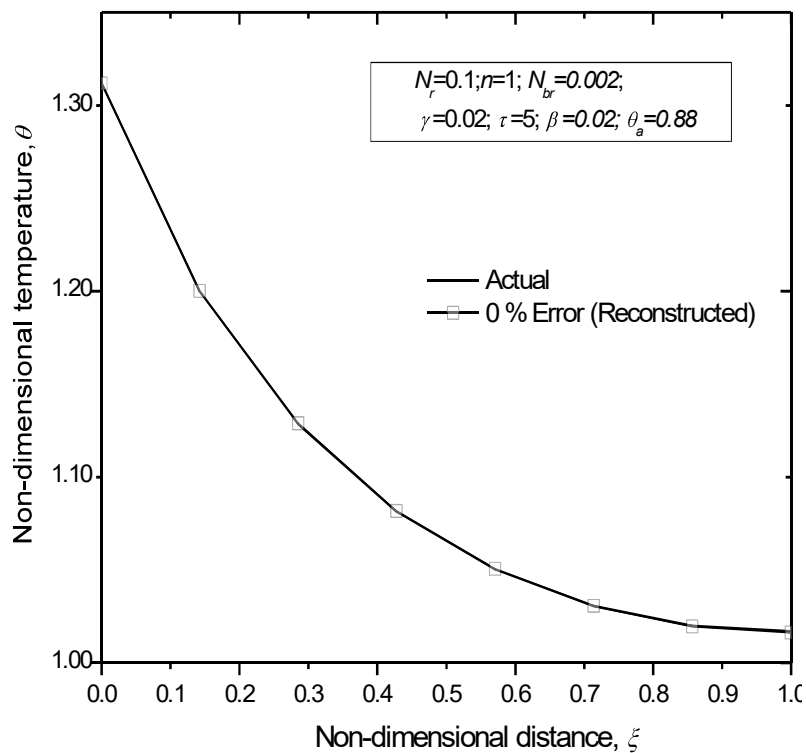
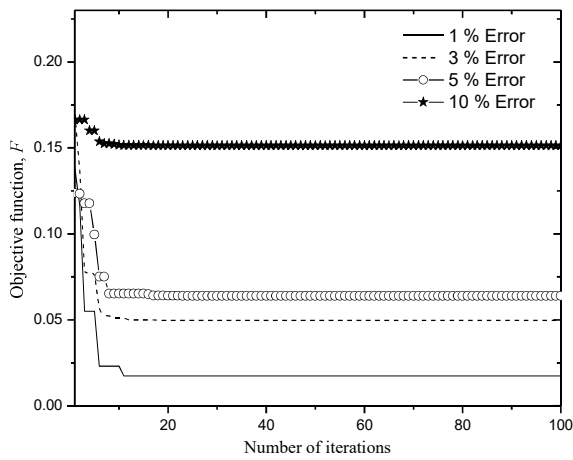


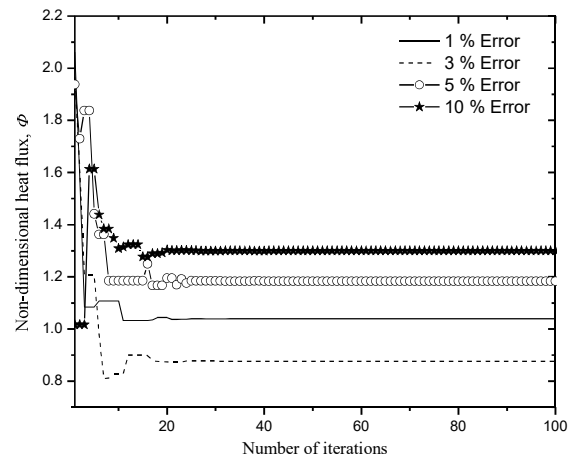
**Figure 4.22.** Comparison of actual and reconstructed non-dimensional temperature field for cylindrical pin fin,  $e_r=0$ .

**Table 4.9** Comparison of values for different runs of DE with temperature field of pin fin containing measurement error,  $e_r \neq 0$ . Range:  $[\phi, h_b] = [0-10; 2-25]$ .

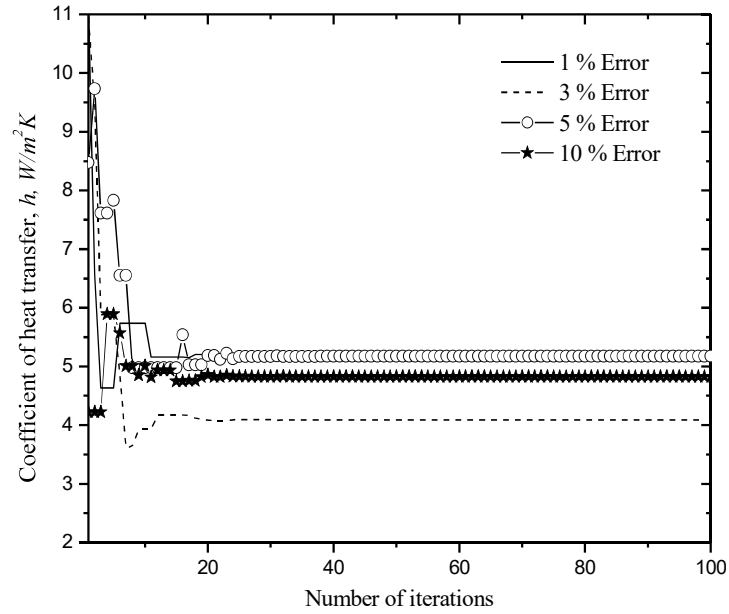
Run	Error, $e_r$ %	Heat flux, $\phi$	Coefficient of heat transfer, $h_b$ (W/m <sup>2</sup> K)	$(N_c, Bi)$	Fitness function, $F$
Exact values considered in the forward problem (2,0.07)					
0.98					
With various measurement errors, $e_r \neq 0$					
<b><math>e_r=1\%</math></b>					
1		1.04	5.18	(2.10,0.014)	$1.8 \times 10^{-2}$
2		1.04	5.18	(2.10,0.014)	$1.8 \times 10^{-2}$
3		1.04	5.18	(2.10,0.014)	$1.8 \times 10^{-2}$
4		1.04	5.18	(2.10,0.014)	$1.8 \times 10^{-2}$
<b><math>e_r=3\%</math></b>					
1		0.88	4.08	(1.65,0.011)	$4.9 \times 10^{-2}$
2		0.88	4.08	(1.65,0.011)	$4.9 \times 10^{-2}$
3		0.88	4.08	(1.65,0.011)	$4.9 \times 10^{-2}$
4		0.88	4.08	(1.65,0.011)	$4.9 \times 10^{-2}$
<b><math>e_r=5\%</math></b>					
1		1.18	5.17	(2.10,0.014)	$6.3 \times 10^{-2}$
2		1.18	5.17	(2.10,0.014)	$6.3 \times 10^{-2}$
3		1.18	5.17	(2.10,0.014)	$6.3 \times 10^{-2}$
4		1.18	5.17	(2.10,0.014)	$6.3 \times 10^{-2}$
<b><math>e_r=10\%</math></b>					
1		1.29	4.82	(1.95,0.013)	$1.5 \times 10^{-1}$
2		1.29	4.82	(1.95,0.013)	$1.5 \times 10^{-1}$
3		1.29	4.82	(1.95,0.013)	$1.5 \times 10^{-1}$
4		1.29	4.82	(1.95,0.013)	$1.5 \times 10^{-1}$



(a)



(b)



(c)

**Figure 4.23.** Variation of estimated unknown parameters; (a) objective function ( $F$ ) (b) heat flux ( $\phi$ ), (c) heat transfer coefficient ( $h$ ), with iterations of DE without measurement error,  $e_r \neq 0$

Though, the objective functions still achieve value of order between  $O(10^{-4}) \leq F \leq O(10^{-2})$ . This indicates that DE gives good convergence for retrieval of parameters. Next, the accuracy and reliability of retrieved are confirmed with the reconstruction of temperature field from the estimated values. The reconstruction has been presented for each measurement error which corresponds to first run in Figure 4.24. The reconstruction have been compared with the exact temperature field which corresponds to forward/experimental data. In Figure 4.24, It is observed that the deviation of temperature field obtained from estimated value of  $(\phi, h_b)$  from exact ones is increases as the error percentage increases. The maximum error obtained in the reconstruction is found to be 0.064 % for  $e_r = 0\%$ , 0.798 % for  $e_r = 1\%$ , 1.128 % for  $e_r = 3\%$ , 3.756 % for  $e_r = 5\%$  and 6.851 % for  $e_r = 10\%$ .

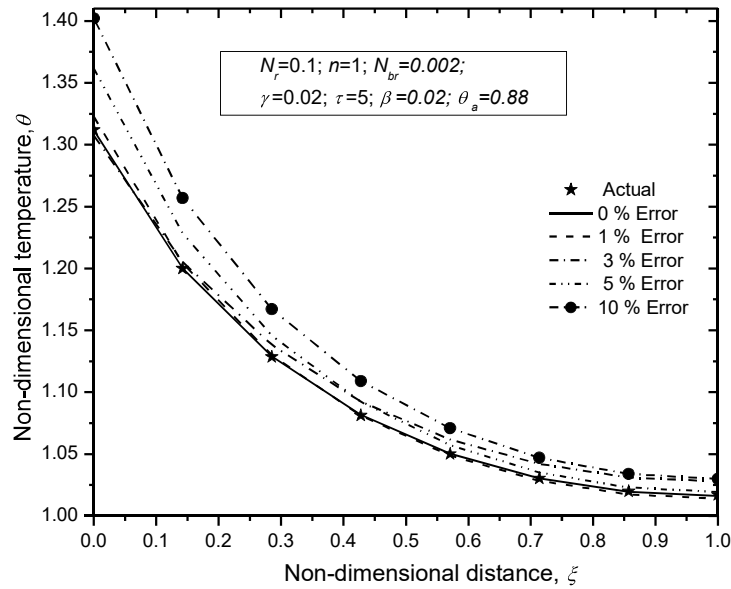


**Figure 4.24.** Comparison of actual and reconstructed temperature field of the fin considering the different error,  $e_r \neq 0$ .

It is observed from the above reconstruction error that the retrieved parameters are acceptable up to 3% measurement error because of less reconstruction error. The retrieved parameters for more than 3% measurement error found to be less accurate and less reliable. So, it is recommended to use retrieved parameters up to 3% measurement error for accurate reconstruction.

#### **4.5. Estimation of multiple tumor parameter in brain tissue using inverse analysis techniques**

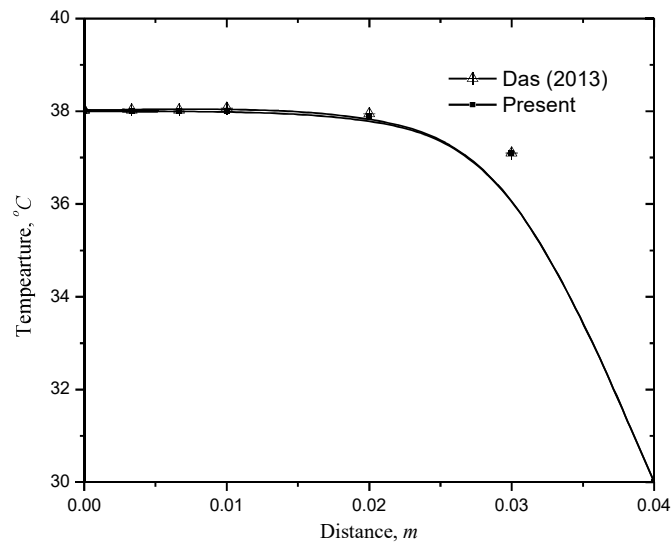
Presence of the tumor altered the temperature of the body that may be the different perfusion rate or heat generation in the tumor. If we anyhow knows that temperature we can easily find out the location, size, and presence of the tumor in the specified portion. In the present work, we are find out the perfusion rate of the different parts of the brain if there is abnormality found in the temperature than there may be some melanoma.

For the forward method, to solve the bioheat equation as discussed in formulation part is solved by the MATLAB's pdepe solver for the single skin layer. But with the introduction of multi-layer, pdepe solver is unable to discretize the governing equation. To overcome this issue the Finite

Element Method is used to obtain the temperature distribution in the Scalp, bone and the brain tissue. This temperature at the particular point is further treat as the input for the inverse method.

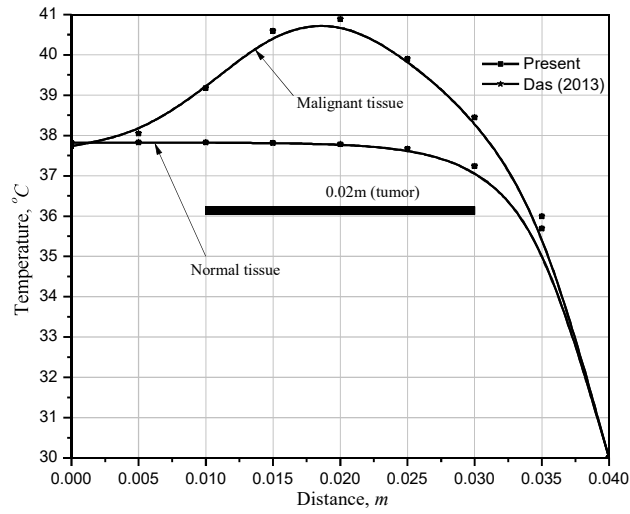
#### 4.5.1. Validation

We validated the result of forward problem obtained by the pdepe solver for the single layer normal tissue with the result available in the literature [41] and found in good agreement with each other as shown in Figure 4.25. The parameters are used for the validation are  $T_a=37$  °C, the density  $\rho=\rho_{bd}=1052$  kg/m<sup>3</sup>,  $c_p=c_{pbd}=3800$  J/kgK,  $Q_m=400$  W/m<sup>3</sup>,  $Q_s=0$  and  $\eta_{bd}=0.0001$  s<sup>-1</sup> and  $k=0.5$  wm<sup>-1</sup>K<sup>-1</sup>



**Figure 4.25.** Comparison of the present result for temperature distribution for single layer normal brain tissue with Das (2013)

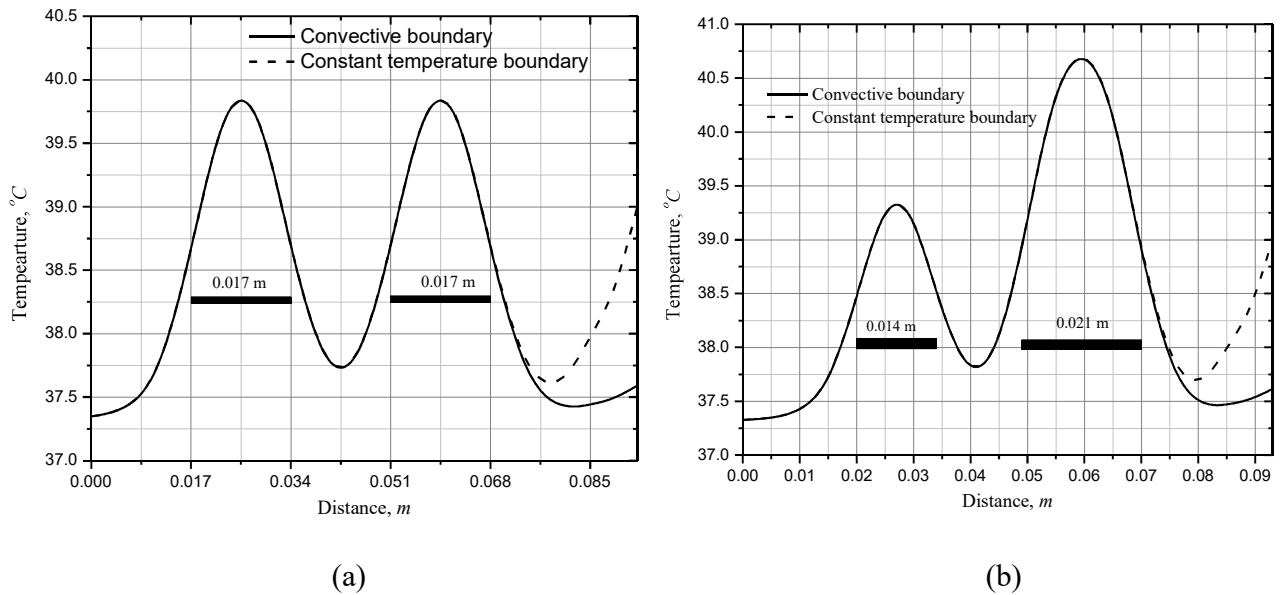
Further, the results for the multilayer cancerous brain from the FEM is compared with the results from the literature [41] and found in good agreement with the literature are shown in figure 4.26 The parameters are used for the validation are  $T_a=36.7$  °C, the density  $\rho=\rho_{bd}=1040$  kg/m<sup>3</sup>,  $c_p=c_{pbd}=3650$  J/kgK,  $Q_{mn}=25000$  W/m<sup>3</sup>,  $Q_{mc}=25000$ W/m<sup>3</sup>,  $Q_s=0$ ,  $\eta_{bd}=0.0081$  s<sup>-1</sup>,  $\eta_{bdc}=0.0005$  s<sup>-1</sup> and  $k=0.4$  wm<sup>-1</sup>K<sup>-1</sup>

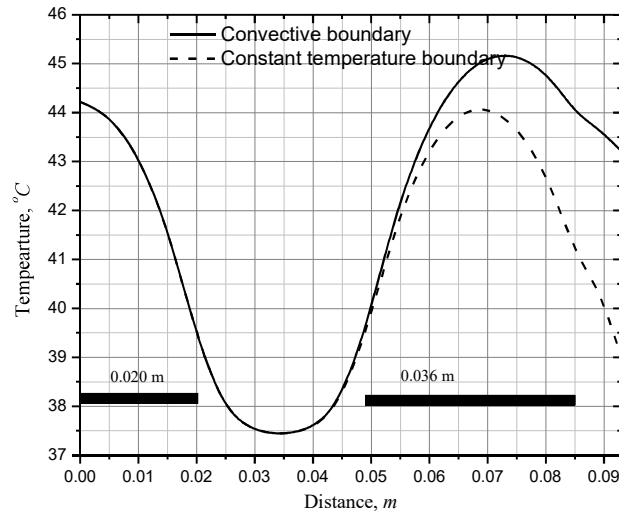


**Figure 4.26.** Comparison of the present result for temperature distribution for multi-layer brain tissue with Das (2013)

#### 4.5.2. Forward results

In present work multi-layer brain is considered, as we discussed pdepe was unable to solve the multi-layer problem to overcome this we adopted FEM. The temperature distribution is obtained for the varying boundary conditions i.e. convective, constant temperature and insulated. One side of the brain is maintain adiabatic and other side is convective or constant temperature. The temperature distribution is also obtained by varying the size and location of the tumor to analysis their effects. The temperature distribution is shown in the Figure 4.27.





(c)

**Figure 4.27.** Comparison of Temperature distribution in the brain tissue with (a) different boundary with multiple tumor of same size (b) multiple tumor of different size and (c) multiple tumor with different size-location.

### 4.5.3. Inverse Results

In present work, multiple tumor with same size is consider having one side insulated and other is maintained at constant temperature. The Differential Evolution is used as the inverse algorithm to simultaneously estimate the multiple parameters. The objective function in the form of,

$$\text{Minimization, } F = \left\{ \theta - \tilde{\theta}(P_1, P_2, P_3, P_4, P_5, P_6, P_7) \right\}^2$$

The normal brain and the cancerous brain tissue temperature distribution shown in the Figure 4.28. Due to the presence of the tumor, the temperature profile did not appear as smooth like normal brain tissue. This is attributed to the fact that the blood perfusion rate and internal heat generation values are different for the tumor so that act like a heat source in that part and have high temperature as compared to the surrounding surface. The properties of all the parts of the brain tissue and the malignant tissue are shown in the Table 4.10.

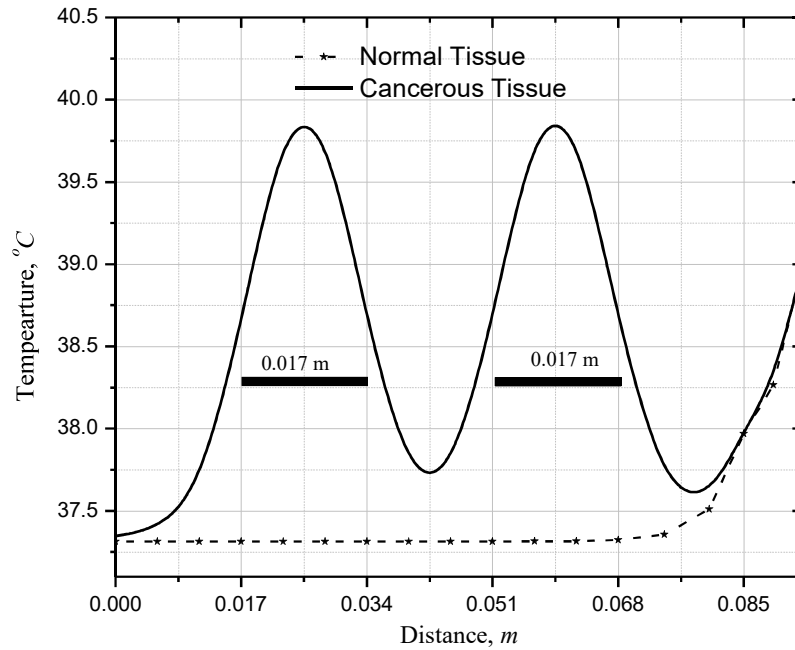


**Figure 4.28.** Comparison of temperature distribution in the brain tissue with and without tumor.

**Table 4.9.** Properties of brain tissue and tumor [57],[41]

Parameters	blood	Scalp	Bone	Brain tissue	Tumor
Specific heat, $c_p$	3800	4000	2300	3700	3700
Density, $\rho$	1050	1000	1500	1050	1050
Thermal Conductivity, $k$	-	0.34	1.16	0.50	0.50
Perfusion rate, $\eta$	-	0.00033	0.0003	0.00833	0.0005
Metabolic heat generation rate, $Q_m$	-	363.4	368.3	10437	25000
Thickness	-	0.004	0.004	0.085	0.017

DE used to find the values of these unknowns, we consider a brain tissue has insulated at one end and other end is provided with constant temperature. There are seven unknown parameter ( $P_1, P_2, P_3, P_4, P_5, P_6, P_7$ ) are estimated by numerical method as forward method and for inverse

differential evolution (DE) is adopted. The three different run have been considered by DE to get confidence in the retrieved parameters which comes in the range provided by us, shown in Table 4.11. It shows the comparison of estimated and exact values of different unknowns, obtained by using DE. The optimization process has been terminated when the objective function ( $F$ ) acquired the minimum value after multiple iterations. In present work, 100 iterations are taken. In the present work, the population size of 25, scaling factor,  $S=0.7$  and crossover probability,  $CR=0.9$  has been considered for DE algorithm.

**Table 4.10.** Comparison of values for different runs of DE with temperature field of pin fin containing no measurement error,  $e_r=0$ . Range:  $[P_1, P_2, P_3, P_4, P_5, P_6, P_7] = [0.0001-0.01]$ ;

Brain tissue	Blood perfusion rate, $\eta_{bd} \text{ s}^{-1}$			
Run	Exact ( $P_1, P_2, P_3, P_4, P_5, P_6, P_7$ )	Estimated ( $P_1, P_2, P_3, P_4, P_5, P_6, P_7$ )	Error (%) ( $P_1, P_2, P_3, P_4, P_5, P_6, P_7$ )	$F$
<b>1</b>	[0.0083, 0.0005, 0.0083, 0.0005, 0.0083, 0.0003, 0.00033]	[0.0083, 0.0005, 0.0083, 0.0005, 0.0083, 0.0003, 0.0005]	[0, 0, 0, 0, 0, 0, 0.017]	$5.9 \times 10^{-2}$
<b>2</b>		[0.0083, 0.0005, 0.0083, 0.0005, 0.0083, 0.0003, 0.0004]	[0, 0, 0, 0, 0, 0, 0.007]	$5.1 \times 10^{-2}$
<b>3</b>		[0.0083, 0.0005, 0.0083, 0.0005, 0.0083, 0.0003, 0.0003]	[0, 0, 0, 0, 0, 0, 0.003]	$5.1 \times 10^{-2}$

It is observed that for the first run the values of Last perfusion rate i.e.  $P_7$  is different than the exact one and all others are same. In 2<sup>nd</sup> and 3<sup>rd</sup> run very less difference in estimated and exact one and showing same results with same objective function value. The iterative variation of unknown parameters ( $P_1, P_2, P_3, P_4, P_5, P_6, P_7$ ) and objective function ( $F$ ) using DE and without measurement error,  $e_r=0$  are shown in Fig. 4.29 (a-b). The obtainable iterative variation equals to the third run of the DE in Table 4.11. The Objective function ( $F$ ) continuous decreases and remain same after 75 iterations. The objective function have value  $F \approx 0$  ( $10^{-2}$ ) for all the runs for estimation of unknowns, ( $P_1, P_2, P_3, P_4, P_5, P_6, P_7$ ). From fig. 4.29 (b), there is a fluctuation in the perfusion rate in the brain tissue which shows the presence of abnormality. The estimated perfusion profile which matches the exactly with the exact values of perfusion rate shows the presence of multiple tumor. Based on the estimated values of the unknown parameters, a new temperature field is reconstructed and compared

with the actual temperature field as shown in Fig. 4.30. The actual and reconstructed temperature field are excellent match with each other.

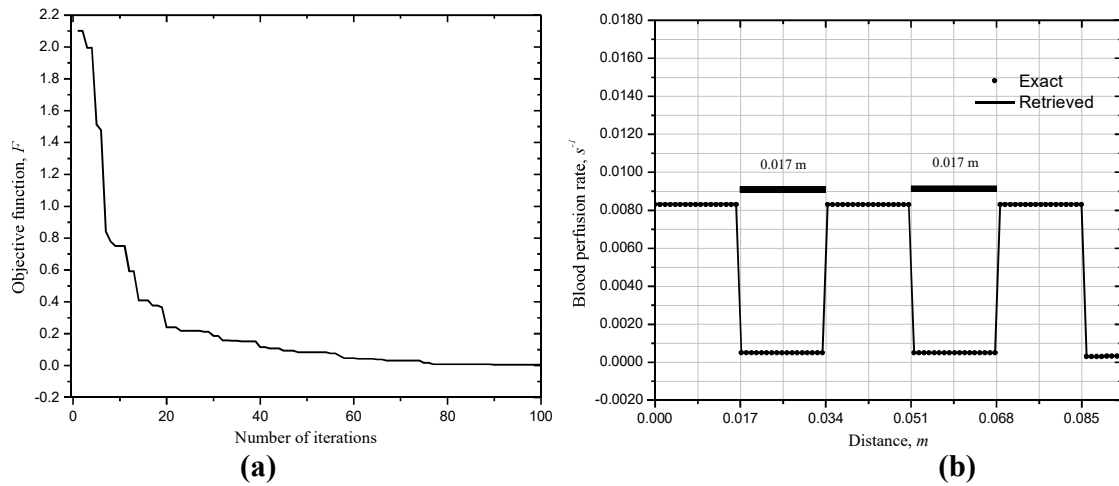


**Figure 4.29.** (a)Variation of objective function (F) with iterations of DE (b) Comparison of estimated and exact values of perfusion rate,  $\eta_b$  in 1-D brain tissue.

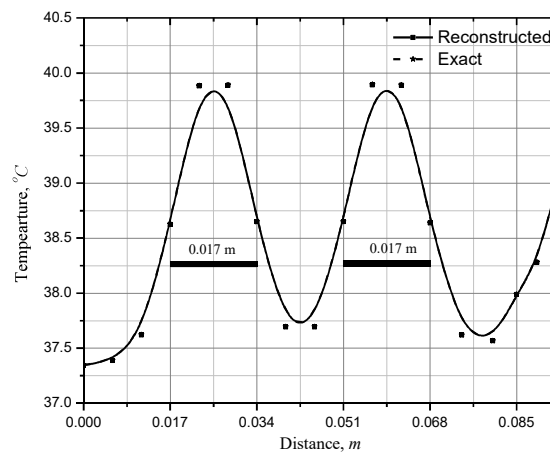


**Figure 4.30.** Comparison of actual and reconstructed non-dimensional temperature field for brain tissue.

It is observed that the maximum deviation of temperature field obtained from estimated value of  $(P_1, P_2, P_3, P_4, P_5, P_6 \text{ and } P_7)$  from exact ones is found to be 0.008

# CONCLUSION AND FUTURE DIRECTIONS

---

### 5.1. Conclusion

The present work considers application of an inverse method on transient state problem describing heat dissipation from a nonlinear longitudinal circular pin fin with disparate tip conditions to estimate the heat flux and heat transfer coefficient. Bioheat problems are also studied considering transient state heat transfer in brain tissue to estimate presence of tumor and blood perfusion rate.. For the circular pin fin, the air is considered as working fluid. The heat transfer coefficient, thermal conductivity, and emissivity is assumed as temperature dependent. For the forward results, the MATLAB based Pdepe tool was applied easily on the problem with sufficient accuracy for nonlinear partial differential equation in one-dimensional space and time. The non-dimensional parameters values used in the present method is obtained from the experiment work. It is observed that the temperature distribution obtained from the present work for convective- radiative tip are in good agreement with analytical work as described earlier in validation section. The solution is obtained for different tip conditions, viz., insulated tip, convective tip, radiative tip, convective-radiative tip and constant temperature tip. From the present study, it is observed that large heat transfer is take place in convective-radiative tip condition. The insulated tip condition have higher local temperature at the tip. The temperature profile curve trend obtained from the MATLAB and experimental work show very satisfactory agreement. Variable heat transfer coefficient exponent ' $n$ ' introduces the nonlinearity and affects the solutions. To understand the ' $n$ ' affects different cases has been studied. The investigation reveals that ' $n$ ' has opposite effect on surface and tip. The impact of Non-dimensional parameters ( $N_r$ ,  $N_c$ ,  $Bi$ ,  $N_{br}$ ,  $\gamma$ , and  $\beta$ ) has been also studied on temperature distribution. As a result, it can be concluded that MATLABs inbuilt Pdepe tool is simple and reliable tool. The results obtained from Pdepe tool gives reasonable results as compared to another analytical or semi-analytical methods. GSSM is used to optimize the objective function

to retrieve time-dependent and independent heat flux in pin fin, a case study has been performed for three different types of heat flux namely constant, linear-triangular with on-off conditions and non-linear realistic, each under static conditions. It has been concluded that for constant heat flux under static conditions, a tolerance level of 5% is acceptable for temperature with a maximum error of 3.72% in reconstruction. Linear triangular heat flux with on-off conditions under static conditions, a tolerance level of 3% is acceptable for temperature with a maximum error of 6% in reconstruction. Non-linear realistic heat flux under static conditions, a tolerance level of 4% is acceptable for temperature with a maximum error of 4% in reconstruction. A similar trend is observed for retrieved heat flux when temperatures are measured through experiments, which concludes that non-linear realistic heat flux under dynamic conditions is retrieved appreciate well using the inverse analysis. It has been concluded that retrieved heat flux is well in agreement with the actual heat flux as confirmed by experiments. The maximum uncertainties in reconstructed heat flux are 5%, 6% and 2% and 9.5% and 8%, 9% for  $V=80V$  and  $I=0.027A$ ,  $V=60V$  and  $I=0.018A$  and  $V=70V$  and  $I=0.022A$  respectively, when heat flux is input for longer duration and for specified duration respectively. Gradient free Differential Evolution is used to simultaneously estimate the heat flux and heat transfer coefficient of the same problem. The forward problem is solved by numerical based MATLAB's pdepe tool and the some input are taken from the experimental outcomes. The temperature field,  $\theta$  is obtained from the forward method and the measurement errors are also added in the exact field to get the idea of real situation. It is noted that the retrieved parameters are unique even with different runs of DE. The DE is used as the inverse algorithm for estimating the two unknown parameters,  $(\phi, h_b)$ . It is find out from present study that the same value of the combination is came out for with error,  $e_r=0$  and without error,  $e_r \neq 0$  cases in multiple runs. The objective function gives very close value for both the considerations. But incorporating measurement error, it recommends that reconstructed temperature field is poor beyond 3% error. The application of inverse methods are also applied on the bioheat problem that is to estimate the presence and perfusion rate in the brain tissue. For the forward problem Finite Element Method is adopted which give much accurate results for the temperature field. The adopted forward method is validated with the results of the method in literature and found in satisfactory agreement. For the sake of inverse Differential Evolution method is adopted, three runs are made to perform the different results and getting the different combinations of the unknown parameters which satisfy the prescribed temperatures. It is observed that the maximum

deviation of temperature field obtained from estimated value of ( $P_1, P_2, P_3, P_4, P_5, P_6,$  and  $P_7$ ) from exact ones is found to be 0.008 %.

Thus the present study helps to estimate the heat flux, heat transfer coefficient from the available temperature. It is helpful in the electronic module. For example, if we want a particular temperature value than we have idea how much amount of heat flux is utilized. As the invasive techniques of estimation of the tumor are so much costly so the present method reveals the non-invasive method of estimating the any melanoma in the brain by known temperature distribution

## **5.2. Future Direction**

The future scope of this work is that this methodology can be applied in any problem with less effort and time can be saved on the analysis part of the problem. In the future, this work can be extended to higher dimensions, as the current study has been made in one-dimension only. Further temperature-dependent thermal conductivity or the convective heat transfer coefficient can be retrieved either individually using the concept of one parameter reconstruction using GSSM, or some other optimization strategy can be implemented to obtain a suitable combination of unknown parameters of interest. For the bioheat problem, we can also apply the inverse methods to the real model in 3-D and use different methods to get more precise results.

## List of Publications

1. “Experimental and numerical thermal analysis (using Pdepe code) of a nonlinear longitudinal circular pin fin with disparate tip conditions”, **Sarvjeet Singh** and Rohit Kumar Singla, “*International Communication in Heat and Mass Transfer*”-2019 (Under review).
2. “Computational Thermal Analysis of a Conductive, Convective and Radiative Circular Pin Fin”, In Proceedings of “*International Conference on Differential Equation and Control Problems-Modeling, Analysis and Computation (ICDECP-19)*”, held at Indian Institute of Technology Mandi, H.P., India from 17th June 2019 to 19th June, 2019. (Paper Presented).
3. “Inverse problem to retrieve heat flux and heat transfer coefficient for a solid pin fin”, **Sarvjeet Singh** and Rohit Kumar Singla, In Proceedings of “*IHMTC-2019: 25th National and 3rd International ISHMT-ASTFE Heat and Mass Transfer Conference*”, to be held at IIT Roorkee, India from 28th Dec, 2019 to 31th Dec, 2019. (Submitted).
4. “ESTIMATION OF MULTIPLE TUMOR PARAMETERS IN A HUMAN BRAIN *TISSUE USING INVERSE OPTIMIZATION*”, **Sarvjeet Singh**, Meenal Singhal, and Rohit Kumar Singla, In Proceedings of “*The Second International Conference on Mathematical Modelling, Applied Analysis and Computation-2019 (ICMMAAC-19)*”, August 8-10, 2019, JECRC University, Jaipur, India. (Paper Accepted).

## References

---

---

- [1] Y. A. Cengel and A. J. Ghajar, “for Chapter 2 HEAT CONDUCTION EQUATION,” pp. 1–101, 2015.
- [2] Bejan, *CONVECTION HEAT Other books by Adrian Bejan* : 2016.
- [3] D. B. Rodrigues, P. J. S. Pereira, P. Limão-vieira, P. R. Stauffer, and P. F. Maccarini, “International Journal of Heat and Mass Transfer Study of the one dimensional and transient bioheat transfer equation : Multi-layer solution development and applications,” *Int. J. Heat Mass Transf.*, vol. 62, pp. 153–162, 2013.
- [4] Edinburgh and UK, “APPLIED PHYSIOLOGY,” in *Contemporary Ergonomics 2001*, 2010, pp. 3–8.
- [5] “J. Hadamard, 1923, Lectures on Cauchy’s Problem in Linear Partial Differential Equations, Yale University Press, New Haven CT.”
- [6] S. Donea, J., & Giuliani, “Finite element analysis of steady-state nonlinear heat transfer problems,” *Nucl. Eng. Des.*, vol. 30, no. 2, pp. 205–213, 1974.
- [7] J. W. Baughn, P. T. Ireland, T. V Jones, and N. Saniei, “A Comparison of the Transient and Heated-Coating Methods for the Measurement of Local Heat Transfer Coefficients on a Pin Fin,” *ASME J. Heat Transf.*, vol. 111, no. 1989, pp. 877–881, 1989.
- [8] S. Kiwan and M. A. Al-Nimr, “Using Porous Fins for Heat Transfer Enhancement,” *J. Heat Transfer*, vol. 123, no. 4, p. 790, 2002.
- [9] S. B. Coşkun and M. T. Atay, “Fin efficiency analysis of convective straight fins with temperature dependent thermal conductivity using variational iteration method,” *Appl. Therm. Eng.*, vol. 28, no. 17–18, pp. 2345–2352, 2008.

- [10] V. P. Singh, V. Kumar, and D. Kumar, “Numerical solution of diffusion model of brown stock washing beds of finite length using MATLAB,” *Proc. - EMS 2008, Eur. Model. Symp. 2nd UKSim Eur. Symp. Comput. Model. Simul.*, no. 13, pp. 295–300, 2008.
- [11] C. C. Wang and C. Y. Yang, “Inverse method in simultaneously estimate internal heat generation and root temperature of the T-shaped fin,” *Int. Commun. Heat Mass Transf.*, vol. 37, no. 9, pp. 1312–1320, 2010.
- [12] R. J. Moitsheki and C. Harley, “Steady thermal analysis of two-dimensional cylindrical pin fin with a nonconstant base temperature,” *Math. Probl. Eng.*, vol. 2011, pp. 7–11, 2011.
- [13] D. T. W. Lin, C. Y. Yang, J. C. Li, and C. C. Wang, “Inverse estimation of the unknown heat flux boundary with irregular shape fins,” *Int. J. Heat Mass Transf.*, vol. 54, no. 25–26, pp. 5275–5285, 2011.
- [14] and H. S. B. Singh, Tejpratap, Sanjeev Shrivastava, “Analysis of Unsteady Heat Conduction Through Short Fin With Applicability of,” *Int. J. Mech. Eng. Robot.*, vol. 2, no. 1, pp. 269–283, 2013.
- [15] M. P. Shah, K. S. Mehra, S. Gautam, and P. Negi, “Transient and Steady State Analysis of Fin Using FEM for Different Material,” *Int. J. Res. Appl. Sci. Eng. Technol.*, vol. 2, no. Vi, pp. 36–40, 2014.
- [16] A. H. R. T. L, “Experimental Analysis of Heat Transfer Enhancement Using Fins in Pin Fin Apparatus,” *Int. J. Core Eng. Manag.*, vol. 2, no. 1, pp. 123–132, 2015.
- [17] Y. P. Reddy, B. J. Kumar, D. Srinivasulu, and C. S. Rao, “Temperature Distribution Analysis of Composite Pin Fin By Experimental and Finite Element Method,” *Int. J. Innov. Res. Sci. Eng. Technol.*, vol. 4, no. 10, pp. 1021–1028, 2015.
- [18] X. Y. Cui, Z. C. Li, H. Feng, and S. Z. Feng, “Steady and transient heat transfer analysis using a stable node-based smoothed finite element method,” *Int. J. Therm. Sci.*, vol. 110, pp. 12–25, 2016.
- [19] G. Sevilgen, “A numerical analysis of a convective straight fin with temperature-dependent

- thermal conductivity,” *Therm. Sci.*, vol. 21, no. 2, pp. 939–952, 2017.
- [20] R. Jooma and C. Harley, “Heat Transfer in a Porous Radial Fin: Analysis of Numerically Obtained Solutions,” *Adv. Math. Phys.*, vol. 2017, 2017.
- [21] S. Gupta and S. Singh, “Analytical Thermal Analysis on Straight Triangular Fins,” *Int. J. Sci. Eng. Res.*, vol. 8, no. 12, pp. 353–357, 2017.
- [22] R. Das and B. Kundu, “Estimation of Internal Heat Generation in a Fin Involving All Modes of Heat Transfer Using Golden Section Search Method,” *Heat Transf. Eng.*, vol. 39, no. 1, pp. 58–71, 2018.
- [23] H. T. Chen and J. Y. Lin, “Simultaneous estimations of temperature-dependent thermal conductivity and heat capacity,” *Int. J. Heat Mass Transf.*, vol. 41, no. 14, pp. 2237–2244, 1998.
- [24] U. C. Chen, W. J. Chang, and J. C. Hsu, “Two-dimensional inverse problem in estimating heat flux of pin fins,” *Int. Commun. Heat Mass Transf.*, vol. 28, no. 6, pp. 793–801, 2001.
- [25] W. L. Chen, Y. C. Yang, and H. L. Lee, “Inverse problem in determining convection heat transfer coefficient of an annular fin,” *Energy Convers. Manag.*, vol. 48, no. 4, pp. 1081–1088, 2007.
- [26] C. A. A. Mota, H. R. B. Orlande, M. O. M. De Carvalho, V. Kolehmainen, and J. P. Kaipio, “Bayesian estimation of temperature-dependent thermophysical properties and transient boundary heat flux,” *Heat Transf. Eng.*, vol. 31, no. 7, pp. 570–580, 2010.
- [27] H. L. Lee, W. J. Chang, W. L. Chen, and Y. C. Yang, “Inverse heat transfer analysis of a functionally graded fin to estimate time-dependent base heat flux and temperature distributions,” *Energy Convers. Manag.*, vol. 57, pp. 1–7, 2012.
- [28] K. Bamdad and H. R. Ashorynejad, “Inverse analysis of a rectangular fin using the lattice Boltzmann method,” *Energy Convers. Manag.*, vol. 97, pp. 290–297, 2015.
- [29] W. L. Chen, H. M. Chou, and Y. C. Yang, “Inverse estimation of the unknown base heat

- flux in irregular fins made of functionally graded materials,” *Int. Commun. Heat Mass Transf.*, vol. 87, no. August, pp. 157–163, 2017.
- [30] C. H. Huang and M. H. Chen, “An estimation of the optimum shape and perforation diameters for pin fin arrays,” *Int. J. Heat Mass Transf.*, vol. 131, pp. 72–84, 2019.
- [31] M. Raudenský, K. A. Woodbury, J. Kral, and T. Brezina, “Genetic algorithm in solution of inverse heat conduction problems,” *Numer. Heat Transf. Part B Fundam.*, vol. 28, no. 3, pp. 293–306, 1995.
- [32] B. V. Babu and K. K. N. Sastry, “Estimation of heat transfer parameters in a trickle-bed reactor using differential evolution and orthogonal collocation,” *Comput. Chem. Eng.*, vol. 23, no. 3, pp. 327–339, 1999.
- [33] L. D. Chiwiacowsky and H. F. De Campos Velho, “Different approaches for the solution of a backward heat conduction problem,” *Inverse Probl. Eng.*, vol. 11, no. 6, pp. 471–494, 2003.
- [34] J. Taler, “Determination of local heat transfer coefficient from the solution of the inverse heat conduction problem,” *Forsch. im Ingenieurwesen/Engineering Res.*, vol. 71, no. 2, pp. 69–78, 2007.
- [35] D. Copiello and G. Fabbri, “Multi-objective genetic optimization of the heat transfer from longitudinal wavy fins,” *Int. J. Heat Mass Transf.*, vol. 52, no. 5–6, pp. 1167–1176, 2009.
- [36] A. S. A. Alghamdi, “Inverse estimation of boundary heat flux for heat conduction model,” *JKAU Eng. Sci.*, vol. 21, no. 1, pp. 73–95, 2010.
- [37] S. Mitra and C. Balaji, “International Journal of Heat and Mass Transfer A neural network based estimation of tumour parameters from a breast thermogram,” *Int. J. Heat Mass Transf.*, vol. 53, no. 21–22, pp. 4714–4727, 2010.
- [38] R. Das, “A simplex search method for a conductive-convective fin with variable conductivity,” *Int. J. Heat Mass Transf.*, vol. 54, no. 23–24, pp. 5001–5009, 2011.

- [39] C. H. Huang and W. L. Chang, "An inverse design method for optimizing design parameters of heat sink modules with encapsulated chip," *Appl. Therm. Eng.*, vol. 40, pp. 216–226, 2012.
- [40] R. Das, "Application of genetic algorithm for unknown parameter estimations in cylindrical fin," *Appl. Soft Comput. J.*, vol. 12, no. 11, pp. 3369–3378, 2012.
- [41] K. Das, R. Singh, and S. C. Mishra, "Numerical analysis for determination of the presence of a tumor and estimation of its size and location in a tissue," *J. Therm. Biol.*, vol. 38, no. 1, pp. 32–40, 2013.
- [42] R. Das and K. T. Ooi, "Application of simulated annealing in a rectangular fin with variable heat transfer coefficient," *Inverse Probl. Sci. Eng.*, vol. 21, no. 8, pp. 1352–1367, 2013.
- [43] A. Bhowmik, R. K. Singla, P. K. Roy, D. K. Prasad, R. Das, and R. Repaka, "Predicting geometry of rectangular and hyperbolic fin profiles with temperature-dependent thermal properties using decomposition and evolutionary methods," *Energy Convers. Manag.*, vol. 74, pp. 535–547, 2013.
- [44] R. Das, "Forward and inverse solutions of a conductive, convective and radiative cylindrical porous fin," *Energy Convers. Manag.*, vol. 87, pp. 96–106, 2014.
- [45] S. Panda, A. Bhowmik, R. Das, R. Repaka, and S. C. Martha, "Application of homotopy analysis method and inverse solution of a rectangular wet fin," *Energy Convers. Manag.*, vol. 80, pp. 305–318, 2014.
- [46] K. Das and S. C. Mishra, "Non-invasive estimation of size and location of a tumor in a human breast using a curve fitting technique ☆," *Int. Commun. Heat Mass Transf.*, vol. 56, pp. 63–70, 2014.
- [47] S. Panda and R. Das, "Inverse analysis of a radial porous fin using genetic algorithm," *2015 8th Int. Conf. Contemp. Comput. IC3 2015*, no. 1, pp. 167–170, 2015.
- [48] A. Bhowmik and R. Repaka, "International Journal of Heat and Mass Transfer Estimation of growth features and thermophysical properties of melanoma within 3-D human skin

- using genetic algorithm and simulated annealing,” *Int. J. Heat Mass Transf.*, vol. 98, pp. 81–95, 2016.
- [49] K. Agrawal, “An analytical approach for inverse heat conduction problem,” *SSRG Int. J. Mech. Eng.*, vol. 3, no. 9, pp. 362–365, 2016.
- [50] I. Conference *et al.*, “ScienceDirect Blood Perfusion Parameter Estimation in Tumors by Blood Perfusion Parameter Estimation in Tumors by means of a Genetic Algorithm Blood Perfusion Parameter Estimation in Tumors by means of a Genetic Algorithm Melo of a Genetic Algorithm,” *Procedia Comput. Sci.*, vol. 108, pp. 1384–1393, 2017.
- [51] H. Kumar and G. Nagarajan, “A Bayesian inference approach: estimation of heat flux from fin for perturbed temperature data,” *Sadhana - Acad. Proc. Eng. Sci.*, vol. 43, no. 4, pp. 1–16, 2018.
- [52] M. Bahador, M. M. Keshtkar, and A. Zariee, “Numerical and experimental investigation on the breast cancer tumour parameters by inverse heat transfer method using genetic algorithm and image processing,” *Sāadhanā*, vol. 0123456789, 2018.
- [53] H. H. Pennes, “Analysis of tissue and arterial blood temperatures in the resting human forearm. 1948.,” *J. Appl. Physiol.*, vol. 85, no. 1, pp. 5–34, 1998.
- [54] J. Kiefer, “Sequential Minimax Search for a Maximum,” *Proc. Am. Math. Soc.*, vol. 4, no. 3, p. 502, 2006.
- [55] K. Price and R. Storn, “Differential Evolution – A Simple and Efficient Heuristic for Global Optimization over Continuous Spaces,” *J. Glob. Optim.*, no. 11, pp. 341–359, 1997.
- [56] S. Parthasarathy and C. Balaji, “Estimation of parameters in multi-mode heat transfer problems using Bayesian inference - Effect of noise and a priori,” *Int. J. Heat Mass Transf.*, vol. 51, no. 9–10, pp. 2313–2334, 2008.
- [57] L. Zhu and C. Diao, “Theoretical simulation of temperature distribution in the brain during mild hypothermia treatment for brain injury,” *Med. Biol. Eng. Comput.*, vol. 39, no. 6, pp. 681–687, 2001.

# HMT

---

## ORIGINALITY REPORT

---

<b>15%</b>	<b>6%</b>	<b>14%</b>	<b>0%</b>
SIMILARITY INDEX	INTERNET SOURCES	PUBLICATIONS	STUDENT PAPERS

---

## PRIMARY SOURCES

---

<b>1</b>	Rodrigues, D.B., P.J.S. Pereira, P. Limão-Vieira, P.R. Stauffer, and P.F. Maccarini. "Study of the one dimensional and transient bioheat transfer equation: Multi-layer solution development and applications", International Journal of Heat and Mass Transfer, 2013. Publication	<b>3%</b>
<b>2</b>	D.B. Rodrigues, P.J.S. Pereira, P. Limão-Vieira, P.R. Stauffer, P.F. Maccarini. "Study of the one dimensional and transient bioheat transfer equation: Multi-layer solution development and applications", International Journal of Heat and Mass Transfer, 2013 Publication	<b>2%</b>
<b>3</b>	<a href="http://www.coursehero.com">www.coursehero.com</a> Internet Source	<b>2%</b>
<b>4</b>	<a href="http://sith.ipb.ac.rs">sith.ipb.ac.rs</a> Internet Source	<b>1%</b>
<b>5</b>	<a href="http://www.irjet.net">www.irjet.net</a> Internet Source	<b>1%</b>

---

6

Pranab Kanti Roy, Ashis Mallick, Hiranmoy Mondal, Sicelo Goqo, Precious Sibanda. "Numerical study on rectangular-convex-triangular profiles with all variable thermal properties", International Journal of Mechanical Sciences, 2017

Publication

---

<1%

7

V.P. Singh. "Numerical Solution of Diffusion Model of Brown Stock Washing Beds of Finite Length Using MATLAB", 2008 Second UKSIM European Symposium on Computer Modeling and Simulation, 09/2008

Publication

---

<1%

8

Coskun, S.B.. "Fin efficiency analysis of convective straight fins with temperature dependent thermal conductivity using variational iteration method", Applied Thermal Engineering, 200812

Publication

---

<1%

9

Kuljeet Singh, Ranjan Das. "Generalized inverse analysis for fins of different profiles with all temperature-dependent parameters", Heat and Mass Transfer, 2015

Publication

---

<1%

10

Leandro dos Santos Coelho, Alireza Askarzadeh. "An enhanced bat algorithm approach for reducing electrical power

<1%

consumption of air conditioning systems based on differential operator", Applied Thermal Engineering, 2016

Publication

11

[jes.ecsdl.org](http://jes.ecsdl.org)

Internet Source

<1%

12

Han-Taw Chen, Jae-Yuh Lin. "Simultaneous estimations of temperature dependent thermal conductivity and heat capacity", International Journal of Heat and Mass Transfer, 1998

Publication

<1%

13

International Journal of Numerical Methods for Heat & Fluid Flow, Volume 11, Issue 5 (2006-09-19)

Publication

<1%

14

Engineering Heat Transfer, 1988.

Publication

<1%

15

[iet-journals.org](http://iet-journals.org)

Internet Source

<1%

16

Eric Li. "Modeling and simulation of bioheat transfer in the human eye using the 3D alpha finite element method ( $\alpha$ FEM)", International Journal for Numerical Methods in Biomedical Engineering, 2010

Publication

<1%

17

Bhattacharjya, Rajib Kumar, Ambuj Srivastava,

and Mysore G. Satish. "Hybrid-Optimization Approach for Estimating Parameters of a Virus Transport Process in Aquifer", Journal of Hazardous Toxic and Radioactive Waste, 2013.

Publication

<1%

18

documents.mx

Internet Source

<1%

19

Kuljeet Singh, Ranjan Das, Rohit K Singla. "Closed-form solution for a rectangular stepped fin involving all variable thermal parameters and nonlinear boundary conditions", Proceedings of the Institution of Mechanical Engineers, Part E: Journal of Process Mechanical Engineering, 2016

Publication

<1%

20

George A. Oguntala, Gbeminiyi M. Sobamowo, Raed Abd-Alhameed, James M. Noras. "Numerical Study of Performance of Porous Fin Heat Sink of Functionally Graded Material for Improved Thermal Management of Consumer Electronics", IEEE Transactions on Components, Packaging and Manufacturing Technology, 2019

Publication

<1%

21

Cui Xiangyang, Li Guangyao, Zheng Gang, Wu Suzhen. "NS-FEM/ES-FEM for contact problems in metal forming analysis",

<1%

22

A. A. Abou El Ela. "Optimal power flow using differential evolution algorithm", Electrical Engineering, 07/16/2009

Publication

---

<1%

23

Alghamdi , A. S. A.. "Inverse Estimation of Boundary Heat Flux for Heat Conduction Model \ Journal of King Abdulaziz University : Engineering Science .- 2010 , Vol. 21 , No. 1 , pp. 73 - 95.", Journal of King Abdulaziz University: Engineering Sciences, 2010

Publication

---

<1%

24

Fung-Bao Liu. "Inverse estimation of wall heat flux by using particle swarm optimization algorithm with Gaussian mutation", International Journal of Thermal Sciences, 2012

Publication

---

<1%

25

International Journal of Numerical Methods for Heat & Fluid Flow, Volume 24, Issue 7 (2014-09-16)

Publication

---

<1%

26

Srikumar Panda, Arka Bhowmik, Ranjan Das, Ramjee Repaka, Subash C. Martha. "Application of homotopy analysis method and inverse solution of a rectangular wet fin", Energy Conversion and Management, 2014

<1%

---

27	<a href="http://ijpg.org">ijpg.org</a> Internet Source	<1%
28	Wang, C.C.. "Inverse method in simultaneously estimate internal heat generation and root temperature of the T-shaped fin", International Communications in Heat and Mass Transfer, 201011 Publication	<1%
29	Rohit K. Singla, Ranjan Das. "A differential evolution algorithm for maximizing heat dissipation in stepped fins", Neural Computing and Applications, 2017 Publication	<1%
30	<a href="http://d.researchbib.com">d.researchbib.com</a> Internet Source	<1%

---

Exclude quotes      On  
Exclude bibliography      On

Exclude matches      < 8 words